UNIVERSITY OF CALIFORNIA SAN DIEGO

Understanding the chemokine scavenging function of C-C chemokine receptor type 2 (CCR2)

A Dissertation submitted in partial satisfaction of the requirements
for the degree Doctor of Philosophy

in

Biomedical Sciences

by

Thomas Shroka

Committee in charge:

Professor Tracy Handel, Chair
Professor William Joiner
Professor Samara Reck-Peterson
Professor Roger Sunahara
Professor JoAnn Trejo

2022

The Dissertation of Thomas Shroka is approved, and it is acceptable in quality and form for publication on microfilm and electronically.

University of California San Diego

2022

DEDICATION

I dedicate this work to my family, friends, and colleagues. All of whom helped make this work possible.

TABLE OF CONTENTS

LIST OF FIGURES

LIST OF ABBREVIATIONS

GPCR	G protein-coupled receptor
CCR	C-C chemokine receptor type
CXCR	C-X-C chemokine receptor type
ACKR	atypical chemokine receptor type
GRK	G protein receptor kinase
PM	plasma membrane
CME	clathrin mediated endocytosis
CIE	clathrin independent endocytosis
CCP	clathrin coated pit
PTx	Pertussis toxin
HEK293	human embryonic kidney 293 cell
APEX	ascorbate peroxidase
MS	mass spectroscopy
BRET	Bioluminescence resonance energy transfer
Rluc	luciferase from *Renilla reniformis*
rGFP	GFP from *Renilla reniformis*
ECL	extracellular loop
ICL	intracellular loop
TM	trans-membrane
GFP	green fluorescent protein
PE	Phycoerythrin

GEF	guanyl nucleotide exchange factor
THP-1	human acute monocytic leukemia cell
TMT	tandem mass tag
TGN	trans-golgi network

ACKNOWLEDGEMENTS

Thanks of course to the committee for dedicating their time, thoughts, and expertise throughout my thesis work. Thanks especially to Tracy Handel for years of mentoring and guidance, without which this work would not be possible. I cannot thank Tracy enough for her dedication to not only my research, but the research of the lab as a whole. And for the countless hours she spends towards ensuring the success of the lab as well as all pharmacology trainees. Although not part of my committee, but a consistent collaborator and mentor, Irina Kufareva also deserves individual mention. She has been critical to my success and training throughout the entirety of my thesis research. I am also extremely appreciative of all the guidance and support provided to me by the various post-docs, fellow graduate students, and undergraduate students who I have had the pleasure of working with over the years. I am also tremendously grateful for the friendships I have formed throughout my time here, within the lab, the BMS program, as well as outside the UCSD community.

I am of course overwhelmingly thankful to my fiancée and partner Renee, who has been more supportive and has made every aspect of my life (PhD included) more enjoyable than I ever could have hoped. And to my parents, Mike and Kim Shroka, who I cannot thank enough for their unbelievable support throughout the years.

Chapter 2, in full, is a reprint of the material currently in press at Science Signaling. (T.M. Shroka, I. Kufareva, C.L. Salanga, T.M. Handel (2022)). “The dual function chemokine receptor, CCR2, drives migration and chemokine scavenging by distinct mechanisms.” The dissertation author was the primary researcher and author of this material.

Chapter 3 is adapted from a manuscript currently in preparation for submission for publication. (T.M. Shroka, A. Lona, C. Sanchez, C.L. Salanga, I. Kufareva, T.M. Handel (2022)). “Proximal proteome of C-C chemokine receptor 2 (CCR2) reveals novel endocytic trafficking patterns.” The dissertation author was the primary researcher and author of this material.

Chapter 4 contains unpublished material. The dissertation author was the primary author of this chapter.

VITA

2012 Bachelor of Science in Biology, The Ohio State University

2014 Bachelor of Science in Health Sciences, Cleveland State University

2022 Doctor of Philosophy in Biomedical Sciences, University of California San Diego

PUBLICATIONS

A. Astashchanka, T. M. Shroka, B. M. Jacobsen, Mucin 2 (MUC2) modulates the aggressiveness of breast cancer. *Breast Cancer Res Treat*. **173**, 289–299 (2019).

J. C. Harrell, T. M. Shroka, B. M. Jacobsen, Estrogen induces c-Kit and an aggressive phenotype in a model of invasive lobular breast cancer. *Oncogenesis*. **6**, 396 (2017).

W. M. Baldwin, C. A. Su, T. M. Shroka, R. L. Fairchild, Experimental models of cardiac transplantation: design determines relevance. *Curr Opin Organ Transplant*. **19**, 525–530 (2014).

FIELD OF STUDY

Biomedical Sciences

ABSTRACT OF THE DISSERTATION

Understanding the chemokine scavenging function of C-C chemokine receptor type 2 (CCR2)

by

Thomas Shroka

Doctor of Philosophy in Biomedical Sciences

University of California San Diego, 2022

Professor Tracy Handel, Chair

Migration of monocytes into tissues is driven by activation of the G protein-coupled receptor CCR2 in response to inflammatory chemokine CCL2 and is critical to normal immune responses. In addition to cell migration, CCR2 has a largely unappreciated scavenging function, by which it sequesters excess chemokine from the extracellular environment. It is hypothesized that this scavenging function allows CCR2 to control its own chemokine gradient, while its ability to recycle rather than downregulate allows it to

maintain responsiveness in the presence of high chemokine concentration. Similarly, this function may be responsible for the difficulty observed when attempting to pharmacologically inhibit CCR2 activity. Therefore, an understanding of the molecular drivers underlying this chemokine scavenging is essential for developing effective therapeutics.

Chemokine scavenging was widely regarded as a function of only atypical chemokine receptors (ACKRs), while scavenging by G protein-coupled chemokine receptors has largely been ignored. In our soon to be published study (Chapter 2), we show that scavenging by CCR2 occurs in a manner independent of G proteins, G protein receptor kinases, arrestins, or clathrin, suggesting that a yet unknown non-canonical mechanism is largely responsible for this function. We therefore took a discovery-based approach using proximity labeling proteomics to further define the interactome of CCR2 along G protein-dependent and -independent pathways (Chapter 3). Finally, we discuss speculative, yet exciting, explanations of observations made in our latest findings and consider possible future experimental directions (Chapter 4). Collectively, the work presented herein highlights the complexity of CCR2 function, and significantly contributes to understanding and identifying the molecular drivers involved in chemokine scavenging.

CHAPTER 1

INTRODUCTION

GPCRs, CHEMOKINES AND CHEMOKINE RECEPTORS

The chemokine signaling system consists of 22 chemokine receptors and nearly 50 chemokine ligands which regulate the movement of numerous cell types (*1*, *2*). Chemokine receptors expressed on the cell surface drive the migratory function by responding to gradients of chemokines which provide directional cues (*3*–*5*). The chemokine system plays a crucial role in development, such as driving directional extension of primary neurons, and in the innate and adaptive immune responses by driving migration of immune cells to sites of inflammation (*6*–*9*). Consequently, dysregulation of the chemokine signaling system can result in autoimmune and other inflammatory diseases, such as pulmonary and cardiac fibrosis, neurological disorders, cardiovascular disease and atherosclerosis (*10*–*12*).

Chemokine receptors makeup the largest family of the rhodopsin-like (also known as class A) G protein-coupled receptors (GPCRs) (*13*). Structurally, GPCRs consist of a membrane-spanning domain comprised of seven trans-membrane helices, three connecting intracellular and three extracellular loops, and an intracellular C-terminal tail (*14*). These receptors activate a vast array of cell signaling pathways to external stimuli by binding of ligands to the extracellular facing orthostatic pocket of the receptor, which results in a confirmational shift of the receptor to provide access for heterotrimeric G proteins to the intracellular core of the receptor. Acting as a guanyl nucleotide exchange factor (GEF), the receptor modifies Gα proteins to their active GTP-bound state which can then activate downstream pathways (*15*). The complete GPCR family consists of over 800 different receptors, making them largest class of cell surface receptors (*16*). Furthermore, there are approximately 14 different Gα subunits (not including individual subunit isoforms) some of which are ubiquitously expressed, whereas others are cell type specific (*17*). These

individual Gα subunits are able to activate a plethora of effector proteins and sell signaling pathways (*18*). To further complicate the GPCR and G protein signaling dynamics, some GPCRs are capable of responding to several different agonist ligands, as well as activate multiple types of Gα subunits (*19*). Moreover, tissues and individual cells typically express at least 100 different GPCRs (*20*), making them one of the most predominant class of membrane proteins, as well one of the most functionally significant contributors to cellular responses to external stimuli. Due to these complexities, it becomes increasingly obvious why research regarding this family of surface receptors is endlessly pursued.

Not surprisingly, considering their extensive role in intracellular signaling and a pharmacologically accessible extracellular binding pocket, GPCRs are the target of over 60% of all FDA approved therapeutics (*21*). However, there are only three FDA approved therapeutics targeting chemokine receptors, and are for treatment of HIV infection (targeting CCR5), stem cell mobilization (targeting CXCR4), and T-cell lymphoma (targeting CCR4) but none have been approved for treatment of inflammatory or autoimmune diseases (*22*, *23*). A possible explanation for why chemokine receptors have proven so difficult to target therapeutically could be due to the extensive interoperability between chemokine receptors and their chemokine ligands, as shown in **Figure 1.1** (*24*). This interoperability between chemokines and chemokine receptors is also complicated by the specific cell-type expression of chemokine receptors, such that chemokine receptors are not strictly restricted to being expressed on only inflammatory or only immunosuppressive cells and are expressed on non-immune cell-types as well. (*25*). Additionally, multiple chemokines can be expressed in the same cell types, such as CCR1 and CCR2 in monocytes which respond to several shared ligands and further complicates the study of these receptors.

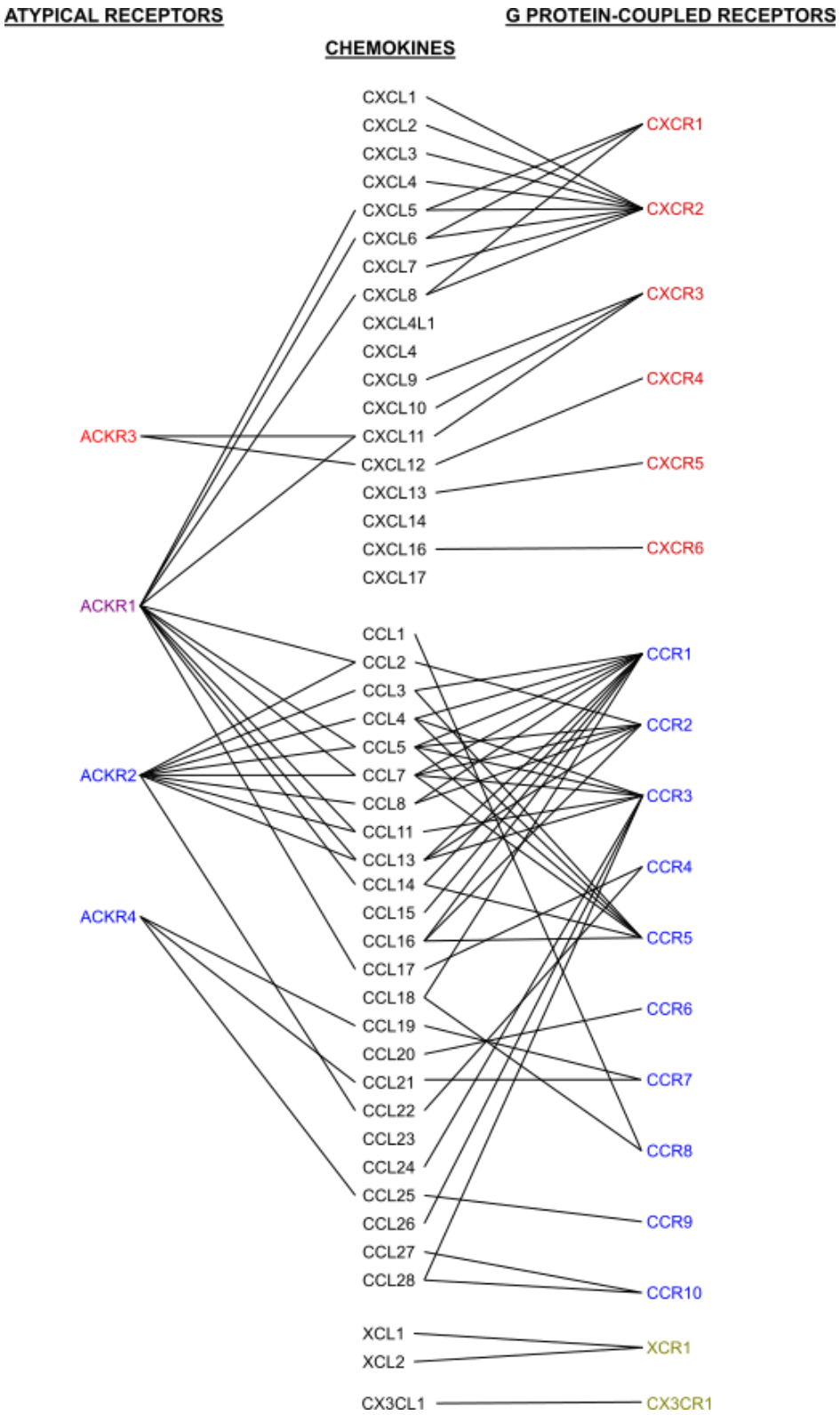

Figure 1.1. Interoperability of chemokines and chemokines receptors. Visualization of chemokines and their chemokine ligand. Adapted from Bachelerie et al. 2014 (*26*).

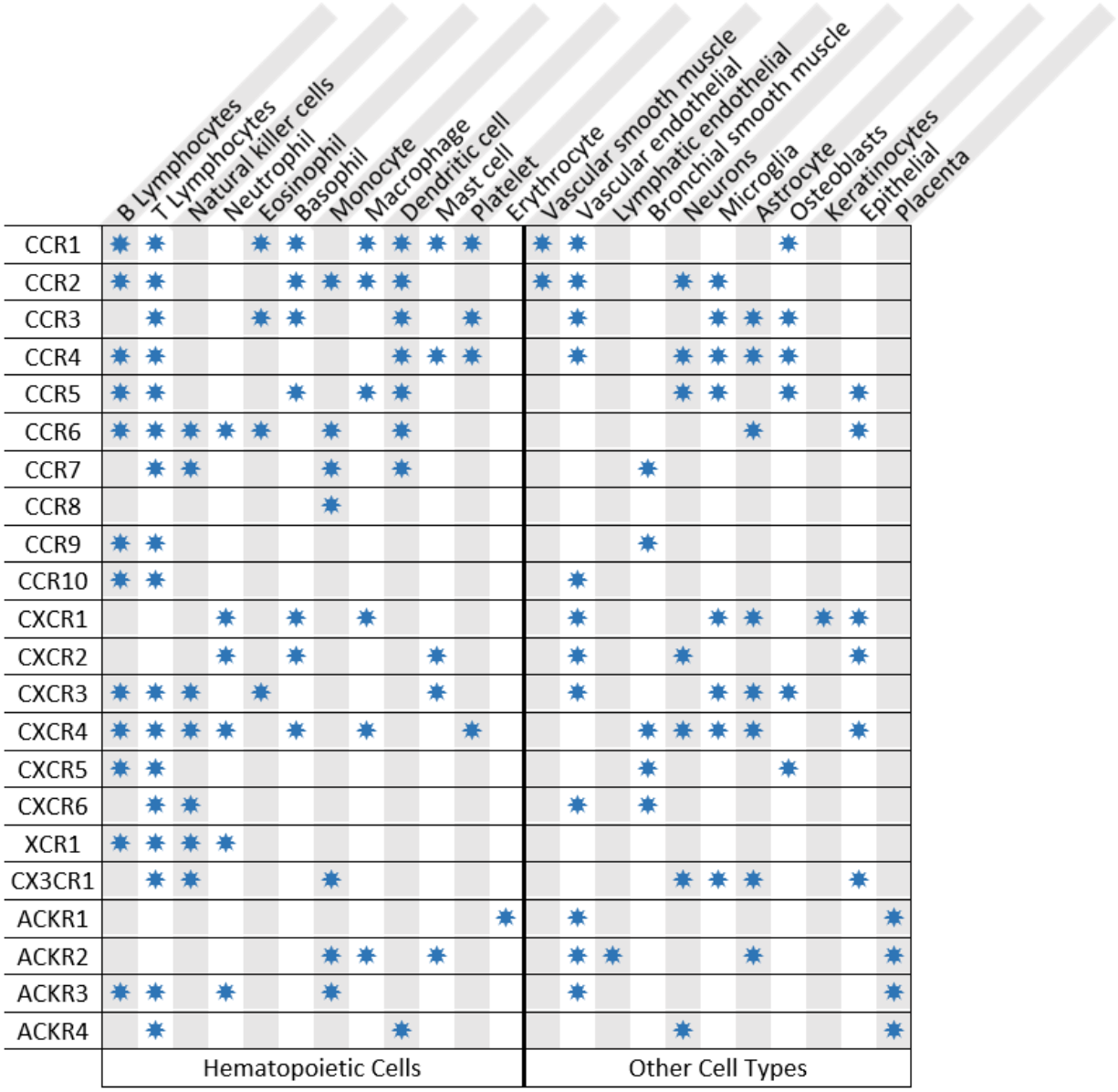

Figure 1.2. Overview of chemokine receptor cellular expression. Chemokine receptors are expressed throughout a wide variety of cell types and are expressed alongside other receptors within the same cell types. Adapted from Scholten et al, 2011 (*13*).

The study of chemokine receptors is inherently tied to the study of their chemokine ligands. Chemokines (short for chemoattractant cytokines) are small (~10 kDa) secreted proteins with a remarkably conserved structure, consisting of a beta sheet, a short flexible N-terminus, and a C-terminal helix (*27*). Chemokine names are derived according to the cysteine motif pattern of residues located near the N-terminus (i.e., C, CC, CXC, or CX3C) (*28*). Notably, chemokines differ from other cytokines by being the only members of the cytokine family that bind and activate GPCRs (*29*). Chemokines were originally discovered for their role in driving the directional migration of immune cells, however they have since been shown to be involved in development, angiogenesis, leukocyte trafficking, cancer and metastasis, as well as host defense from infectious disease (*9*, *10*, *30*).

As with other GPCRs, stimulation of chemokine receptors by chemokine agonists, leads to the recruitment and activation of heterotrimeric G proteins which in turn activate signaling pathways that control the cell motility machinery (*31–33*). Upon activation of the receptor, the outward movement of transmembrane helices V and VI, creates space in the intracellular facing core of the receptor in which heterotrimeric G proteins can bind (*34*). The agonist-bound activated GPCR then acts as a GEF resulting in formation of the active GTP-bound Gα-subunit and dissociation from Gβγ, where both G protein subunits can activate downstream effectors (*35*).

Following activation of G protein, GPCRs (primarily the Ser/Thr residues of their C-terminus) are phosphorylated by G protein-coupled receptor kinases (GRKs) (*36*). The GRKs 2/3/5/6 are the only ubiquitously expressed GRKs; GRK-1 and -7 are visual GKRs and GRK4 is only expressed in the testis (*37*). Since GRKs are primarily cytosolic proteins, they require specific mechanisms to associate with the plasma membrane (PM) where the

receptors reside. GRK2/3 contain a pleckstrin homology (PH) domain which is able to bind Gβγ located at PM (*38, 39*) whereas GRK5/6 are not dependent on Gβγ but rather associate with the membrane via palmitoylation of their C-terminal cysteines and interaction with PM phospholipids (*40–43*).

Following receptor phosphorylation by GRKs, arrestins are then recruited to the receptor where they make extensive electrostatics interactions with the phospho-residues of the receptor C-terminus as well as interactions with the exposed cytoplasmic face and core of the receptor (*44, 45*). Remarkably, there have been only four arrestins discovered in mammalian biology, with arrestin-1 and -4 being visual arrestins and only two non-visual arrestins, arrestin-2 and -3 (a.k.a. β-arrestin-1 and -2), meaning that within most tissues, of the 800 identified GPCRs there are only two arrestins acting on these receptors (*46–49*). The role of arrestins in terminating G protein signaling by GPCRs is well established. They accomplish this by interacting with and outcompeting G proteins for the same cytoplasmic core location of active GPCRs, and as their name suggests, arrest further GPCR mediate G protein signaling (*44*). Arrestins also facilitate internalization and shuttling of the receptor into the endosomal trafficking pathway by interaction with endocytic machinery, AP2 and clathrin (*50*). Following internalization, GPCRs are trafficked along a complex network of endocytic pathways, involving hundreds of proteins mediators and effectors.

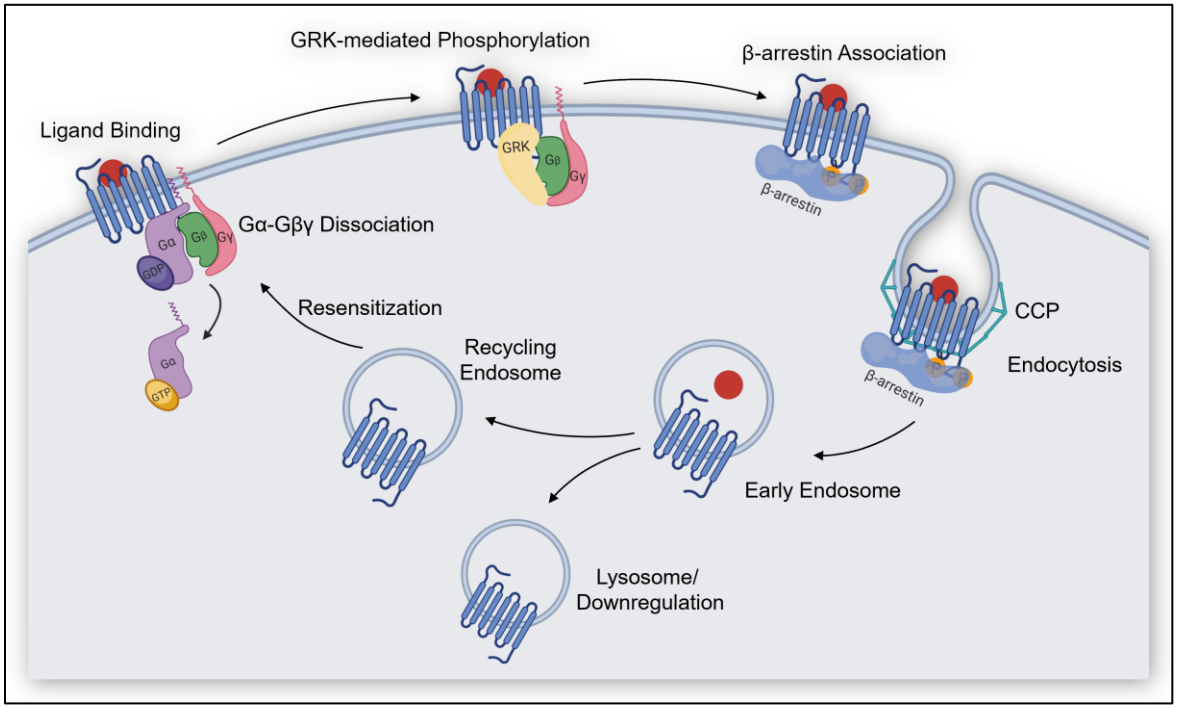

Figure 1.3. Canonical GPCR activation and endocytosis. Following ligand binding activation of the GPCR results in a conformational shift resulting in G protein coupling and guanine nucleotide exchange of GDP for GTP on the Gα-subunit of the heterotrimeric G protein (Gαβγ), after which Gα dissociates and activates downstream effectors. Subsequent phosphorylation of the C-terminus of the receptor results in β-arrestin association which make extensive electrostatic interactions with the phosphorylated receptor. β-arrestin acts as a scaffold for the AP2-complex and clathrin, internalizing the receptor via CCP. The endocytosed receptor is then shuttled along the endocytic trafficking network via a plethora of mediators resulting in either receptor recycling or degradation via lysosomal degradation.

C-C CHEMOKINE RECEPTOR TYPE 2 (CCR2) AND CHEMOKINE SCAVENGING

CCR2 is a canonical G protein-coupled chemokine receptor and a key regulator of monocyte migration (*3, 51*). Due to the crucial role that monocytes play in many diseases, CCR2 has become an important therapeutic target (*52*). Preclinical studies indicate the potential of CCR2 blockade for the treatment of cardiovascular diseases including atherosclerosis and heart failure, pulmonary, cardiac and liver fibrosis and numerous other inflammatory diseases (*53–61*). The receptor has also been the target of serval clinical trials for diabetic nephropathy, non-small cell lung cancer, non-alcoholic steatohepatitis (NASH), non-alcoholic fatty liver disease (NAFLD), and pancreatic ductal adenocarcinomas (PDAC) (*62–68*). However, many of these clinical trials were unsuccessful due to lack of efficacy.

Our lab and other labs have shown that beyond its G protein signaling capabilities involved in monocyte migration, CCR2 is also able to scavenge its chemokine ligands. However, this second function is largely overlooked, poorly understood, and could be a primary cause of the lack of efficacy observed when targeting chemokine receptors (*69, 70*). Scavenging by CCR2 is particularly important due its primary chemokine ligand, CCL2 (formerly known as MCP-1) which has both constitutive and inducible expression throughout the body (*71*). Previous in vivo studies have shown that in CCR2 null or CCR2 antagonist treated mice have increased plasma levels of CCL2, and this same affect has been observed in patients undergoing clinical trials of CCR2 pharmacological antagonists (*72–76*). This is especially unwanted due to the inflammatory role of CCL2, and although CCR2 is being inhibited in these scenarios, the increased plasma concentration of CCL2 can potentially overcome this inhibition and activate unblocked receptor. Additionally, elevated

expression levels of CCL2 are associated with several disease pathologies, including multiple sclerosis plaques, Alzheimer disease, rheumatoid arthritis (RA), osteoporosis, and invasive breast cancer (*77–81*). To overcome this inability to therapeutically target CCR2 as well as other chemokine receptors, further studies of CCR2's complete functional mechanisms are required for a more thorough understanding of receptor biology and to determine the best strategies for interfering with its function.

The initiation of an immune response is an immensely important physiological function and is a carefully regulated process (*82*). However, the resolution of an inflammatory response is an equally important function (*83*). As described above, the chemokine receptor family plays a crucial role in an effective inflammatory response by driving migration of immune cells to sites of injury via their G protein signaling following activation by chemokine ligands. Additionally, resolution of the inflammatory response is also mediated by chemokine receptors. The uptake of extracellular chemokine (i.e., scavenging) by atypical chemokine receptors (ACKRs) is one means by which this resolutory function is achieved (*84*). These four receptors (ACKR1-4) are unique due to the fact that they do not couple to or activate G protein, but rather act as professional chemokine scavengers (*85*). Unlike G protein-coupled chemokine receptors, ACKRs are typically expressed on non-immune cell types, such as erythrocytes (red blood cells), lymphatic or vascular endothelial cells; with the exception of ACKR2 (a.k.a. D6) and ACKR3 which have been reported to be expressed on some leukocytes (*84*). This function has been shown to have a physiologically important role, especially in development and the immune response, by modulating the amount of chemokine available to activate other G protein-coupled chemokine receptors and drive certain cellular functions (*86, 87*). As stated

previously, our lab and other have shown that CCR2 and several other canonical G protein-coupled chemokine receptors are able to scavenge extracellular chemokine as well as drive G protein signaling functions (*69, 88*). It is hypothesized that the dual functions of CCR2 allow it to promote canonical activation of cell motility and concurrently scavenge chemokine in order to maintain responsiveness of monocytes, such that cells migrate without desensitizing when faced with high concentrations of chemokine in inflammatory situations. Due to CCR2 sharing ligands with other chemokine receptors CCR1, CCR3 and CCR5, it may also act as an atypical receptor by modulating the responsiveness of receptors expressed on different cells by altering the availability of specific chemokines, thereby regulating the function of these other receptors. Beyond just CCR2, we currently have a relatively poor understanding of the detailed mechanisms underlying how chemokines and their receptors collectively coordinate inflammatory responses and resolution. However, due to CCR2's unique dual G protein-coupled and scavenging functions, its role in both inflammatory and immunosuppressive responses, and its clinical relevancy, determining the mechanisms underlying CCR2 function deserves greater attention.

REFERENCES

1. C. E. Hughes, R. J. B. Nibbs, A guide to chemokines and their receptors. *Febs J.* **285**, 2944–2971 (2018).

2. P. M. Murphy, M. Baggiolini, I. F. Charo, C. A. Hébert, R. Horuk, K. Matsushima, L. H. Miller, J. J. Oppenheim, C. A. Power, International Union of Pharmacology. XXII. Nomenclature for Chemokine Receptors. *Pharmacol. Rev.* **52**, 145–176 (2000).

3. C. Shi, E. G. Pamer, Monocyte recruitment during infection and inflammation. *Nat. Rev. Immunol.* **11**, 762–774 (2011).

4. J. W. Griffith, C. L. Sokol, A. D. Luster, Chemokines and chemokine receptors: positioning cells for host defense and immunity. *Annu. Rev. Immunol.* **32**, 659–702 (2014).

5. F. Melchers, A. G. Rolink, C. Schaniel, The Role of Chemokines in Regulating Cell Migration during Humoral Immune Responses. *Cell*. **99**, 351–354 (1999).

6. D. Malhotra, J. Shin, L. Solnica-Krezel, E. Raz, Spatio-temporal regulation of concurrent developmental processes by generic signaling downstream of chemokine receptors. *eLife*. **7**, e33574 (2018).

7. J. Wang, H. Knaut, Chemokine signaling in development and disease. *Dev. Camb. Engl.* **141**, 4199–4205 (2014).

8. I. F. Charo, R. M. Ransohoff, The Many Roles of Chemokines and Chemokine Receptors in Inflammation. *N. Engl. J. Med.* **354**, 610–621 (2006).

9. Y. Le, Y. Zhou, P. Iribarren, J. Wang, Chemokines and chemokine receptors: their manifold roles in homeostasis and disease. *Cell. Mol. Immunol.* **1**, 95–104 (2004).

10. D. Raman, T. Sobolik-Delmaire, A. Richmond, Chemokines in health and disease. *Exp. Cell Res.* **317**, 575–589 (2011).

11. R. M. Ransohoff, L. Liu, A. E. Cardona, Chemokines and chemokine receptors: multipurpose players in neuroinflammation. *Int. Rev. Neurobiol.* **82**, 187–204 (2007).

12. A. E. I. Proudfoot, Chemokine receptors: multifaceted therapeutic targets. *Nat. Rev. Immunol.* **2**, 106–115 (2002).

13. D. J. Scholten, M. Canals, D. Maussang, L. Roumen, M. J. Smit, M. Wijtmans, C. de Graaf, H. F. Vischer, R. Leurs, Pharmacological modulation of chemokine receptor function. *Br. J. Pharmacol.* **165**, 1617–1643 (2012).

14. B. K. Kobilka, G Protein Coupled Receptor Structure and Activation. *Biochim. Biophys. Acta*. **1768**, 794–807 (2007).

15. W. I. Weis, B. K. Kobilka, The Molecular Basis of G Protein–Coupled Receptor Activation. *Annu. Rev. Biochem.* **87**, 897–919 (2018).

16. R. Fredriksson, M. C. Lagerström, L.-G. Lundin, H. B. Schiöth, The G-protein-coupled receptors in the human genome form five main families. Phylogenetic analysis, paralogon groups, and fingerprints. *Mol. Pharmacol.* **63**, 1256–1272 (2003).

17. V. Syrovatkina, K. O. Alegre, R. Dey, X.-Y. Huang, Regulation, Signaling and Physiological Functions of G-proteins. *J. Mol. Biol.* **428**, 3850–3868 (2016).

18. N. Tuteja, Signaling through G protein coupled receptors. *Plant Signal. Behav.* **4**, 942–947 (2009).

19. J. W. Wisler, H. A. Rockman, R. J. Lefkowitz, Biased G protein-coupled receptor signaling: Changing the paradigm of drug discovery. *Circulation*. **137**, 2315–2317 (2018).

20. P. A. Insel, A. Wilderman, A. C. Zambon, A. N. Snead, F. Murray, N. Aroonsakool, D. S. McDonald, S. Zhou, T. McCann, L. Zhang, K. Sriram, A. M. Chinn, A. V. Michkov, R. M. Lynch, A. C. Overland, R. Corriden, G Protein–Coupled Receptor (GPCR) Expression in Native Cells: "Novel" endoGPCRs as Physiologic Regulators and Therapeutic Targets. *Mol. Pharmacol.* **88**, 181–187 (2015).

21. T. Schöneberg, A. Schulz, H. Biebermann, T. Hermsdorf, H. Römpler, K. Sangkuhl, Mutant G-protein-coupled receptors as a cause of human diseases. *Pharmacol. Ther.* **104**, 173–206 (2004).

22. Y. L. Kasamon, H. Chen, R. A. de Claro, L. Nie, J. Ye, G. M. Blumenthal, A. T. Farrell, R. Pazdur, FDA Approval Summary: Mogamulizumab-kpkc for Mycosis Fungoides and Sézary Syndrome. *Clin. Cancer Res. Off. J. Am. Assoc. Cancer Res.* **25**, 7275–7280 (2019).

23. M. O'Hayre, C. L. Salanga, T. M. Handel, D. J. Hamel, Emerging Concepts and Approaches for Chemokine-Receptor Drug Discovery. *Expert Opin. Drug Discov.* **5**, 1109–1122 (2010).

24. T. J. Schall, A. E. I. Proudfoot, Overcoming hurdles in developing successful drugs targeting chemokine receptors. *Nat. Rev. Immunol.* **11**, 355–363 (2011).

25. C. Murdoch, A. Finn, Chemokine receptors and their role in inflammation and infectious diseases. *Blood*. **95**, 3032–3043 (2000).

26. F. Bachelerie, A. Ben-Baruch, A. M. Burkhardt, C. Combadiere, J. M. Farber, G. J. Graham, R. Horuk, A. H. Sparre-Ulrich, M. Locati, A. D. Luster, A. Mantovani, K. Matsushima, P. M. Murphy, R. Nibbs, H. Nomiyama, C. A. Power, A. E. I. Proudfoot, M. M. Rosenkilde, A. Rot, S. Sozzani, M. Thelen, O. Yoshie, A. Zlotnik, International Union of Basic and Clinical Pharmacology. LXXXIX. Update on the Extended Family of Chemokine Receptors and Introducing a New Nomenclature for Atypical Chemokine Receptors. *Pharmacol. Rev.* **66**, 1–79 (2014).

27. M. C. Miller, K. H. Mayo, Chemokines from a Structural Perspective. *Int. J. Mol. Sci.* **18**, 2088 (2017).

28. K. Bacon, M. Baggiolini, H. Broxmeyer, R. Horuk, I. Lindley, A. Mantovani, K. Maysushima, P. Murphy, H. Nomiyama, J. Oppenheim, A. Rot, T. Schall, M. Tsang, R. Thorpe, J. Van Damme, M. Wadhwa, O. Yoshie, A. Zlotnik, K. Zoon, IUIS/WHO

Subcommittee on Chemokine Nomenclature, Chemokine/chemokine receptor nomenclature. *J. Interferon Cytokine Res. Off. J. Int. Soc. Interferon Cytokine Res.* **22**, 1067–1068 (2002).

29. M. J. Cameron, D. J. Kelvin, *Cytokines, Chemokines and Their Receptors* (Landes Bioscience, 2013; https://www.ncbi.nlm.nih.gov/books/NBK6294/).

30. J. W. Griffith, C. L. Sokol, A. D. Luster, Chemokines and Chemokine Receptors: Positioning Cells for Host Defense and Immunity. *Annu. Rev. Immunol.* **32**, 659–702 (2014).

31. Al-Aoukaty, Rolstad, Giaid, Maghazachi, MIP-3α, MIP-3β and fractalkine induce the locomotion and the mobilization of intracellular calcium, and activate the heterotrimeric G proteins in human natural killer cells. *Immunology*. **95**, 618–624 (1998).

32. H. Arai, I. F. Charo, Differential regulation of G-protein-mediated signaling by chemokine receptors. *J. Biol. Chem.* **271**, 21814–21819 (1996).

33. S. L. Ritter, R. A. Hall, Fine-tuning of GPCR activity by receptor-interacting proteins. *Nat. Rev. Mol. Cell Biol.* **10**, 819–830 (2009).

34. Common activation mechanism of class A GPCRs | eLife, (available at https://elifesciences.org/articles/50279).

35. W. M. Oldham, H. E. Hamm, Heterotrimeric G protein activation by G-protein-coupled receptors. *Nat. Rev. Mol. Cell Biol.* **9**, 60–71 (2008).

36. J. A. Pitcher, N. J. Freedman, R. J. Lefkowitz, G protein-coupled receptor kinases. *Annu. Rev. Biochem.* **67**, 653–692 (1998).

37. C. Ribas, P. Penela, C. Murga, A. Salcedo, C. García-Hoz, M. Jurado-Pueyo, I. Aymerich, F. Mayor, The G protein-coupled receptor kinase (GRK) interactome: Role of GRKs in GPCR regulation and signaling. *Biochim. Biophys. Acta BBA - Biomembr.* **1768**, 913–922 (2007).

38. K. Touhara, J. Inglese, J. A. Pitcher, G. Shaw, R. J. Lefkowitz, Binding of G protein beta gamma-subunits to pleckstrin homology domains. *J. Biol. Chem.* **269**, 10217–10220 (1994).

39. W. J. Koch, J. Inglese, W. C. Stone, R. J. Lefkowitz, The binding site for the beta gamma subunits of heterotrimeric G proteins on the beta-adrenergic receptor kinase. *J. Biol. Chem.* **268**, 8256–8260 (1993).

40. R. H. Stoffel, R. R. Randall, R. T. Premont, R. J. Lefkowitz, J. Inglese, Palmitoylation of G protein-coupled receptor kinase, GRK6. Lipid modification diversity in the GRK family. *J. Biol. Chem.* **269**, 27791–27794 (1994).

41. X. Jiang, J. L. Benovic, P. B. Wedegaertner, Plasma Membrane and Nuclear Localization of G Protein–coupled Receptor Kinase 6A. *Mol. Biol. Cell.* **18**, 2960–2969 (2007).

42. J. A. Pitcher, Z. L. Fredericks, W. C. Stone, R. T. Premont, R. H. Stoffel, W. J. Koch, R. J. Lefkowitz, Phosphatidylinositol 4,5-Bisphosphate (PIP2)-enhanced G Protein-coupled Receptor Kinase (GRK) Activity: LOCATION, STRUCTURE, AND REGULATION OF THE PIP2 BINDING SITE DISTINGUISHES THE GRK SUBFAMILIES*. *J. Biol. Chem.* **271**, 24907–24913 (1996).

43. M. M. Thiyagarajan, R. P. Stracquatanio, A. N. Pronin, D. S. Evanko, J. L. Benovic, P. B. Wedegaertner, A Predicted Amphipathic Helix Mediates Plasma Membrane Localization of GRK5*. *J. Biol. Chem.* **279**, 17989–17995 (2004).

44. V. V. Gurevich, E. V. Gurevich, The structural basis of arrestin-mediated regulation of G-protein-coupled receptors. *Pharmacol. Ther.* **110**, 465–502 (2006).

45. E. V. Gurevich, V. V. Gurevich, Arrestins: ubiquitous regulators of cellular signaling pathways. *Genome Biol.* **7**, 236 (2006).

46. H. Attramadal, J. L. Arriza, C. Aoki, T. M. Dawson, J. Codina, M. M. Kwatra, S. H. Snyder, M. G. Caron, R. J. Lefkowitz, Beta-arrestin2, a novel member of the arrestin/beta-arrestin gene family. *J. Biol. Chem.* **267**, 17882–17890 (1992).

47. C. M. Craft, D. H. Whitmore, A. F. Wiechmann, Cone arrestin identified by targeting expression of a functional family. *J. Biol. Chem.* **269**, 4613–4619 (1994).

48. M. J. Lohse, J. L. Benovic, J. Codina, M. G. Caron, R. J. Lefkowitz, β-Arrestin: a Protein that Regulates β-adrenergic Receptor Function. *Science*. **248**, 1547–1550 (1990).

49. A. Murakami, T. Yajima, H. Sakuma, M. J. McLaren, G. Inana, X-Arrestin: a new retinal arrestin mapping to the X chromosome. *FEBS Lett.* **334**, 203–209 (1993).

50. R. H. Oakley, S. A. Laporte, J. A. Holt, L. S. Barak, M. G. Caron, Association of beta-arrestin with G protein-coupled receptors during clathrin-mediated endocytosis dictates the profile of receptor resensitization. *J. Biol. Chem.* **274**, 32248–32257 (1999).

51. H. W. Zimmermann, V. Sterzer, H. Sahin, CCR1 and CCR2 antagonists. *Curr. Top. Med. Chem.* **14**, 1539–1552 (2014).

52. T. O'Connor, L. Borsig, M. Heikenwalder, CCL2-CCR2 Signaling in Disease Pathogenesis. *Endocr. Metab. Immune Disord. Drug Targets*. **15**, 105–118 (2015).

53. M. Struthers, A. Pasternak, CCR2 antagonists. *Curr. Top. Med. Chem.* **10**, 1278–1298 (2010).

54. J. E. Pease, R. Horuk, Chemokine receptor antagonists: Part 1. *Expert Opin. Ther. Pat.* **19**, 39–58 (2009).

55. J. E. Pease, R. Horuk, Chemokine receptor antagonists: part 2. *Expert Opin. Ther. Pat.* **19**, 199–221 (2009).

56. C. N. França, M. C. O. Izar, M. N. S. Hortêncio, J. B. do Amaral, C. E. S. Ferreira, I. D. Tuleta, F. A. H. Fonseca, Monocyte subtypes and the CCR2 chemokine receptor in cardiovascular disease. *Clin. Sci. Lond. Engl. 1979.* **131**, 1215–1224 (2017).

57. K. Yumimoto, S. Sugiyama, K. Mimori, K. I. Nakayama, Potentials of C-C motif chemokine 2-C-C chemokine receptor type 2 blockers including propagermanium as anticancer agents. *Cancer Sci.* **110**, 2090–2099 (2019).

58. X. Zhang, X. Qin, C. Y. Qin, Y. Yin, Y. Chen, H. Zhu, Expression of monocyte chemoattractant protein-1 and CC chemokine receptor 2 in non-small cell lung cancer and its significance. *Cancer Immunol. Immunother. CII*. **62**, 563–570 (2013).

59. B. B. Moore, R. Paine, P. J. Christensen, T. A. Moore, S. Sitterding, R. Ngan, C. A. Wilke, W. A. Kuziel, G. B. Toews, Protection from pulmonary fibrosis in the absence of CCR2 signaling. *J. Immunol. Baltim. Md 1950*. **167**, 4368–4377 (2001).

60. I. Bot, N. V. Ortiz Zacarías, W. E. A. de Witte, H. de Vries, P. J. van Santbrink, D. van der Velden, M. J. Kröner, D.-J. van der Berg, D. Stamos, E. C. M. de Lange, J. Kuiper, A. P. IJzerman, L. H. Heitman, A novel CCR2 antagonist inhibits atherogenesis in apoE deficient mice by achieving high receptor occupancy. *Sci. Rep.* **7**, 52 (2017).

61. Charo Israel F., Blinding the Monocytes to Protect the Heart. *Circulation*. **127**, 2006–2008 (2013).

62. T. Sullivan, Z. Miao, D. J. Dairaghi, A. Krasinski, Y. Wang, B. N. Zhao, T. Baumgart, L. S. Ertl, A. Pennell, L. Seitz, J. Powers, R. Zhao, S. Ungashe, Z. Wei, L. Boring, C.-L. Tsou, I. Charo, R. D. Berahovich, T. J. Schall, J. C. Jaen, CCR2 antagonist CCX140-B provides renal and glycemic benefits in diabetic transgenic human CCR2 knockin mice. *Am. J. Physiol. - Ren. Physiol.* **305**, F1288–F1297 (2013).

63. M. Jamal-Hanjani, G. A. Wilson, N. McGranahan, N. J. Birkbak, T. B. K. Watkins, S. Veeriah, S. Shafi, D. H. Johnson, R. Mitter, R. Rosenthal, M. Salm, S. Horswell, M.

Escudero, N. Matthews, A. Rowan, T. Chambers, D. A. Moore, S. Turajlic, H. Xu, S.-M. Lee, M. D. Forster, T. Ahmad, C. T. Hiley, C. Abbosh, M. Falzon, E. Borg, T. Marafioti, D. Lawrence, M. Hayward, S. Kolvekar, N. Panagiotopoulos, S. M. Janes, R. Thakrar, A. Ahmed, F. Blackhall, Y. Summers, R. Shah, L. Joseph, A. M. Quinn, P. A. Crosbie, B. Naidu, G. Middleton, G. Langman, S. Trotter, M. Nicolson, H. Remmen, K. Kerr, M. Chetty, L. Gomersall, D. A. Fennell, A. Nakas, S. Rathinam, G. Anand, S. Khan, P. Russell, V. Ezhil, B. Ismail, M. Irvin-Sellers, V. Prakash, J. F. Lester, M. Kornaszewska, R. Attanoos, H. Adams, H. Davies, S. Dentro, P. Taniere, B. O'Sullivan, H. L. Lowe, J. A. Hartley, N. Iles, H. Bell, Y. Ngai, J. A. Shaw, J. Herrero, Z. Szallasi, R. F. Schwarz, A. Stewart, S. A. Quezada, J. Le Quesne, P. Van Loo, C. Dive, A. Hackshaw, C. Swanton, Tracking the Evolution of Non–Small-Cell Lung Cancer. *N. Engl. J. Med.* **376**, 2109–2121 (2017).

64. D. de Zeeuw, P. Bekker, E. Henkel, C. Hasslacher, I. Gouni-Berthold, H. Mehling, A. Potarca, V. Tesar, H. J. L. Heerspink, T. J. Schall, CCX140-B Diabetic Nephropathy Study Group, The effect of CCR2 inhibitor CCX140-B on residual albuminuria in patients with type 2 diabetes and nephropathy: a randomised trial. *Lancet Diabetes Endocrinol.* **3**, 687–696 (2015).

65. T. M. Nywening, A. Wang-Gillam, D. E. Sanford, B. A. Belt, R. Z. Panni, B. M. Cusworth, A. T. Toriola, R. K. Nieman, L. A. Worley, M. Yano, K. J. Fowler, A. C. Lockhart, R. Suresh, B. R. Tan, K.-H. Lim, R. C. Fields, S. M. Strasberg, W. G. Hawkins, D. G. DeNardo, S. P. Goedegebuure, D. C. Linehan, Targeting tumour-associated macrophages with CCR2 inhibition in combination with FOLFIRINOX in patients with borderline resectable and locally advanced pancreatic cancer: a single-centre, open-label, dose-finding, non-randomised, phase 1b trial. *Lancet Oncol.* **17**, 651–662 (2016).

66. D. Linehan, M. S. Noel, A. F. Hezel, A. Wang-Gillam, F. Eskens, S. Sleijfer, I. M. E. Desar, F. Erdkamp, J. Wilmink, J. Diehl, A. Potarca, N. Zhao, S. Miao, J. Deng, J. Hillson, P. Bekker, T. J. Schall, R. Singh, Overall survival in a trial of orally administered CCR2 inhibitor CCX872 in locally advanced/metastatic pancreatic cancer: Correlation with blood monocyte counts. *J. Clin. Oncol.* **36**, 92–92 (2018).

67. M. Vilums, A. J. M. Zweemer, Z. Yu, H. de Vries, J. M. Hillger, H. Wapenaar, I. A. E. Bollen, F. Barmare, R. Gross, J. Clemens, P. Krenitsky, J. Brussee, D. Stamos, J. Saunders, L. H. Heitman, A. P. IJzerman, Structure–Kinetic Relationships—An Overlooked Parameter in Hit-to-Lead Optimization: A Case of Cyclopentylamines as Chemokine Receptor 2 Antagonists. *J. Med. Chem.* **56**, 7706–7714 (2013).

68. S. L. Friedman, B. A. Neuschwander-Tetri, M. Rinella, A. J. Sanyal, Mechanisms of NAFLD development and therapeutic strategies. *Nat. Med.* **24**, 908–922 (2018).

69. B. N. Zhao, J. J. Campbell, C. L. Salanga, L. S. Ertl, Y. Wang, S. Yau, T. Dang, Y. Zeng, J. P. McMahon, A. Krasinski, P. Zhang, I. Kufareva, T. M. Handel, I. F. Charo, R. Singh, T. J. Schall, CCR2-Mediated Uptake of Constitutively Produced CCL2: A

Mechanism for Regulating Chemokine Levels in the Blood. *J. Immunol. Baltim. Md 1950*. **203**, 3157–3165 (2019).

70. S. Volpe, E. Cameroni, B. Moepps, S. Thelen, T. Apuzzo, M. Thelen, CCR2 acts as scavenger for CCL2 during monocyte chemotaxis. *PloS One*. **7**, e37208 (2012).

71. S. L. Deshmane, S. Kremlev, S. Amini, B. E. Sawaya, Monocyte Chemoattractant Protein-1 (MCP-1): An Overview. *J. Interferon Cytokine Res.* **29**, 313–326 (2009).

72. J. Gilbert, J. Lekstrom-Himes, D. Donaldson, Y. Lee, M. Hu, J. Xu, T. Wyant, M. Davidson, MLN1202 Study Group, Effect of CC chemokine receptor 2 CCR2 blockade on serum C-reactive protein in individuals at atherosclerotic risk and with a single nucleotide polymorphism of the monocyte chemoattractant protein-1 promoter region. *Am. J. Cardiol.* **107**, 906–911 (2011).

73. M. V. Perez-Gomez, M. D. Sanchez-Niño, A. B. Sanz, B. Zheng, C. Martín-Cleary, M. Ruiz-Ortega, A. Ortiz, B. Fernandez-Fernandez, Targeting inflammation in diabetic kidney disease: early clinical trials. *Expert Opin. Investig. Drugs*. **25**, 1045–1058 (2016).

74. C. E. Vergunst, D. M. Gerlag, L. Lopatinskaya, L. Klareskog, M. D. Smith, F. van den Bosch, H. J. Dinant, Y. Lee, T. Wyant, E. W. Jacobson, D. Baeten, P. P. Tak, Modulation of CCR2 in rheumatoid arthritis: a double-blind, randomized, placebo-controlled clinical trial. *Arthritis Rheum.* **58**, 1931–1939 (2008).

75. T. M. Nywening, A. Wang-Gillam, D. E. Sanford, B. A. Belt, R. Z. Panni, B. M. Cusworth, A. T. Toriola, R. K. Nieman, L. A. Worley, M. Yano, K. J. Fowler, A. C. Lockhart, R. Suresh, B. R. Tan, K.-H. Lim, R. C. Fields, S. M. Strasberg, W. G. Hawkins, D. G. DeNardo, S. P. Goedegebuure, D. C. Linehan, Targeting tumour-associated macrophages with CCR2 inhibition in combination with FOLFIRINOX in patients with borderline resectable and locally advanced pancreatic cancer: a single-centre, open-label, dose-finding, non-randomised, phase 1b trial. *Lancet Oncol.* **17**, 651–662 (2016).

76. R. J. Aiello, B. D. Perry, P.-A. Bourassa, A. Robertson, W. Weng, D. R. Knight, A. H. Smith, K. S. Frederick, A. Kalgutkar, R. P. Gladue, CCR2 receptor blockade alters blood monocyte subpopulations but does not affect atherosclerotic lesions in apoE(-/-) mice. *Atherosclerosis*. **208**, 370–375 (2010).

77. C. McManus, J. W. Berman, F. M. Brett, H. Staunton, M. Farrell, C. F. Brosnan, MCP-1, MCP-2 and MCP-3 expression in multiple sclerosis lesions: an immunohistochemical and in situ hybridization study. *J. Neuroimmunol.* **86**, 20–29 (1998).

78. E. Prat, P. Baron, L. Meda, E. Scarpini, D. Galimberti, G. Ardolino, A. Catania, G. Scarlato, The human astrocytoma cell line U373MG produces monocyte chemotactic

protein (MCP)-1 upon stimulation with beta-amyloid protein. *Neurosci. Lett.* **283**, 177–180 (2000).

79. S. Singh, D. Anshita, V. Ravichandiran, MCP-1: Function, regulation, and involvement in disease. *Int. Immunopharmacol.* **101**, 107598 (2021).

80. X.-W. Yang, X.-S. Wang, F.-B. Cheng, F. Wang, L. Wan, F. Wang, H.-X. Huang, Elevated CCL2/MCP-1 Levels are Related to Disease Severity in Postmenopausal Osteoporotic Patients. *Clin. Lab.* **62**, 2173–2181 (2016).

81. A. Rogic, I. Pant, L. Grumolato, R. Fernandez-Rodriguez, A. Edwards, S. Das, A. Sun, S. Yao, R. Qiao, S. Jaffer, R. Sachidanandam, G. Akturk, R. Karlic, M. Skobe, S. A. Aaronson, High endogenous CCL2 expression promotes the aggressive phenotype of human inflammatory breast cancer. *Nat. Commun.* **12**, 6889 (2021).

82. J. Charles A Janeway, P. Travers, M. Walport, M. J. Shlomchik, Principles of innate and adaptive immunity. *Immunobiol. Immune Syst. Health Dis. 5th Ed.* (2001) (available at https://www.ncbi.nlm.nih.gov/books/NBK27090/).

83. M. A. Sugimoto, L. P. Sousa, V. Pinho, M. Perretti, M. M. Teixeira, Resolution of Inflammation: What Controls Its Onset? *Front. Immunol.* **7** (2016) (available at https://www.frontiersin.org/articles/10.3389/fimmu.2016.00160).

84. R. Bonecchi, G. J. Graham, Atypical Chemokine Receptors and Their Roles in the Resolution of the Inflammatory Response. *Front. Immunol.* **7** (2016) (available at https://www.frontiersin.org/articles/10.3389/fimmu.2016.00224).

85. M. H. Ulvmar, E. Hub, A. Rot, Atypical chemokine receptors. *Exp. Cell Res.* **317**, 556–568 (2011).

86. C. Tobia, P. Chiodelli, A. Barbieri, S. Buraschi, E. Ferrari, S. Mitola, G. Borsani, J. Guerra, M. Presta, Atypical Chemokine Receptor 3 Generates Guidance Cues for CXCL12-Mediated Endothelial Cell Migration. *Front. Immunol.* **10** (2019) (available at https://www.frontiersin.org/articles/10.3389/fimmu.2019.01092).

87. B. Boldajipour, H. Mahabaleshwar, E. Kardash, M. Reichman-Fried, H. Blaser, S. Minina, D. Wilson, Q. Xu, E. Raz, Control of chemokine-guided cell migration by ligand sequestration. *Cell*. **132**, 463–473 (2008).

88. A. E. Cardona, M. E. Sasse, L. Liu, S. M. Cardona, M. Mizutani, C. Savarin, T. Hu, R. M. Ransohoff, Scavenging roles of chemokine receptors: chemokine receptor deficiency is associated with increased levels of ligand in circulation and tissues. *Blood*. **112**, 256–263 (2008).

CHAPTER 2

Title: The dual function chemokine receptor, CCR2, drives migration and chemokine scavenging by distinct mechanisms

Authors: Thomas M. Shroka[1,2], Irina Kufareva[2], Catherina L. Salanga[2], Tracy M. Handel[2*]

Affiliations:

[1]Biomedical Sciences Program, School of Medicine, University of California San Diego, La Jolla, CA 92093, USA.

[2]Skaggs School of Pharmacy and Pharmaceutical Sciences, University of California San Diego, La Jolla, CA 92093, USA.

*Corresponding author. Email: thandel@health.ucsd.edu

Abstract: The G protein-coupled C-C chemokine receptor 2 (CCR2) is a key driver of monocyte infiltration into tissues following gradients of chemokine during acute and chronic inflammation. However, it also functions as a scavenger receptor whereby it sequesters chemokine from the extracellular environment. Historically, scavenging has been described for atypical chemokine receptors (ACKRs) that themselves do not signal through G proteins but instead control chemokine availability for other G protein-coupled chemokine receptors (GPCRs). By regulating chemokine levels, scavenging contributes indirectly to cell migration, resolution of inflammatory responses, and prevents down-regulation of canonical

GPCRs. Thus, CCR2 is a dual function receptor that drives chemotaxis via G protein-dependent signaling, and scavenges chemokine by mechanisms that are currently unknown. To determine if scavenging is regulated by common GPCR mediators, we used CRISPR knockout cell lines coupled with a panel of cell-based assays and fluorescence microscopy. Here we show that CCR2 scavenges by constitutively internalizing to remove chemokine from the extracellular space and recycles back to the cell surface for further rounds of ligand consumption. This process occurs in a manner independent of G proteins, G protein receptor kinases, β-arrestins, or clathrin, suggesting a functional population that works by non-canonical mechanisms. The mechanism is distinct from "professional" scavenger receptors like ACKR3, where GRKs and/or β-arrestins have been shown to play a role. These findings set the stage for understanding the molecular regulators that dictate CCR2 scavenging versus migration and may have implications for drug discovery targeting this therapeutically important receptor.

One Sentence Summary: In addition to its role in driving G protein-dependent cell migration, the chemoattractant receptor CCR2 scavenges chemokine by constitutively internalizing with ligand and rapidly recycling to the cell surface in a manner independent of G proteins and other canonical regulators of GPCRs.

INTRODUCTION

Chemokine receptors belong to a family of transmembrane proteins that control the migration of many different cell types, particularly leukocytes, in response to specific chemokine ligands. Upon binding chemokine, most of these receptors couple to the Gi class

of heterotrimeric G proteins, which in turn activate the cell motility machinery. While most chemokine receptors are G protein-coupled receptors (GPCRs), four receptors are referred to as atypical chemokine receptors (ACKRs) because they don't couple to G proteins or directly mediate cell migration (*1*). Instead, some of these ACKRs (ACKR2, ACKR3, and ACKR4) scavenge chemokines to regulate extracellular ligand concentrations, which maintains the responsiveness of canonical G protein-coupled chemokine receptors that share the same ligand(s) (*2*). For example, proper migration and positioning of cortical interneurons not only requires CXCR4, which is directly responsible for driving neuronal migration towards CXCL12, but also ACKR3, which scavenges CXCL12; in the absence of ACKR3-mediated CXCL12 scavenging, CXCR4-mediated migration is markedly defective due to overstimulation and downregulation of CXCR4 (*3*). Other data suggests that chemokine uptake by atypical receptors also contributes to the resolution phase of inflammatory responses and the creation of chemokine gradients that promote leukocyte migration and extravasation (*2*, *4–8*).

Scavenging is not restricted to atypical receptors, however. Early receptor knockout studies of canonical chemokine receptors (CCR2, CXCR2, CXCR3 and CX3CR1) revealed elevated plasma levels of their cognate chemokines, suggestive of a chemokine-removal mechanism mediated by these receptors (*9*). CCR2, a key regulator of monocyte migration, was later confirmed as a scavenger receptor (*10, 11*) and in one study was shown to scavenge more efficiently than the atypical receptor ACKR2 (*6*). Thus, CCR2 is a dual function receptor that directly regulates both cell migration and scavenging, in contrast to

professional scavenger receptors that cooperate with canonical GPCRs to facilitate migration.

For both atypical and canonical receptors, scavenging involves internalization and recycling of the receptor with concomitant clearance of the ligand from the extracellular space. However, knowledge of the detailed interactions and pathways that regulate scavenging is sparse and at times contradictory. In this study, we therefore investigated the molecular mechanisms by which CCR2 scavenges, focusing on the role of intracellular proteins usually associated with GPCR function and internalization. Our data suggests that in addition to the well-known canonical G protein-dependent receptor population that controls migration, a second functional population scavenges CCL2 in a manner independent of G proteins, GRKs, arrestins and clathrin; it also accounts for the largest proportion of chemokine removed from the extracellular space by CCR2. This scavenging receptor population operates by constitutively internalizing and recycling through mechanisms that have yet to be defined. In contrast with CCR2, we also show that CCR1, another G protein-coupled receptor on monocytes that scavenges chemokine, does so in a G protein-independent but β-arrestin-dependent manner. This suggests that different mechanisms may be operative for different receptors, possibly to avoid pathway competition in the context of inflammatory situations and complex chemokine stimuli. CCR2 (and CCR1) have been pursued as targets for inflammatory diseases (*12*) and the presence of a scavenging population may affect the efficacy of antagonists directed against these receptors, warranting an understanding of the mechanisms.

RESULTS

Internalization and chemokine scavenging by CCR2 occurs independent of Gα proteins

Like canonical chemokine receptors, CCR2 requires the activation of Gαiβγ heterotrimers as the first step in a cascade of events that regulate cell migration. Subsequent interactions are less well understood but are assumed to involve common mechanisms associated with GPCR signaling. This includes phosphorylation of the receptor C-terminus by G protein receptor kinases (GRKs); specifically, GRK2 and GRK3 have been shown to follow agonist stimulation and result in CCR2 desensitization (*13*). β-arrestin recruitment is then triggered by CCR2 phosphorylation (*14–17*), and as for many GPCRs, implicated in the internalization of the receptor (*18, 19*). We sought to systematically investigate if and how these mediators (G proteins, GRKs and β-arrestin) contribute to internalization and scavenging by CCR2, starting with G proteins.

In contrast to CCR2-mediated cell migration, previous studies have shown that scavenging by CCR2 is Gi-independent by pharmacological inhibition using Pertussis Toxin (PTx) (*10, 11*). Using CRISPR knockout (KO) of G proteins in human embryonic kidney (HEK) 293 cell lines, scavenging was also shown to be independent of $G\alpha_{q/11}$ which couples to CCR2 (*10*, *11*, *20*). However, because Gαi and $G\alpha_{q/11}$ were assessed individually, which could lead to compensation effects, and other Gα protein subtypes have not been tested, we conducted additional studies with CRISPR KO cell lines of Gαi (Gαi KO) or all Gα proteins (Gα_all KO) (*21*). For these experiments, CCL2 was incubated with the indicated CCR2-expressing KO cell line and the amount of CCL2 remaining in the media after 16 h was quantified by

ELISA. As shown in **Fig. 2.1A**, the ability of CCR2 to scavenge CCL2 was perturbed only slightly in the Gα_all KO cells and even less so in Gαi KO cells compared to the parental (WT) HEK293 cells. As discussed later, we interpret the slight reduction in the clearance of CCL2 from the media in the Gα_all KO cells to be due to a slight contribution from Gαi and some other G protein (likely $G\alpha_{q/11}$) due to the canonical G protein-dependent population, which by default internalizes some chemokine along with the receptor. However, the bulk of chemokine scavenged was not dependent on G proteins, which is consistent with prior work (*10*, *11*).

β-arrestin1 and β-arrestin2 were previously reported to associate with CCR2 following stimulation with agonist in a manner partially dependent on Gαi (*19*). Since β-arrestin is often involved in receptor internalization and receptor internalization is critical for chemokine scavenging, we extended these studies to examine CCL2-triggered β-arrestin recruitment to the plasma membrane (PM) in Gαi KO and Gα_all KO HEK293 cells. To monitor β-arrestin trafficking/translocation, we used enhanced bystander bioluminescence resonance energy transfer (ebBRET) between RlucII-tagged β-arrestin1/2 and fluorescently (rGFP) tagged PM marker bound CAAX (*22*). The advantage of this ebBRET assay is that it allows the use of WT CCR2 without any C-terminal tags, which can potentially affect receptor trafficking and/or interactions. As shown in **Fig. 2.1, B** and **C**, recruitment of both β-arrestin1 and 2 was significantly diminished in the absence of Gαi and almost completely lost when all Gα proteins were absent. This is likely due to the loss of GRK2- and GRK3-mediated phosphorylation of the receptor C-terminus. Both kinases contain pleckstrin homology (PH) domains and because their recruitment to the PM depends on the binding of

this domain to active Gβγ (*23*, *24*), phosphorylation is expected to be significantly diminished in G protein KO cells (*13*). Similar results were also observed by BRET with direct recruitment of GFP10-β-arrestin to CCR2-RlucII (**fig. 2.S1**).

Since a substantial decrease in β-arrestin recruitment in the absence of G proteins would be expected to impair receptor internalization, we also investigated the ability of CCR2 to internalize in the Gαi and Gα_all KO cells using CCR2-RlucII and rGFP-CAAX BRET pairs. As compared to WT HEK293 cells, Gα KO cells showed only a minor loss of CCL2-induced receptor internalization (**Fig. 2.1D**), which was surprising given the lack of β-arrestin recruitment. Similar results were also observed when using CCR2-RlucII association with early endosome marker rGFP-FYVE as an orthogonal measure of receptor internalization (**fig. 2.S2**). However, we had previously shown that CCR2 also internalizes constitutively in the absence of chemokine (*11*), but these BRET-based methods are not capable of detecting it. This is because processes that occur continuously and effectively at equilibrium, like constitutive internalization, give rise to a baseline BRET state; and it is only after a perturbation, such as ligand addition, that a BRET signal corresponding to a *change* in receptor internalization, can be detected above the baseline (**fig. 2.S3A**). Therefore, to monitor constitutive receptor internalization, another method is required. For this reason, we developed a "pre-label "flow cytometry assay (*11*) in which the receptor at the cell surface is labeled at 4°C, a temperature that is non-permissive to internalization and therefore enables on to quantify the initial level of surface receptor. Upon warming the cells to 37°C (without ligand), constitutive internalization and endocytic trafficking of the receptor resume, and the amount of labeled receptor at the cell surface decreases. The

amount of original (i.e. pre-labeled) receptor *remaining* at the surface can then be detected with a fluorescent secondary antibody (**fig. 2.S3B)**, and loss of receptor due to constitutive internalization quantified by the decrease in fluorescence signal compared to that at 4°C. As shown in **Fig. 2.1E**, constitutive internalization of CCR2 was unaffected by the loss of Gαi or all Gα proteins; in fact if anything, slightly more receptor internalized in the KO cells. Confirmation of G protein-independent receptor internalization was visualized by confocal fluorescence microscopy using surface-labeled SNAP-CCR2 (**Fig. 2.1F**). Taken together, these data suggest that CCR2 internalizes in a ligand-dependent and -independent manner (i.e. constitutively) and scavenges chemokine independent of G proteins, similar to atypical chemokine receptors (*1*).

GRKs and receptor C-terminal phosphorylation are not required for CCR2 internalization and scavenging

Phosphorylation of the C-terminus of agonist stimulated GPCRs is a crucial step in the recruitment of β-arrestins, and often results in arrestin-mediated receptor internalization (*25–27*). Previous studies have suggested that phosphorylation of CCR2 contributes to receptor internalization (*28, 29*), but which GRKs play a role and whether phosphorylation contributes to constitutive as well as agonist-induced internalization is unclear. To address these questions, we conducted receptor internalization and chemokine scavenging experiments in CCR2-expressing HEK293A CRISPR KO cells lacking either GRK2/3, GRK5/6, or GRK2/3/5/6. Using the ELISA assay, we found that while the GRK2/3 cells trended towards reduced scavenging, only the GRK2/3/5/6 KO cell lines showed a reduction that reached significance (**Fig. 2.2A**). However, even in these cells, the difference compared

to CCR2 in the WT cell background was minor. Recruitment of β-arrestins was then assessed by ebBRET (**Fig. 2.2, B** and **C**) and in both the GRK2/3 and GRK2/3/5/6 KO cell lines, a substantial loss of CCL2-mediated β-arrestin recruitment was observed. This is consistent with prior studies indicating GRK2 contributes to CCR2 phosphorylation (*28*). The further decrease in β-arrestin2 recruitment in the GRK2/3/5/6 KO cells indicates that GRK5 and/or 6 has only a minor effect. Finally, we assessed internalization of CCR2 in the absence of GRKs by our BRET and flow cytometry-based approaches. CCL2-dependent internalization was partially decreased in the GRK2/3 KO and almost completely lost in the GRK2/3/5/6 KO cells (**Fig. 2.2D**), whereas constitutive receptor internalization was unaffected (**Fig. 2.2E**). Fluorescence microscopy imaging of CCR2 internalization in the various cell lines also confirmed that constitutive internalization of CCR2 is independent of GRKs (**Fig. 2.2F**).

Although GRKs contribute to the phosphorylation of CCR2, we aimed to determine whether *any* C-terminal phosphorylation is required for chemokine scavenging using a mutant of CCR2 (CCR2-ST/9A) with nine C-terminal serine/threonine residues mutated to alanine. Serine residue Ser^{356} at the extreme C-terminus of CCR2 was left unchanged as it is part of a putative class II PDZ-binding motif, which may be required for receptor trafficking or recycling (*30*, *31*). Moreover, the addition of the S356A mutation to CCR2-ST/9A (CCR2-ST/10A) showed identical behavior to the CCR2-ST/9A mutant (**fig. 2.S4**). Consistent with the GRK KO cells, the CCR2-ST/9A mutant showed only a minor loss of CCL2 scavenging (**Fig. 2.3A**), but a significant loss of β-arrestin recruitment (**Fig. 2.3, B** and **C**) and CCL2-dependent internalization (**Fig. 2.3D**). However, as with the loss of Gα proteins or GRKs,

constitutive internalization of CCR2 was unaffected (**Fig. 2.3, E** and **F**). To ensure the loss of extracellular CCL2 is due to chemokine uptake into the cell and not just binding at the surface, we used fluorescence microscopy to visualize scavenging of CCL2-mCherry. As shown in **fig. 2.S5**, CCL2-mCherry was efficiently scavenged in the absence of GRK2/3/5/6 and C-terminal serine/threonine residues. The combination of these GRK and phosphorylation-mutant results suggest that CCR2 phosphorylation is important for β-arrestin recruitment and canonical ligand-induced internalization but is not required for constitutive internalization and chemokine scavenging. The data also further support the role of constitutive CCR2 internalization in chemokine scavenging.

β-arrestins play a minor role in chemokine scavenging by CCR2

Upon activation and phosphorylation by GRKs, many GPCRs interact with β-arrestins, which mediate internalization by engaging endocytic machinery components such as AP2 and clathrin (*32, 33*). The above data showing the sensitivity of β-arrestin recruitment to the loss of Gα proteins, GRKs and C-terminal phosphorylation suggests a canonical role for β-arrestins in CCR2 function, similar to many GPCRs. Consistent with this, β-arrestin has been reported to be recruited to CCR2 following chemokine stimulation (*19*), as well as involved in receptor desensitization in primary monocytes, where disruption of GRK2-mediated receptor phosphorylation and β-arrestin recruitment leads to increased monocyte migration (*34, 35*). Through their effects on internalization, β-arrestins have also been reported to contribute to chemokine scavenging by atypical receptors ACKR2 (*36*) and ACKR4 (*37*). Similarly, some studies suggest scavenging by ACKR3 is dependent on β-arrestins (*38*), although other reports indicate it is β-arrestin independent (*39, 40*). The

reduction of CCL2-stimulated β-arrestin recruitment but not CCL2 scavenging in the G protein KO, GRK KO, and phosphorylation-mutant experiments reported above suggests that β-arrestins are not necessary for scavenging by CCR2. However, these experiments do not exclude that a constitutive interaction between CCR2 and β-arrestin, not detected in the β-arrestin recruitment assay, plays a role. As a more direct approach, we investigated CCR2-mediated scavenging using an HEK293 cell line in which both β-arrestin1 and 2 were knocked out by CRISPR. As shown in **Figure 2.4A,** the loss of β-arrestin1 and 2 resulted in a small (~19%) but measurable loss of scavenging. Moreover and as shown in **fig. 2.S6**, CCL2-mCherry was efficiently scavenged in the absence of β-arrestin1/2. Knockout of β-arrestin1/2 also led to a complete loss of CCL2-induced receptor internalization (**Fig. 2.4B**), similar to the effects of the GRK2/3/5/6 deletion. However, constitutive receptor internalization was unaffected as determined by flow cytometry (**Fig. 2.4C**) and confirmed by confocal microscopy (**Fig. 2.4D**). We confirmed these observations in a monocytic cell line (THP-1), which endogenously expresses CCR2 but has both β-arrestin1 and β-arrestin2 knocked down by CRISPR (**fig. 2.S7**). As for the CCR2 expressing HEK293 cells, only a small (~19%) reduction in scavenging (**Fig. 2.4E**) as well as an even smaller (~8%) loss of constitutive internalization (**Fig. 2.4F**) was observed.

Previous studies show that loss of GRK2-mediated receptor phosphorylation and β-arrestin recruitment results in increased monocyte migration (*34*, *35*). We therefore tested this in the β-arrestin1/2 KD THP-1 cells and observed a significant increase in migration, but only at CCL2 concentrations of 100 nM and above (**Fig. 2.4G**). This is consistent with the role of β-arrestin in receptor desensitization; however, the lack of increased migration in the β-

arresitn1/2 KD cells at lower, more physiological levels of CCL2 indicates that CCR2 remains responsive even when β-arrestin is present. Together with minor contributions of G proteins and GRKs to scavenging (described above), but their requirement for β-arrestin recruitment, this data suggests that the small role played by β-arrestins in the cellular uptake of chemokine is associated with canonical G protein, GRK, and β-arrestin dependent internalization of CCR2. The data also suggests that constitutive internalization, which appears to play a major role in CCR2-mediated scavenging, is β-arrestin independent.

Chemokine scavenging occurs independent of clathrin-mediated endocytosis

The above data strongly implicate constitutive internalization as a consistent feature of CCR2 scavenging. However, the pathways by which CCR2 (and other chemokine receptors) constitutively internalize are poorly understood. Although clathrin is often involved in canonical ligand-dependent internalization of many GPCRs (*41*), some GPCRs constitutively internalize through clathrin-coated pits independent of phosphorylation and β-arrestin. This has been well documented for protease-activated receptor-1 (PAR1) and the thromboxane-A2β receptor (*42–44*). We therefore evaluated the ability of CCR2 to internalize and scavenge using a dominant-negative form of dynamin-2 (DNM2-K44A) that inhibits clathrin-mediated endocytosis (CME) (*45*). As shown in **Figure 2.5A**, DNM2-K44A had no effect on the ability of CCR2 to scavenge chemokine and only a small effect on constitutive internalization (**Fig. 2.5, B** and **C**). By contrast, CCL2-dependent internalization was shown to be significantly affected by the dominant-negative dynamin mutant (**Fig. 2.5D**) consistent with a canonical mechanism of internalization. This was also assessed by

confocal microscopy using a dynamin inhibitor, Dyngo-4a (*46*), which showed no effect on constitutive internalization (**fig. 2.S8**).

CCR2 undergoes rapid recycling and is resistant to degradation

The above data suggests that CCR2-mediated ligand scavenging is robust and largely unaffected by perturbations of mediators frequently associated with GPCR function. To further probe CCR2 scavenging mechanisms, we investigated its endosomal trafficking patterns in comparison to the scavenging receptor ACKR3 (*47*, *48*) and the non-scavenging receptor CXCR4 (*11*). BRET experiments were conducted using C-terminally RlucII-tagged receptors in combination with rGFP-tagged Rab4, Rab11 or Rab7 endosomal markers that represent fast recycling, slow recycling and late endosomal association, respectively (*49*). As shown in **Figure 2.6, A** to **C**, CCR2 rapidly sorted into fast recycling Rab4 endosomes and Rab7 late endosomes but did not associate with slow recycling Rab11 endosomes. Sorting of CCR2 into fast recycling Rab4 endosomes was more extensive and sustained compared to the atypical scavenging receptor ACKR3, which sorted more into slow recycling endosomes. Additionally, although Rab7 is generally regarded to be associated with lysosomal degradation, Rab7 is also known to recycle through the trans-golgi network (TGN) (*50–52*). Due to the lack of observed degradation (shown below) we believe CCR2 is trafficking through this TGN recycling pathway. In contrast to CCR2 and ACKR3, the G protein-coupled chemokine receptor, CXCR4, showed minimal association with recycling endosomes, consistent with the fact that it does not scavenge chemokine. Ultimately, these results highlight the general differences between endosomal trafficking patterns observed in chemokine receptor endocytosis.

Using a BRET-based method (*22*), we also demonstrated that CCR2 departs the plasma membrane following chemokine stimulation but robustly recycles back upon chemokine washout (**Fig. 2.6, D** to **F**) or after addition of CCR2 inhibitor BMS681 (**fig. 2.S9**). In fact, compared to the professional scavenger, ACKR3, which also constitutively internalizes and recycles, CCR2 recycles back to the plasma membrane more efficiently. As an orthogonal strategy, we used a surface receptor labeling method, adapted from Montpas et al., 2017 (*39*). Again, this experiment revealed that cell surface CCR2 decreases upon chemokine stimulation but is quickly replenished following CCL2 removal (**Fig. 2.6G**). Finally, although CCR2 associates with Rab7 late endosomes, western blots revealed that the expression level of CCR2 is maintained following CCL2 stimulation, in contrast to the control GPCR, PAR1 (**Fig. 2.6, H** and **I**) which was degraded following agonist addition. These data suggest that CCR2 has distinct trafficking mechanisms compared to other chemokine and non-chemokine receptors, which is not surprising since it functions as both an atypical scavenging receptor and a canonical GPCR. The ability to rapidly recycle and avoid depletion may also contribute to its ability to efficiently scavenge chemokine.

CCR2 and CCR1 have distinct mechanisms of scavenging

CCR1 is another chemokine receptor expressed on monocytes that regulates migration (*53, 54*). We and others previously showed that despite being a G protein-coupled chemokine receptor like CCR2, CCR1 also scavenges chemokine (*55*, *56*). Furthermore, we determined that CCR1 is constitutively phosphorylated, constitutively interacts with β-arrestin2 and constitutively internalizes in a β-arrestin2-dependent manner (*55*). Given that scavenging relies on constitutive internalization, we hypothesized that chemokine scavenging by CCR1

may be β-arrestin-dependent. As shown in **Figure 2.7A**, a major reduction (~54%) of CCL14 scavenging by CCR1 was indeed observed in the β-arrestin KO cells, which contrasts with CCR2 where β-arrestin only plays a minor role in chemokine sequestration (19%).

Given the different β-arrestin dependencies of CCR1 and CCR2, as well as the general role of β-arrestins in receptor desensitization, we also evaluated the impact of the loss of β-arrestin on Gαi activation using Gαi-Nluc and Gβγ-cpVenus in a BRET-based Gαβγ dissociation assay (*37*). In the β-arrestin KO cells, both CCR1 and CCR2 triggered similar, sustained Gαi:Gβγ dissociation upon stimulation with chemokine, as might be expected (**Fig. 2.7, B** and **C**). However, in WT cells, CCR1 quickly activated Gαi, but then Gαi and Gβγ rapidly reassociated, likely because the receptor returns to a state in which it is constitutively phosphorylated and associated with β-arrestin (**Fig. 2.7D**). By contrast, CCR2 has a similar activation profile in the presence or absence of β-arrestin (**Fig. 2.7E**), indicating that β-arrestin mediated desensitization of CCR2 does not occur to the same extent as for CCR1. The prolonged activation of G protein as observed in this assay may reflect the ability of CCR2 to avoid desensitization and/or downregulation (as shown in **Fig. 2.6H**), allowing cells to migrate, even when exposed to high concentrations of chemokine (*10*). Consistent with these findings, activation by the formyl peptide receptor-1 (FPR1) results in heterologous desensitization of CCR1 but not CCR2 (*57*). Comparisons to endosomal trafficking of CCR1 were attempted but proved unsuccessful due to the lack of cell surface expression of C-terminally RlucII-tagged CCR1 (CCR1-RlucII) (**fig. 2.S10**). Together, the results suggest that β-arrestin regulates scavenging and signaling of CCR1 to a

greater extent than CCR2. Moreover, the greater susceptibility of CCR1 to desensitization may reflect a functional hierarchy of these two receptors in monocytes.

DISCUSSION

The physiological importance of clearing circulating chemokines as well as chemokines from tissue microenvironments has been documented most extensively for the atypical chemokine receptors. These receptors work in concert with G protein-coupled chemokine receptors to regulate extracellular chemokine availability in the context of normal immunological responses and inflammatory conditions. However, early chemokine receptor KO studies hinted at a possible role for scavenging by several canonical GPCRs (*9*), which was later validated for CCR1, CCR2 and CCR5 (*2, 10, 11, 55, 56*). In fact, scavenging of chemokine CCL2 by CCR2 was shown to be more efficient than that of the atypical receptor, ACKR2, on the same cell (*58*). In this study we sought to define the mechanisms that regulate CCR2 scavenging as they are poorly understood.

Like most chemokine receptors, CCR2 is a GPCR that activates G proteins, is phosphorylated by GRKs, recruits β-arrestin and is internalized upon agonist stimulation (*13, 19, 29*). However, here we show that in contrast to its function in controlling cell migration, CCR2 robustly scavenges chemokine in a manner that is largely independent of these classical GPCR signaling pathways. We hypothesize that the minor contributions to scavenging from G proteins, GRKs and β-arrestins are attributable to chemokine uptake that occurs by default in the context of canonical GPCR agonist-stimulated pathways. However, the bulk of chemokine scavenging arises from constitutive "passive" internalization of

CCR2 via mediators that have yet to be identified. Thus, CCR2 appears to have two mechanistically distinct functional populations, one that regulates migration and one involved in scavenging (**Fig. 2.8**). Receptor molecules in these populations likely interchange, with constitutively internalized and recycling CCR2 acting as a feeder pathway that provides non-desensitized receptor for persistent CCL2-stimulated cell migration via the canonical signaling pathway. The importance of rapid receptor recycling for continuous CCR2 signaling at the leading edge of monocytes was in fact suggested by Volpe and coworkers to explain the fact that receptor internalization does not reduce the responsiveness of the cells as they migrate towards CCL2 (*10*). The fact that a large population of internalized/recycling CCR2 molecules do not need to be resensitized by dephosphorylation may contribute to the efficiency by which signaling-ready receptor molecules can be replenished at the leading edge of migrating cells from the scavenger pathway.

We originally hypothesized that β-arrestin might be an essential component of CCR2 scavenging because of its common role in receptor internalization. Additionally, previous studies from our lab identified CCR1 as a scavenger that relies on β-arrestin to constitutively internalize (*55*), a key feature of scavenging, and herein we confirm that β-arrestin does indeed play a major role in chemokine sequestration by CCR1. However, unlike CCR1, we found that CCR2 constitutively internalizes in the absence of β-arrestin and that knockout of β-arrestin has only a small impact on scavenging (where its small contribution likely arises from the agonist-stimulated canonical pathway). Consistent with these contrasting dependencies on β-arrestin, CCR2 scavenges largely independent of GRKs and phosphorylation of its C-terminus whereas CCR1 is basally phosphorylated (*55*). Thus, it

appears that different receptors use different mechanisms for scavenging. Since CCR1 and CCR2 are both chemoattractant receptors on monocytes that predominantly scavenge distinct ligands, the use of different scavenging mechanisms might be important for avoiding competition for pathway regulators, which could impair chemokine clearance. CCR2 and CCR1 also differ with respect to the duration of G protein activation, with CCR1-activated G proteins returning more rapidly to an inactive state when β-arrestin is present. The prolonged activation of G proteins following stimulation by CCR2 both in the presence and absence of β-arrestin may reflect its relative functional independence from arrestin.

While CCR2 scavenges chemokine independent of the most common agonist-triggered GPCR internalization mechanisms, constitutive internalization and recycling is crucial. In fact, our previous studies showed that in monocytes, the entire surface population of CCR2 constitutively turns over and is replaced in under 30 minutes (*11*). Accordingly, we investigated the role of clathrin. However, perturbing CME did not inhibit CCR2-mediated chemokine scavenging. β-arrestin often acts as an adapter along with AP-2 to bridge clathrin (*32*, *33*, *59*), and these results are therefore consistent with a lack of a role for β-arrestin in scavenging. Thus future endeavors will be focused on identifying mediators of clathrin-independent endocytosis (CIE). Possibilities include the Rho family cdc42 and Arf family GTPases, which have been identified as regulators of both clathrin- and dynamin-independent internalization pathways and recycling of membrane proteins, including GPCRs. For example, Arf3 has been shown to be required for maintaining the integrity of the recycling endosome (*60*), while other members are involved in CIE (*61–63*). Arf6 has also been shown to be involved in actin cytoskeleton remodeling, phagocytosis and

migration, as well as regulating the recycling of GPCRs, such as the β2-adrenergic receptor (*64–66*). Cdc42 is involved in macropinocytosis and phagocytosis in macrophages and dendritic cells, as well as transmigration of monocytes, all of which express CCR2, and could contribute to its passive scavenging (*67–69*). Pathways involved in the natural turnover of the cell membrane and the constitutive endocytic processes may also play a role (*70*). For example, GPCRs and other membrane proteins can sense and sort according to membrane curvature (*71*). The specific niches in which CCR2 resides within the membrane and its capacity to recycle back to the surface following constitutive endocytosis could influence its ability to scavenge. These pathways are less understood but may involve micro- and macropinocytosis mentioned above, as well as the CLIC-GEEC pathway, and other CME and CIE mechanisms (*72–74*).

In addition to understanding the molecular controls of scavenging, a key question relates to the functional relevance of scavenging by canonical receptors. As suggested above and by Volpe and coworkers (*10*), scavenging may allow cells to continuously migrate by remaining responsive to chemoattractant, which may be particularly important for monocytes during pro-inflammatory immune responses. In the case of CCR2, sustained G protein activation following agonist stimulation (**Fig. 7**) may also contribute to persistent migration, thereby synergizing with scavenging and rapid recycling. Along these lines, peripheral blood mononuclear cells (PBMCs) and peritoneal macrophages from CCR2-KO mice exhibit reduced binding capability and migration to the CCR1 ligand CCL3, but the same susceptibility to desensitization and downregulation is not observed for CCR2 (*9*). However, migration without desensitizing may be inappropriate for certain cell types in

some contexts, explaining why some canonical receptors, like CXCR4, do not scavenge but instead rely on atypical receptors when scavenging is needed. Scavenging by canonical chemokine receptors may also enable migrating cells to create their own chemokine gradients and undergo self-directed migration, or contribute to dampening or terminating the inflammatory response when such a response is no longer needed (*5*, *75–80*). Finally, since some ligands of CCR2 are shared with other chemokine receptors (such as chemokine CCL7 with receptor CCR1), scavenging by CCR2 may impact other chemokine receptors and affect the migration of cells that express both receptors in cis, for example monocytes that express both CCR1 and CCR2, or in trans. Along these lines, desensitization and downregulation of CCR1 has been observed in PBMCs from CCR2-KO mice that fail to scavenge CCR2 ligands (*9*).

A final question is what regulates whether CCR2 scavenges chemokine or is directed into G protein-dependent pathways to promote cell migration, and what determines the balance of scavenging versus migration? Prior studies have shown that treatments mimicking inflammation (LPS or IFNγ plus IL-10) cause monocytes and dendritic cells to switch purely to scavenging by receptors CCR1, CCR2 and CCR5 (*56*). They simultaneously become incapable of promoting cell migration as if uncoupled from G proteins, despite continued cell surface expression of the receptors. This is likely due to inhibition of some component of the cell motility machinery rather than a receptor-specific phenomenon, but whether there are also receptor-specific switches that determine relative amounts of scavenging versus migration remains to be determined. Changes in trafficking patterns could change the balance; for example, the β2 adrenergic and M3 muscarinic receptors are reported to

constitutively internalize via CIE and shift to clathrin-dependent endocytosis after agonist stimulation (*81*).

The scavenging function of chemokine receptors needs to be considered when evaluating the safety and therapeutic efficacy of blocking receptor-ligand binding, especially considering the above potential roles of scavenging. CCR2 is being pursued as a target for a number of diseases (*12*, *82*–89) but inhibition with small molecule antagonists leads to inhibition of scavenging and elevated plasma levels of CCL2 (*90–93*), the consequences of which are unknown (*11*). The presence of elevated levels of chemokine may also compete with receptor antagonists thereby decreasing the efficacy of therapeutic drugs aimed at blocking CCR2-mediated cell migration (*90, 91*). To fully understand the role of scavenging in normal physiology and potential consequences of blocking it, a better understanding of the regulatory mechanisms will be required. This study represents a first step in this direction by demonstrating that CCR2 has two functional populations, one that controls migration through canonical G protein mechanisms and one that controls scavenging through G protein-independent mechanisms. The results also provide a framework for understanding a significant body of prior studies aimed at defining the network of intracellular proteins involved in CCR2 pharmacology.

MATERIALS AND METHODS

Cell lines

All KO and parental (WT) control HEK293 cells were a kind gift of Dr. Asuka Inoue (Tohoku University, Japan). HEK293 cells lacking functional $G\alpha_i$ (Gi KO), or a

combination of $G\alpha_i$, $G\alpha_o$, $G\alpha_q$, $G\alpha_z$, $G\alpha_{olf}$, $G\alpha_{11}$, $G\alpha_s$, $G\alpha_{12}$ and $G\alpha_{13}$ knockouts (ΔGs/i/o/olf/q/z/11/12/13 = G_all KO) were generated by CRISPR/Cas9 as previously reported (*21*, *94*). A dual β-arrestin1 and β-arrestin2 knockout (β-arrestin1/2 KO) was prepared by CRISPR/Cas9 targeting of ARRB1 and ARRB2 as described previously (*95*). Similarly, CRISPR/Cas9 was used to generate GRK2/3 KO, GRK5/6 KO and GRK2/3/5/6 KO in the HEK293A cell line (*96*). THP-1 β-arrestin1/2 KD and corresponding THP-1 neg-gRNA control cells were prepared using lentiCRISPRv2 (*97*), a gift from Dr. Feng Zhang (Broad Institute, MA, USA) and gRNAs generated using CHOPCHOPv3 (*98*). THP-1 β-arrestin1/2 KD was confirmed by western blot (**fig. S6**) using anti-β-arrestin1 (#D8O3J, Cell Signaling Technology, MA, USA), and anti-β-arrestin2 (#C16D9, Cell Signaling Technology, MA, USA) antibodies. Stable chemokine receptor-expressing cells (CCR1 or CCR2) were generated in the HEK293 WT and all KO cell lines by lentiviral transduction using pLenti-CMV-Hygro expression vector, a gift from Eric Campeau & Paul Kaufman (University of Massachusetts Medical School, MA, USA) (*99*) and receptor surface expression confirmed by flow cytometry (Guava EasyCyte™ 8HT, Luminex) with an anti-hCCR2-PE (phycoerythrin) antibody (FAB151P, R&D Systems). Cell lines were cultured in Dulbecco's modified Eagle's medium (DMEM), supplemented with GlutaMax (Gibco) and 10% fetal bovine serum (FBS) and grown at 37°C with 5% CO_2.

DNA plasmids and cloning

The pcDNA3.1(+) constructs of β-arrestin1-RlucII, β-arrestin2-RlucII, rGFP-CAAX, rGFP-Rab4 and rGFP-Rab11 (*22*) were kindly gifted by Dr. Michel Bouvier (Université de Montréal, Canada). The FLAG-PAR1 construct was kindly gifted by Dr. JoAnn Trejo (UC

San Diego, La Jolla, CA, USA). The rGFP-Rab7 construct was generated by PCR amplification of the Rab7 coding sequence of EGFP-Rab7A, a gift from Qing Zhong (UC Berkeley, CA, USA) (*100*) and in-frame insertion into the XbaI and PmeI sites of rGFP-Rab4 by DNA ligation. Receptor-RlucII (CCR2, CXCR4, ACKR3) constructs were created by PCR amplification of the coding region of CCR2, CXCR4 and ACKR3; products were subcloned in-frame at the N-terminus of the RlucII sequence into the pcDNA3.1 RlucII vector. The CCR2-ST/9A (S316A, T324A, T338A, T343A, S344A, T345A, T347A, S349A and T350A) phosphorylation-deficient mutant was created using site-directed mutagenesis with the QuikChange mutagenesis kit (Agilent Technologies, La Jolla, CA, USA). To obtain FLAG-SNAP-CCR2, the coding sequence of pcDNA3.1(+) CCR2 vectors were PCR amplified and then inserted into the pRK5–FLAG-ST–CXCR4 plasmid (*101*), containing a mGlu5 receptor signal peptide (*102*) that promotes proper receptor trafficking to the cell surface (kind gift of Dr. Angélique Levoye, University of Paris, France). Introduction of two gRNA into the lentiCRISPRv2 plasmid for the β-arrestin1/2 KD was performed using the Multiplex CRISPR/Cas9 Assembly System a gift from Dr. Takashi Yamamoto (Hiroshima University, Japan) (*103*), following the Golden Gate assembly method as previously described previously (*104*).

Chemokine scavenging ELISA assay

WT non-receptor-expressing or stable receptor-expressing (CCR1 or CCR2) HEK293 cells and corresponding KO cells were seeded in triplicate in 96-well dishes at 50,000 cells/well and allowed to adhere for ~8 h. Subsequently, media was replaced with DMEM/10% FBS media containing 5 nM CCL2 or CCL14 and incubated for ~16 h. Remaining chemokine

levels in the supernatants of cultured cells were measured in triplicate using commercially available CCL2 and CCL14 Invitrogen™ ELISA kits according to manufacturer's instructions (Fisher Scientific, Hampton, NH, USA) and read with a SpectraMax M5 plate reader (Molecular Devices, Sunnyvale, CA, USA). Remaining levels of exogenous chemokine are reported as the percentage of levels in supernatants of the corresponding non-receptor expressing cells.

BRET assays

HEK293 cells were seeded directly into 96-well plates (20,000 cells per well) and transfected the next day using Mirus TransIT-Lt1 transfection reagent at ~70% confluency. Cells were transfected with a BRET donor (1.2 ng of Receptor-RlucII or 0.72 ng of β-arrestin1- or β-arrestin2-RlucII per well) along with 4.8 ng of BRET acceptor per well (for example, rGFP-CAAX, rGFP-Rab4, rGFP-Rab11 or rGFP-Rab7). All assays were performed ~30 h after transfection, modified from methods as previously described (*22*). Cells were washed once with pre-warmed Tyrode's buffer (140 mM NaCl, 2.7 mM KCl, 1 mM $CaCl_2$, 12 mM $NaHCO_3$, 5.6 mM D-glucose, 0.5 mM $MgCl_2$, 0.37 mM NaH_2PO_4, 25 mM HEPES, pH 7.4), followed by addition of cell-permeable RlucII substrate, Prolume Purple (NanoLight Technologies) at a final concentration of 5 μM, ~3 to 6 min before BRET measurements. Three baseline BRET measurements were performed approximately 1 min apart, followed by the addition of the indicated concentrations of chemokine. Subsequent BRET measurements were taken approximately 1 min apart for 50 min or the indicated times.

For evaluation of receptor recycling to the plasma membrane, cells were seeded onto poly-D-lysine coated 96-well plates and transfected as described above. Following 13 min of chemokine stimulation, cells were washed three times with pre-warmed Tyrode's buffer and subsequent BRET measurements were taken approximately 1 min apart for an additional 25 min. Values are presented as the percentage of mock treated (no ligand) [$(BRET_{ligand}/BRET_{basal}) \times 100$]. All BRET measurements were read using a VictorX Light luminescence reader (Perkin Elmer, Waltham, MA, USA) or Spark microplate reader (Tecan, Männedorf, Switzerland).

Receptor constitutive internalization "pre-label" assay

CCR2 receptor surface expression was determined by a pre-label flow cytometry-based internalization assay (*11*, *55*), which measures the number of labeled CCR2 molecules remaining on the cell surface after 45 min of incubation at 37°C. HEK293 cells stably expressing CCR2 were labeled with mouse anti-hCCR2 antibody (Clone# 48607, R&D Systems) or its isotype-matched control for 30 min on ice and protected from light. Unbound antibody was washed away with wash buffer (PBS, 0.5% bovine serum albumin (BSA)). Cells were then resuspended in Assay Buffer (DMEM, 0.5% BSA) and either held at 4°C (which prevents receptor trafficking and internalization) or transferred to 37°C (which allows for normal receptor trafficking) and incubated for 45 min. After incubation, cells were transferred to wet ice and the remaining surface receptor was labeled with anti-mouse antibody conjugated to PE (Clone# 344701, R&D Systems) for 40 min on ice and protected from light. CCR2 expression was assessed by flow cytometry using a Guava Easycyte™ 8HT flow cytometer (Luminex) and analyzed with FlowJo software (FlowJo, Ashland, OR,

USA). The geometric mean fluorescent intensity of analyzed cells was used to quantify surface expression of CCR2 and compared to non-internalized control to determine relative percent of receptor remaining at the surface.

Receptor constitutive internalization microscopy

Constitutive internalization of CCR2 was qualitatively assessed based on a previously described method (*102*). HEK293 cells or the corresponding KO cell lines expressing FLAG-SNAP-CCR2 or FLAG-SNAP-CCR2-ST/9A were seeded onto fibronectin-coated 10 mm glass-bottom dishes (FluoroDish FD3510, WPI). For cells expressing dynamin-2 dominant negative mutant DNM2-K44A, cells were transfected with DNM2-K44A-EGFP, a kind gift of Dr. Jin Zhang (UC San Diego, La Jolla, CA, USA) and re-seeded 24 h after transfection. The next day, cells were stained with 5 μM cell impermeable SNAP-Surface Alexa Fluor 488 or 647 (New England Biolabs) in complete media (DMEM + 10% FBS) at 4°C in the dark for 45 min. Excess SNAP substrate was removed by washing with ice-cold complete media. Cells were imaged in phenol-red free DMEM media containing 2% FBS at 4°C (prevents receptor trafficking and internalization) or transferred to 37°C for 45 min (allows for normal receptor trafficking) and then imaged on an Eclipse Ti2-E (Nikon) equipped with a CSU-X1 (Yokogawa) spinning disk field scanning confocal system and stage top incubator (Tokai Hit).

SNAP-receptor recycling assay

The ability of CCR2 to recover to the cell surface following internalization was assessed based on a modified method as described (*39*). HEK293 cells stably expressing SNAP-tagged CCR2 were preincubated for 2 h with 5 mg/mL cycloheximide. Cells were then left

untreated or stimulated with 100 nM CCL2 at 37°C for 45 min. Subsequently, cells were washed and remaining non-internalized SNAP-CCR2 at the cell surface was blocked at 4°C with SNAP-Surface block (New England Biolabs) for 45 min. The cells were then washed and shifted to 37°C for 15, 45 or 75 min. Following the specified timepoints, cells were transferred to wet ice and receptors were labeled with SNAP-Surface Alexa Fluor 649 (New England Biolabs) at 4°C. Data is displayed as a percentage of receptor compared to surface receptor measured at the start of the protocol.

Chemotaxis assay

Chemotaxis assays were carried out by using Transwell chemotaxis chambers (Corning Inc., Corning, New York, USA). Cells were harvested by centrifugation and resuspended in complete media, Roswell Park Memorial Institute 1640 (RPMI) + 10% FBS, at a density of 6.6×10^5 cells/ml. Various concentrations of CCL2 was added to the bottom of the chambers and covered with a 5-μm pore-sized polycarbonate membrane filter while 5×10^4 cells were added to the top of the filter. After 2 h incubation at 37°C, media containing migrated cells was removed from the bottom chamber and cells were counted by flow cytometry using a Guava Easycyte™ 8HT flow cytometer (Luminex) and analyzed with FlowJo software (FlowJo, Ashland, OR, USA). Data is presented as percentage of migrated cells compared to initial number of cells added before migration.

Receptor degradation assay

CCR2 degradation was assessed as described previously described (*105*). HEK293 cells were seeded in 12-well dishes (1.5×10^5 cells/well) and transfected the next day with either FLAG-CCR2 or FLAG-PAR1 using Mirus TransIT-Lt1 transfection reagent. After 48 h,

cells were treated with 10 µg/mL cycloheximide for 90 min at 37°C. Cells were then incubated in the same media with or without 100 nM CCL2 or 100 µM TFLLRN (PAR1-specific agonist) for 2 h at 37°C. Cells were placed on ice, washed with PBS, and lysed in RIPA lysis buffer (Thermo Fisher Scientific) containing cOmplete™, Mini, EDTA-free Protease Inhibitor Cocktail (Roche). Cell lysates were collected and rotated end-over-end for 1 h at 4°C, and protein concentrations were determined by Pierce™ Rapid Gold bicinchoninic acid (BCA) assay (Thermo Fisher Scientific). Equivalent amounts of lysates were used for immunoprecipitation (IP) using M2 anti-FLAG affinity resin (Millipore Sigma) according to the manufacturer's instructions. Equivalent volumes of IP elution and equal amounts of lysates were resolved by SDS-PAGE and transferred to nitrocellulose membrane (Bio-Rad). Membranes were blocked with 5% nonfat dry milk (Bio-Rad) diluted in wash buffer (50 mm Tris-HCl, pH 7.4, 15 mm NaCl, 0.1% Tween 20) and subsequently washed. IP elution western blots were incubated overnight at 4°C with anti-FLAG antibody (F4725, Millipore Sigma) diluted in TBS containing 5% BSA and lysate blots were incubated overnight at 4°C with anti-α-Tubulin (T6074, Millipore Sigma). Membranes were subsequently washed and probed with corresponding secondary IRDye® 800CW antibody (LI-COR Biosciences) diluted in TBS containing 5% BSA at room temperature for 1 h. Membranes were then washed and imaged on an Odyssey Infrared Imaging System (LI-COR Biosciences). Densitometry was performed using LI-COR Image Studio software.

G protein dissociation assay

HEK293 cells and corresponding KO cells stably expressing CCR1 or CCR2 were seeded directly into 96-well plates (20,000 cells/well) and transfected the next day with pIRES Gα-

Nluc Gβγ-cpVenus, a kind gift from Dr. Daniel Legler (University of Konstanz, Germany) using Mirus TransIT-Lt1 transfection reagent with cells at ~70% confluency (*37*). After ~30 h, cells were washed once with pre-warmed Tyrode's buffer followed by addition of 5 μM luciferase substrate coelenterazine-H (Biotium, CA, USA). Three baseline BRET measurements were performed approximately 1 min apart, followed by addition of indicated concentrations of chemokine ligand and subsequent BRET measurements were taken approximately 1 min apart for 25 min or indicated times.

Statistics

All data points are the mean ± SEM of at least three independent experiments. All data were analyzed using GraphPad Prism with statistically significant differences ($P < 0.05$) using one-way ANOVAs with Dunnett's multiple comparison post hoc test or unpaired t test with Welch's correction post hoc test. For comparison of BRET internalization and β-arrestin recruitment, the area under the curve (AUC) was determined using GraphPad Prism and statistical significance was determined using the appropriate tests mentioned above.

Supplementary Materials

Fig. 2.S1. Direct recruitment of β-arrestin to CCR2 by BRET.

Fig. 2.S2. CCR2 association with early endosome marker rGFP-FYVE.

Fig. 2.S3. Methods for CCL2-induced versus constitutive internalization of CCR2

Fig. 2.S4. CCR2 internalization and β-arrestin recruitment of phosphorylation mutant CCR2-ST/10A.

Fig. 2.S5. CCL2-mCherry is internalized by CCR2 independent of C-terminal phosphorylation.

Fig. 2.S6. CCL2-mCherry is internalized by CCR2 in WT and β-arrestin1/2 KO HEK293 cells.

Fig. 2.S7. CRISPR knockdown of β-arrestin1 and β-arrestin2 in THP-1 cells.

Fig. 2.S8. Constitutive internalization of CCR2 is unaffected by Dyngo-4a.

Fig. 2.S9. CCR2 recycles to the plasma membrane following receptor inhibition with BMS681.

Fig. 2.S10. RlucII-tagged CCR1 does not express on the cell surface.

REFERENCES

1. M. H. Ulvmar, E. Hub, A. Rot, Atypical chemokine receptors. *Exp Cell Res*. **317**, 556–568 (2011).

2. R. J. B. Nibbs, G. J. Graham, Immune regulation by atypical chemokine receptors. *Nat Rev Immunol*. **13**, 815–829 (2013).

3. P. Abe, W. Mueller, D. Schütz, F. MacKay, M. Thelen, P. Zhang, R. Stumm, CXCR7 prevents excessive CXCL12-mediated downregulation of CXCR4 in migrating cortical interneurons. *Development*. **141**, 1857–1863 (2014).

4. R. Bonecchi, G. J. Graham, Atypical Chemokine Receptors and Their Roles in the Resolution of the Inflammatory Response. *Front Immunol*. **7** (2016), doi:10.3389/fimmu.2016.00224.

5. C. A. H. Hansell, C. E. Hurson, R. J. B. Nibbs, DARC and D6: silent partners in chemokine regulation? *Immunol Cell Biol*. **89**, 197–206 (2011).

6. G. J. Graham, M. Locati, A. Mantovani, A. Rot, M. Thelen, The biochemistry and biology of the atypical chemokine receptors. *Immunol Lett*. **145**, 30–38 (2012).

7. A. Mantovani, M. Locati, A. Vecchi, S. Sozzani, P. Allavena, Decoy receptors: a strategy to regulate inflammatory cytokines and chemokines. *Trends Immunol*. **22**, 328–336 (2001).

8. A. Mantovani, R. Bonecchi, M. Locati, Tuning inflammation and immunity by chemokine sequestration: decoys and more. *Nat Rev Immunol*. **6**, 907–918 (2006).

9. A. E. Cardona, M. E. Sasse, L. Liu, S. M. Cardona, M. Mizutani, C. Savarin, T. Hu, R. M. Ransohoff, Scavenging roles of chemokine receptors: chemokine receptor deficiency is associated with increased levels of ligand in circulation and tissues. *Blood*. **112**, 256–263 (2008).

10. S. Volpe, E. Cameroni, B. Moepps, S. Thelen, T. Apuzzo, M. Thelen, CCR2 acts as scavenger for CCL2 during monocyte chemotaxis. *PLoS One*. **7**, e37208 (2012).

11. B. N. Zhao, J. J. Campbell, C. L. Salanga, L. S. Ertl, Y. Wang, S. Yau, T. Dang, Y. Zeng, J. P. McMahon, A. Krasinski, P. Zhang, I. Kufareva, T. M. Handel, I. F. Charo, R. Singh, T. J. Schall, CCR2-Mediated Uptake of Constitutively Produced CCL2: A Mechanism for Regulating Chemokine Levels in the Blood. *J Immunol*. **203**, 3157–3165 (2019).

12. T. O'Connor, L. Borsig, M. Heikenwalder, CCL2-CCR2 Signaling in Disease Pathogenesis. *Endocr Metab Immune Disord Drug Targets*. **15**, 105–118 (2015).

13. A. M. Aragay, M. Mellado, J. M. Frade, A. M. Martin, M. C. Jimenez-Sainz, C. Martinez-A, F. Mayor, Monocyte chemoattractant protein-1-induced CCR2B receptor desensitization mediated by the G protein-coupled receptor kinase 2. *Proc Natl Acad Sci U S A*. **95**, 2985–2990 (1998).

14. C. V. Carman, J. L. Benovic, G-protein-coupled receptors: turn-ons and turn-offs. *Curr Opin Neurobiol*. **8**, 335–344 (1998).

15. J. L. Benovic, H. Kühn, I. Weyand, J. Codina, M. G. Caron, R. J. Lefkowitz, Functional desensitization of the isolated beta-adrenergic receptor by the beta-adrenergic receptor kinase: potential role of an analog of the retinal protein arrestin (48-kDa protein). *Proc Natl Acad Sci U S A*. **84**, 8879–8882 (1987).

16. H. Attramadal, J. L. Arriza, C. Aoki, T. M. Dawson, J. Codina, M. M. Kwatra, S. H. Snyder, M. G. Caron, R. J. Lefkowitz, Beta-arrestin2, a novel member of the arrestin/beta-arrestin gene family. *J Biol Chem*. **267**, 17882–17890 (1992).

17. M. J. Lohse, J. L. Benovic, J. Codina, M. G. Caron, R. J. Lefkowitz, beta-Arrestin: a protein that regulates beta-adrenergic receptor function. *Science*. **248**, 1547–1550 (1990).

18. V. V. Gurevich, E. V. Gurevich, GPCR Signaling Regulation: The Role of GRKs and Arrestins. *Front Pharmacol*. **10**, 125 (2019).

19. Y. A. Berchiche, S. Gravel, M.-E. Pelletier, G. St-Onge, N. Heveker, Different effects of the different natural CC chemokine receptor 2b ligands on beta-arrestin

recruitment, Gαi signaling, and receptor internalization. *Mol Pharmacol*. **79**, 488–498 (2011).

20. M. Mellado, J. M. Rodríguez-Frade, A. J. Vila-Coro, S. Fernández, A. Martín de Ana, D. R. Jones, J. L. Torán, C. Martínez-A, Chemokine receptor homo- or heterodimerization activates distinct signaling pathways. *EMBO J*. **20**, 2497–2507 (2001).

21. M. Grundmann, N. Merten, D. Malfacini, A. Inoue, P. Preis, K. Simon, N. Rüttiger, N. Ziegler, T. Benkel, N. K. Schmitt, S. Ishida, I. Müller, R. Reher, K. Kawakami, A. Inoue, U. Rick, T. Kühl, D. Imhof, J. Aoki, G. M. König, C. Hoffmann, J. Gomeza, J. Wess, E. Kostenis, Lack of beta-arrestin signaling in the absence of active G proteins. *Nat Commun*. **9**, 341 (2018).

22. Y. Namkung, C. Le Gouill, V. Lukashova, H. Kobayashi, M. Hogue, E. Khoury, M. Song, M. Bouvier, S. A. Laporte, Monitoring G protein-coupled receptor and β-arrestin trafficking in live cells using enhanced bystander BRET. *Nat Commun*. **7**, 12178 (2016).

23. W. J. Koch, J. Inglese, W. C. Stone, R. J. Lefkowitz, The binding site for the beta gamma subunits of heterotrimeric G proteins on the beta-adrenergic receptor kinase. *J Biol Chem*. **268**, 8256–8260 (1993).

24. K. Touhara, J. Inglese, J. A. Pitcher, G. Shaw, R. J. Lefkowitz, Binding of G protein beta gamma-subunits to pleckstrin homology domains. *J Biol Chem*. **269**, 10217–10220 (1994).

25. R. J. Lefkowitz, G protein-coupled receptor kinases. *Cell*. **74**, 409–412 (1993).

26. M. J. Lohse, C. Krasel, R. Winstel, F. Mayor, G-protein-coupled receptor kinases. *Kidney Int*. **49**, 1047–1052 (1996).

27. R. T. Premont, J. Inglese, R. J. Lefkowitz, Protein kinases that phosphorylate activated G protein-coupled receptors. *FASEB J*. **9**, 175–182 (1995).

28. A. M. Aragay, M. Mellado, J. M. R. Frade, A. M. Martin, M. C. Jimenez-Sainz, C. Martinez-A, F. Mayor, Monocyte chemoattractant protein-1-induced CCR2B receptor desensitization mediated by the G protein-coupled receptor kinase 2. *PNAS*. **95**, 2985–2990 (1998).

29. C. Franci, J. Gosling, C. L. Tsou, S. R. Coughlin, I. F. Charo, Phosphorylation by a G protein-coupled kinase inhibits signaling and promotes internalization of the monocyte chemoattractant protein-1 receptor. Critical role of carboxyl-tail serines/threonines in receptor function. *J Immunol*. **157**, 5606–5612 (1996).

30. H.-J. Lee, J. J. Zheng, PDZ domains and their binding partners: structure, specificity, and modification. *Cell Commun Signal*. **8**, 8 (2010).

31. G. Romero, M. von Zastrow, P. A. Friedman, Role of PDZ proteins in regulating trafficking, signaling, and function of GPCRs: means, motif, and opportunity. *Adv Pharmacol*. **62**, 279–314 (2011).

32. S. A. Laporte, R. H. Oakley, J. A. Holt, L. S. Barak, M. G. Caron, The interaction of beta-arrestin with the AP-2 adaptor is required for the clustering of beta 2-adrenergic receptor into clathrin-coated pits. *J Biol Chem*. **275**, 23120–23126 (2000).

33. E. Boucrot, S. Saffarian, R. Zhang, T. Kirchhausen, Roles of AP-2 in clathrin-mediated endocytosis. *PLoS One*. **5**, e10597 (2010).

34. D. Jiang, T. Xie, J. Liang, P. W. Noble, β-Arrestins in the immune system. *Prog Mol Biol Transl Sci*. **118**, 359–393 (2013).

35. D. Sharma, N. Parameswaran, Multifaceted role of β-arrestins in inflammation and disease. *Genes Immun*. **16**, 499–513 (2015).

36. E. Galliera, V. R. Jala, J. O. Trent, R. Bonecchi, P. Signorelli, R. J. Lefkowitz, A. Mantovani, M. Locati, B. Haribabu, beta-Arrestin-dependent constitutive internalization of the human chemokine decoy receptor D6. *J Biol Chem*. **279**, 25590–25597 (2004).

37. C. Matti, A. Salnikov, M. Artinger, G. D'Agostino, I. Kindinger, M. Uguccioni, M. Thelen, D. F. Legler, ACKR4 Recruits GRK3 Prior to β-Arrestins but Can Scavenge Chemokines in the Absence of β-Arrestins. *Front Immunol*. **11**, 720 (2020).

38. K. E. Luker, J. M. Steele, L. A. Mihalko, P. Ray, G. D. Luker, Constitutive and chemokine-dependent internalization and recycling of CXCR7 in breast cancer cells to degrade chemokine ligands. *Oncogene*. **29**, 4599–4610 (2010).

39. N. Montpas, G. St-Onge, N. Nama, D. Rhainds, B. Benredjem, M. Girard, G. Hickson, V. Pons, N. Heveker, Ligand-specific conformational transitions and intracellular transport are required for atypical chemokine receptor 3-mediated chemokine scavenging. *J Biol Chem*. **293**, 893–905 (2018).

40. F. Saaber, D. Schütz, E. Miess, P. Abe, S. Desikan, P. Ashok Kumar, S. Balk, K. Huang, J. M. Beaulieu, S. Schulz, R. Stumm, ACKR3 Regulation of Neuronal Migration Requires ACKR3 Phosphorylation, but Not β-Arrestin. *Cell Rep*. **26**, 1473-1488.e9 (2019).

41. M. Kaksonen, A. Roux, Mechanisms of clathrin-mediated endocytosis. *Nat Rev Mol Cell Biol*. **19**, 313–326 (2018).

42. M. M. Paing, A. B. Stutts, T. A. Kohout, R. J. Lefkowitz, J. Trejo, beta -Arrestins regulate protease-activated receptor-1 desensitization but not internalization or Down-regulation. *J Biol Chem*. **277**, 1292–1300 (2002).

43. J. L. Parent, P. Labrecque, M. Driss Rochdi, J. L. Benovic, Role of the differentially spliced carboxyl terminus in thromboxane A2 receptor trafficking: identification of a distinct motif for tonic internalization. *J Biol Chem*. **276**, 7079–7085 (2001).

44. A. Marchese, C. Chen, Y.-M. Kim, J. L. Benovic, The ins and outs of G protein-coupled receptor trafficking. *Trends Biochem Sci*. **28**, 369–376 (2003).

45. H. Damke, T. Baba, D. E. Warnock, S. L. Schmid, Induction of mutant dynamin specifically blocks endocytic coated vesicle formation. *J Cell Biol*. **127**, 915–934 (1994).

46. A. McCluskey, J. A. Daniel, G. Hadzic, N. Chau, E. L. Clayton, A. Mariana, A. Whiting, N. N. Gorgani, J. Lloyd, A. Quan, L. Moshkanbaryans, S. Krishnan, S. Perera, M. Chircop, L. von Kleist, A. B. McGeachie, M. T. Howes, R. G. Parton, M. Campbell, J. A. Sakoff, X. Wang, J.-Y. Sun, M. J. Robertson, F. M. Deane, T. H. Nguyen, F. A. Meunier, M. A. Cousin, P. J. Robinson, Building a better dynasore: the dyngo compounds potently inhibit dynamin and endocytosis. *Traffic*. **14**, 1272–1289 (2013).

47. J. Koenen, F. Bachelerie, K. Balabanian, G. Schlecht-Louf, C. Gallego, Atypical Chemokine Receptor 3 (ACKR3): A Comprehensive Overview of its Expression and Potential Roles in the Immune System. *Mol Pharmacol*. **96**, 809–818 (2019).

48. S. Lau, A. Feitzinger, G. Venkiteswaran, J. Wang, S. W. Lewellis, C. A. Koplinski, F. C. Peterson, B. F. Volkman, M. Meier-Schellersheim, H. Knaut, A negative-feedback loop maintains optimal chemokine concentrations for directional cell migration. *Nat Cell Biol*. **22**, 266–273 (2020).

49. A. Wandinger-Ness, M. Zerial, Rab proteins and the compartmentalization of the endosomal system. *Cold Spring Harb Perspect Biol*. **6**, a022616 (2014).

50. A. Sapmaz, I. Berlin, E. Bos, R. H. Wijdeven, H. Janssen, R. Konietzny, J. J. Akkermans, A. E. Erson-Bensan, R. I. Koning, B. M. Kessler, J. Neefjes, H. Ovaa, USP32 regulates late endosomal transport and recycling through deubiquitylation of Rab7. *Nat Commun*. **10**, 1454 (2019).

51. P. J. Cullen, H. C. Korswagen, Sorting nexins provide diversity for retromer-dependent trafficking events. *Nat Cell Biol*. **14**, 29–37 (2012).

52. M. N. J. Seaman, The retromer complex – endosomal protein recycling and beyond. *Journal of Cell Science*. **125**, 4693–4702 (2012).

53. X. Gong, W. Gong, D. B. Kuhns, A. Ben-Baruch, O. M. Howard, J. M. Wang, Monocyte chemotactic protein-2 (MCP-2) uses CCR1 and CCR2B as its functional receptors. *J Biol Chem*. **272**, 11682–11685 (1997).

54. C. Weber, K. S. Weber, C. Klier, S. Gu, R. Wank, R. Horuk, P. J. Nelson, Specialized roles of the chemokine receptors CCR1 and CCR5 in the recruitment of monocytes and T(H)1-like/CD45RO(+) T cells. *Blood*. **97**, 1144–1146 (2001).

55. C. T. Gilliland, C. L. Salanga, T. Kawamura, J. Trejo, T. M. Handel, The chemokine receptor CCR1 is constitutively active, which leads to G protein-independent, β-arrestin-mediated internalization. *J Biol Chem*. **288**, 32194–32210 (2013).

56. G. D'Amico, G. Frascaroli, G. Bianchi, P. Transidico, A. Doni, A. Vecchi, S. Sozzani, P. Allavena, A. Mantovani, Uncoupling of inflammatory chemokine receptors by IL-10: generation of functional decoys. *Nat Immunol.* **1**, 387–391 (2000).

57. F. Bednar, C. Song, G. Bardi, W. Cornwell, T. J. Rogers, Cross-desensitization of CCR1, but not CCR2, following activation of the formyl peptide receptor FPR1. *J Immunol*. **192**, 5305–5313 (2014).

59. L. B. Ford, V. Cerovic, S. W. F. Milling, G. J. Graham, C. A. H. Hansell, R. J. B. Nibbs, Characterization of conventional and atypical receptors for the chemokine CCL2 on mouse leukocytes. *J Immunol*. **193**, 400–411 (2014).

60. S. A. Laporte, R. H. Oakley, J. Zhang, J. A. Holt, S. S. Ferguson, M. G. Caron, L. S. Barak, The beta2-adrenergic receptor/betaarrestin complex recruits the clathrin adaptor AP-2 during endocytosis. *Proc Natl Acad Sci U S A*. **96**, 3712–3717 (1999).

61. Y. Kondo, A. Hanai, W. Nakai, Y. Katoh, K. Nakayama, H.-W. Shin, ARF1 and ARF3 are required for the integrity of recycling endosomes and the recycling pathway. *Cell Struct Funct.* **37**, 141–154 (2012).

62. R. Karnik, M. J. Ludlow, N. Abuarab, A. J. Smith, M. E. L. Hardy, D. J. S. Elliott, A. Sivaprasadarao, Endocytosis of HERG is clathrin-independent and involves arf6. *PLoS One*. **8**, e85630 (2013).

63. N. Naslavsky, R. Weigert, J. G. Donaldson, Characterization of a nonclathrin endocytic pathway: membrane cargo and lipid requirements. *Mol Biol Cell*. **15**, 3542–3552 (2004).

64. K. Sandvig, M. L. Torgersen, H. A. Raa, B. van Deurs, Clathrin-independent endocytosis: from nonexisting to an extreme degree of complexity. *Histochem Cell Biol*. **129**, 267–276 (2008).

65. Q. Zhang, D. Cox, C. C. Tseng, J. G. Donaldson, S. Greenberg, A requirement for ARF6 in Fcgamma receptor-mediated phagocytosis in macrophages. *J Biol Chem*. **273**, 19977–19981 (1998).

66. L. C. Santy, J. E. Casanova, Activation of ARF6 by ARNO stimulates epithelial cell migration through downstream activation of both Rac1 and phospholipase D. *J Cell Biol*. **154**, 599–610 (2001).

67. E. Macia, M. Partisani, O. Paleotti, F. Luton, M. Franco, Arf6 negatively controls the rapid recycling of the β2 adrenergic receptor. *J Cell Sci*. **125**, 4026–4035 (2012).

68. Y. Egami, T. Taguchi, M. Maekawa, H. Arai, N. Araki, Small GTPases and phosphoinositides in the regulatory mechanisms of macropinosome formation and maturation. *Front Physiol*. **5**, 374 (2014).

69. W. S. Garrett, L. M. Chen, R. Kroschewski, M. Ebersold, S. Turley, S. Trombetta, J. E. Galán, I. Mellman, Developmental control of endocytosis in dendritic cells by Cdc42. *Cell*. **102**, 325–334 (2000).

70. K. S. Weber, L. B. Klickstein, P. C. Weber, C. Weber, Chemokine-induced monocyte transmigration requires cdc42-mediated cytoskeletal changes. *Eur J Immunol*. **28**, 2245–2251 (1998).

71. M. Tanaka, T. Kikuchi, H. Uno, K. Okita, T. Kitanishi-Yumura, S. Yumura, Turnover and flow of the cell membrane for cell migration. *Sci Rep*. **7**, 12970 (2017).

72. K. R. Rosholm, N. Leijnse, A. Mantsiou, V. Tkach, S. L. Pedersen, V. F. Wirth, L. B. Oddershede, K. J. Jensen, K. L. Martinez, N. S. Hatzakis, P. M. Bendix, A. Callan-Jones, D. Stamou, Membrane curvature regulates ligand-specific membrane sorting of GPCRs in living cells. *Nat Chem Biol*. **13**, 724–729 (2017).

73. S. Sabharanjak, P. Sharma, R. G. Parton, S. Mayor, GPI-anchored proteins are delivered to recycling endosomes via a distinct cdc42-regulated, clathrin-independent pinocytic pathway. *Dev Cell*. **2**, 411–423 (2002).

74. M. Kirkham, A. Fujita, R. Chadda, S. J. Nixon, T. V. Kurzchalia, D. K. Sharma, R. E. Pagano, J. F. Hancock, S. Mayor, R. G. Parton, Ultrastructural identification of uncoated caveolin-independent early endocytic vehicles. *J Cell Biol*. **168**, 465–476 (2005).

75. S. Mayor, R. G. Parton, J. G. Donaldson, Clathrin-independent pathways of endocytosis. *Cold Spring Harb Perspect Biol*. **6**, a016758 (2014).

76. D. P. Dyer, K. Pallas, L. Medina-Ruiz, F. Schuette, G. J. Wilson, G. J. Graham, CXCR2 deficient mice display macrophage-dependent exaggerated acute inflammatory responses. *Sci Rep*. **7**, 42681 (2017).

77. E. Bakos, C. A. Thaiss, M. P. Kramer, S. Cohen, L. Radomir, I. Orr, N. Kaushansky, A. Ben-Nun, S. Becker-Herman, I. Shachar, CCR2 Regulates the Immune Response by Modulating the Interconversion and Function of Effector and Regulatory T Cells. *J Immunol*. **198**, 4659–4671 (2017).

78. P. D. Doodes, Y. Cao, K. M. Hamel, Y. Wang, R. L. Rodeghero, T. Kobezda, A. Finnegan, CCR5 is involved in resolution of inflammation in proteoglycan-induced arthritis. *Arthritis Rheum*. **60**, 2945–2953 (2009).

79. A. Ortega-Gómez, M. Perretti, O. Soehnlein, Resolution of inflammation: an integrated view. *EMBO Mol Med*. **5**, 661–674 (2013).

80. G. J. Graham, M. Locati, Regulation of the immune and inflammatory responses by the "atypical" chemokine receptor D6. *J Pathol*. **229**, 168–175 (2013).

81. M. Aswad, S. Assi, S. Schif-Zuck, A. Ariel, CCL5 Promotes Resolution-Phase Macrophage Reprogramming in Concert with the Atypical Chemokine Receptor D6 and Apoptotic Polymorphonuclear Cells. *J Immunol*. **199**, 1393–1404 (2017).

82. M. Scarselli, J. G. Donaldson, Constitutive internalization of G protein-coupled receptors and G proteins via clathrin-independent endocytosis. *J Biol Chem*. **284**, 3577–3585 (2009).

83. M. M. Tu, H. A. Abdel-Hafiz, R. T. Jones, A. Jean, K. J. Hoff, J. E. Duex, A. Chauca-Diaz, J. C. Costello, G. M. Dancik, B. A. J. Tamburini, B. Czerniak, J. Kaye, D. Theodorescu, Inhibition of the CCL2 receptor, CCR2, enhances tumor response to immune checkpoint therapy. *Commun Biol*. **3**, 720 (2020).

84. I. Bot, N. V. Ortiz Zacarías, W. E. A. de Witte, H. de Vries, P. J. van Santbrink, D. van der Velden, M. J. Kröner, D.-J. van der Berg, D. Stamos, E. C. M. de Lange, J. Kuiper, A. P. IJzerman, L. H. Heitman, A novel CCR2 antagonist inhibits atherogenesis in apoE deficient mice by achieving high receptor occupancy. *Sci Rep*. **7**, 52 (2017).

85. E. Pairo-Castineira, S. Clohisey, L. Klaric, A. D. Bretherick, K. Rawlik, D. Pasko, S. Walker, N. Parkinson, M. H. Fourman, C. D. Russell, J. Furniss, A. Richmond, E. Gountouna, N. Wrobel, D. Harrison, B. Wang, Y. Wu, A. Meynert, F. Griffiths, W. Oosthuyzen, A. Kousathanas, L. Moutsianas, Z. Yang, R. Zhai, C. Zheng, G. Grimes, R. Beale, J. Millar, B. Shih, S. Keating, M. Zechner, C. Haley, D. J. Porteous, C. Hayward, J. Yang, J. Knight, C. Summers, M. Shankar-Hari, P. Klenerman, L. Turtle, A. Ho, S. C. Moore, C. Hinds, P. Horby, A. Nichol, D. Maslove, L. Ling, D. McAuley, H. Montgomery, T. Walsh, A. C. Pereira, A. Renieri, X. Shen, C. P. Ponting, A. Fawkes, A. Tenesa, M. Caulfield, R. Scott, K. Rowan, L. Murphy, P. J. M. Openshaw, M. G. Semple, A. Law, V. Vitart, J. F. Wilson, J. K. Baillie, Genetic mechanisms of critical illness in COVID-19. *Nature*. **591**, 92–98 (2021).

86. K. Yumimoto, S. Sugiyama, K. Mimori, K. I. Nakayama, Potentials of C-C motif chemokine 2-C-C chemokine receptor type 2 blockers including propagermanium as anticancer agents. *Cancer Sci*. **110**, 2090–2099 (2019).

87. Q. Liu, Y. Zhou, Z. Yang, The cytokine storm of severe influenza and development of immunomodulatory therapy. *Cell Mol Immunol*. **13**, 3–10 (2016).

88. D. de Zeeuw, P. Bekker, E. Henkel, C. Hasslacher, I. Gouni-Berthold, H. Mehling, A. Potarca, V. Tesar, H. J. L. Heerspink, T. J. Schall, CCX140-B Diabetic Nephropathy Study Group, The effect of CCR2 inhibitor CCX140-B on residual albuminuria in patients with type 2 diabetes and nephropathy: a randomised trial. *Lancet Diabetes Endocrinol*. **3**, 687–696 (2015).

89. T. M. Nywening, A. Wang-Gillam, D. E. Sanford, B. A. Belt, R. Z. Panni, B. M. Cusworth, A. T. Toriola, R. K. Nieman, L. A. Worley, M. Yano, K. J. Fowler, A. C. Lockhart, R. Suresh, B. R. Tan, K.-H. Lim, R. C. Fields, S. M. Strasberg, W. G. Hawkins, D. G. DeNardo, S. P. Goedegebuure, D. C. Linehan, Targeting tumour-associated macrophages with CCR2 inhibition in combination with FOLFIRINOX in patients with borderline resectable and locally advanced pancreatic cancer: a single-centre, open-label, dose-finding, non-randomised, phase 1b trial. *Lancet Oncol*. **17**, 651–662 (2016).

90. M. Xu, Y. Wang, R. Xia, Y. Wei, X. Wei, Role of the CCL2-CCR2 signalling axis in cancer: Mechanisms and therapeutic targeting. *Cell Prolif*. **54**, e13115 (2021).

91. J. Gilbert, J. Lekstrom-Himes, D. Donaldson, Y. Lee, M. Hu, J. Xu, T. Wyant, M. Davidson, MLN1202 Study Group, Effect of CC chemokine receptor 2 CCR2 blockade on serum C-reactive protein in individuals at atherosclerotic risk and with a single nucleotide polymorphism of the monocyte chemoattractant protein-1 promoter region. *Am J Cardiol*. **107**, 906–911 (2011).

92. C. E. Vergunst, D. M. Gerlag, L. Lopatinskaya, L. Klareskog, M. D. Smith, F. van den Bosch, H. J. Dinant, Y. Lee, T. Wyant, E. W. Jacobson, D. Baeten, P. P. Tak, Modulation of CCR2 in rheumatoid arthritis: a double-blind, randomized, placebo-controlled clinical trial. *Arthritis Rheum*. **58**, 1931–1939 (2008).

93. R. J. Aiello, B. D. Perry, P.-A. Bourassa, A. Robertson, W. Weng, D. R. Knight, A. H. Smith, K. S. Frederick, A. Kalgutkar, R. P. Gladue, CCR2 receptor blockade alters blood monocyte subpopulations but does not affect atherosclerotic lesions in apoE(-/-) mice. *Atherosclerosis*. **208**, 370–375 (2010).

94. Y. Wang, L. Cui, W. Gonsiorek, S.-H. Min, G. Anilkumar, S. Rosenblum, J. Kozlowski, D. Lundell, J. S. Fine, E. P. Grant, CCR2 and CXCR4 regulate peripheral blood monocyte pharmacodynamics and link to efficacy in experimental autoimmune encephalomyelitis. *J Inflamm (Lond)*. **6**, 32 (2009).

95. N. Okashah, Q. Wan, S. Ghosh, M. Sandhu, A. Inoue, N. Vaidehi, N. A. Lambert, Variable G protein determinants of GPCR coupling selectivity. *Proc Natl Acad Sci U S A*. **116**, 12054–12059 (2019).

96. M. O'Hayre, K. Eichel, S. Avino, X. Zhao, D. J. Steffen, X. Feng, K. Kawakami, J. Aoki, K. Messer, R. Sunahara, A. Inoue, M. von Zastrow, J. S. Gutkind, Genetic evidence that β-arrestins are dispensable for the initiation of β2-adrenergic receptor signaling to ERK. *Sci Signal*. **10**, eaal3395 (2017).

97. S. Pandey, P. Kumari, M. Baidya, R. Kise, Y. Cao, H. Dwivedi-Agnihotri, R. Banerjee, X. X. Li, C. S. Cui, J. D. Lee, K. Kawakami, J. Maharana, A. Ranjan, M. Chaturvedi, G. D. Jhingan, S. A. Laporte, T. M. Woodruff, A. Inoue, A. K. Shukla, Intrinsic bias at non-canonical, β-arrestin-coupled seven transmembrane receptors. *Mol Cell*. **81**, 4605-4621.e11 (2021).

98. N. E. Sanjana, O. Shalem, F. Zhang, Improved vectors and genome-wide libraries for CRISPR screening. *Nat Methods*. **11**, 783–784 (2014).

99. K. Labun, T. G. Montague, M. Krause, Y. N. Torres Cleuren, H. Tjeldnes, E. Valen, CHOPCHOP v3: expanding the CRISPR web toolbox beyond genome editing. *Nucleic Acids Research*. **47**, W171–W174 (2019).

100. E. Campeau, V. E. Ruhl, F. Rodier, C. L. Smith, B. L. Rahmberg, J. O. Fuss, J. Campisi, P. Yaswen, P. K. Cooper, P. D. Kaufman, A versatile viral system for expression and depletion of proteins in mammalian cells. *PLoS One*. **4**, e6529 (2009).

101. Q. Sun, W. Westphal, K. N. Wong, I. Tan, Q. Zhong, Rubicon controls endosome maturation as a Rab7 effector. *Proc Natl Acad Sci U S A.* **107**, 19338–19343 (2010).

102. A. Levoye, J. M. Zwier, A. Jaracz-Ros, L. Klipfel, M. Cottet, D. Maurel, S. Bdioui, K. Balabanian, L. Prézeau, E. Trinquet, T. Durroux, F. Bachelerie, A Broad G Protein-Coupled Receptor Internalization Assay that Combines SNAP-Tag Labeling, Diffusion-Enhanced Resonance Energy Transfer, and a Highly Emissive Terbium Cryptate. *Front Endocrinol (Lausanne)*. **6**, 167 (2015).

103. F. Ango, S. Albani-Torregrossa, C. Joly, D. Robbe, J. M. Michel, J. P. Pin, J. Bockaert, L. Fagni, A simple method to transfer plasmid DNA into neuronal primary cultures: functional expression of the mGlu5 receptor in cerebellar granule cells. *Neuropharmacology*. **38**, 793–803 (1999).

104. T. Sakuma, A. Nishikawa, S. Kume, K. Chayama, T. Yamamoto, Multiplex genome engineering in human cells using all-in-one CRISPR/Cas9 vector system. *Sci Rep*. **4**, 5400 (2014).

105. T. Cermak, E. L. Doyle, M. Christian, L. Wang, Y. Zhang, C. Schmidt, J. A. Baller, N. V. Somia, A. J. Bogdanove, D. F. Voytas, Efficient design and assembly of custom

TALEN and other TAL effector-based constructs for DNA targeting. *Nucleic Acids Research*. **39**, e82 (2011).

106. M. R. Dores, M. M. Paing, H. Lin, W. A. Montagne, A. Marchese, J. Trejo, AP-3 regulates PAR1 ubiquitin-independent MVB/lysosomal sorting via an ALIX-mediated pathway. *Mol Biol Cell*. **23**, 3612–3623 (2012).

Acknowledgments:

We acknowledge M. Bouvier (Université de Montréal), D. Legler (University of Konstanz), M. Gustavsson (UC San Diego, currently University of Copenhagen), A. Levoye, (University of Paris), A. Inoue (Tohoku University) and B. Moepps (ULM University) for the BRET reagents, plasmid constructs, cell lines, and CCL2-mCherry used in our studies. We thank Minya Pu, MA, of the UC San Diego Moores Cancer Center Biostatistics Shared Resource for critical review of and assistance with the statistical analyses in the manuscript. We also thank Dr. Eric Griffis and the Nikon Imaging Center at UC San Diego for technical support and advice.

Funding:

National Institute of General Medical Sciences NIH R01 grant GM136202 (T.M.H. and I.K)

National Institute of Allergy and Infectious Diseases NIH R21 grant AI149369 (I.K.)

National Institute of General Medical Sciences, Cellular and Molecular Pharmacology Training Grant T32 GM007752 (T.M.S.)

Competing interests: Dr. Handel is a co-founder of Lassogen Inc and serves on the Scientific Advisory Boards of Artica, Abilita Bio, and Abalone Bio. The terms of these arrangement have been reviewed and approved by the University of California, San Diego in

accordance with its conflict of interest policies. The remaining authors declare that they have no competing interests.

FIGURE LEGENDS

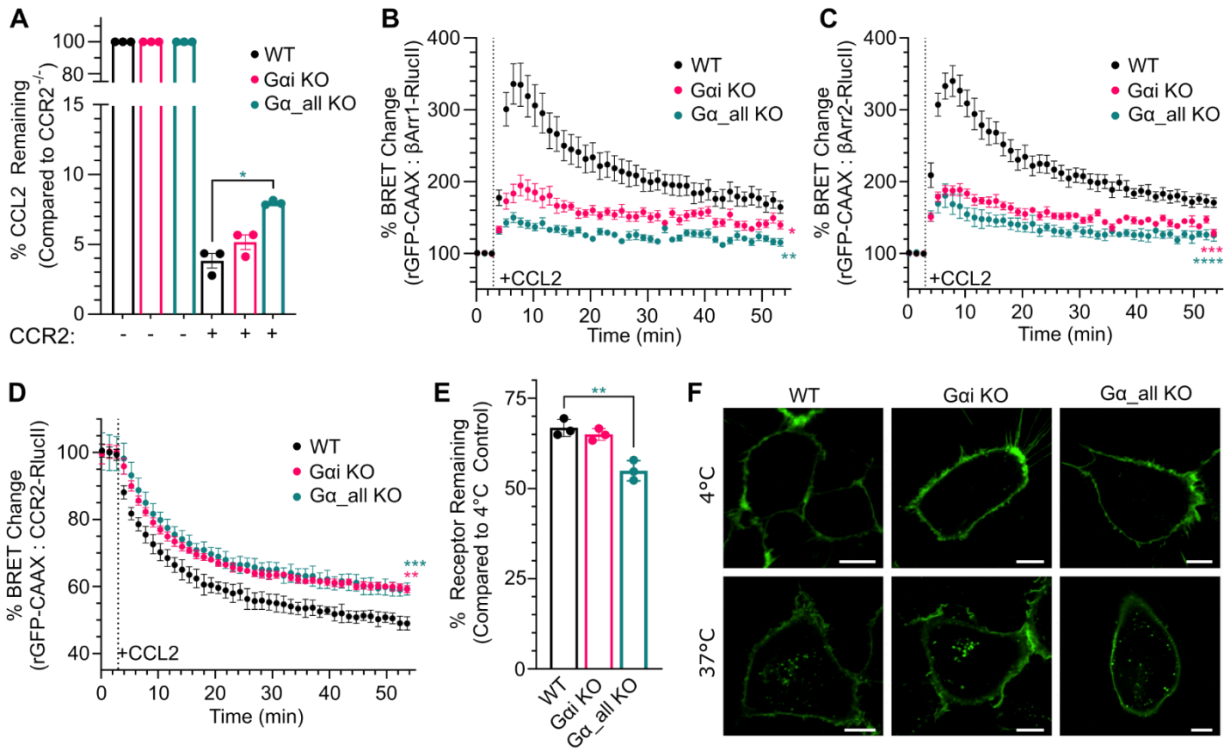

Figure 2.1. Scavenging of CCR2 is G protein-independent. (**A**) WT, Gαi KO and Gα_all KO HEK293 cells stably expressing CCR2 and respective non-expressing cells were cultured in media containing 5 nM CCL2 for 16 h. Remaining levels of CCL2 were measured by ELISA, interpolated from CCL2 standards, and presented as a percentage of non-CCR2 expressing cells. (**B** and **C**) β-arrestin recruitment assessed by ebBRET. Cells transfected with β-arrestin1- or β-arrestin2-RlucII and rGFP-CAAX were stimulated with 100 nM CCL2 or left untreated. Data are presented as a percentage of BRET values for untreated controls. Loss of G protein significantly decreases recruitment of β-arrestin. (**D**) CCR2 internalization assessed by BRET. Cells transfected with CCR2-RlucII and rGFP-CAAX were stimulated with 100 nM CCL2 or left untreated. The BRET ratio changes upon agonist treatment are expressed as a percentage of the BRET ratio observed in untreated controls. (**E**) Constitutive internalization of WT, Gαi KO and Gα_all KO HEK293 cells stably expressing CCR2 were assessed by pre-label flow cytometry (see Methods). Data presented as percentage of surface receptor remaining compared to non-internalized control. (**F**) Constitutive internalization was visualized by fluorescence confocal microscopy in WT, Gαi KO and Gα_all KO HEK293 cells expressing SNAP-CCR2 that was labeled with cell impermeable SNAP-Surface Alexa Fluor 488 at 4°C for 1 h. The cells were then held at 4°C for 45 min (top panel) or transferred to 37°C for 45 min (bottom panel) before being imaged. Scale bars, 10 µm. All data are expressed as the mean ± SEM of n ≥ 3 independent experiments. *P < 0.05, **P < 0.01, ***P < 0.001, ****P < 0.0001 versus controls, one-way analysis of variance (ANOVA) with Dunnet's multiple comparison test.

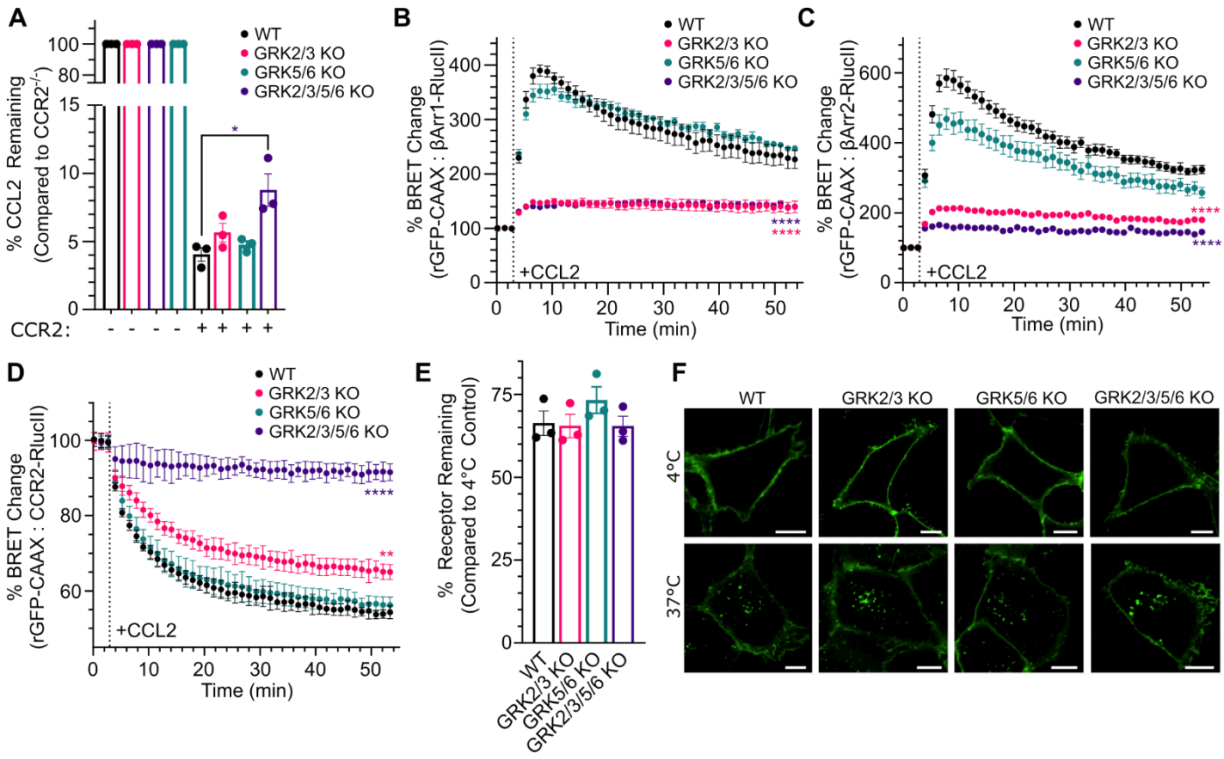

Figure 2.2. CCR2 scavenging of CCL2 is not dependent on GRKs. (**A**) WT HEK293A, HEK293A GRK2/3 KO, HEK293A GRK5/6 KO and HEK293A GRK2/3/5/6 KO cells stably expressing CCR2 and the corresponding CCR2 non-expressing cells were cultured in media containing 5 nM CCL2 for 16 h. Remaining levels of CCL2 were interpolated from CCL2 standards and are presented as the percentage of remaining CCL2 relative to CCR2 non-expressing cells. (**B** and **C**) β-arrestin recruitment assessed by ebBRET. Cells transfected with β-arrestin1- or β-arrestin2-RlucII and rGFP-CAAX were stimulated with 100 nM CCL2 or left untreated. Data are presented as a percentage of BRET values for untreated controls. Loss of GRK2/3, but not GRK5/6, significantly decreases recruitment of β-arrestin. (**D**) CCR2 internalization assessed by BRET. Cells transfected with CCR2-RlucII and rGFP-CAAX were stimulated with 100 nM CCL2 or left untreated. The BRET ratio changes upon agonist treatment are expressed as a percentage of BRET ratio observed in the untreated controls. (**E**) Constitutive internalization of WT HEK293A, HEK293A GRK2/3 KO, HEK293A GRK5/6 KO and HEK293A GRK2/3/5/6 KO stably expressing CCR2 was assessed by pre-label flow cytometry (see Methods). Data are presented as a percentage of surface receptor remaining as compared to non-internalized control. (**F**) Constitutive internalization was visualized by fluorescence confocal microscopy in WT and corresponding GRK KO HEK293A cells expressing SNAP-CCR2 that was labeled with cell impermeable SNAP-Surface Alexa Fluor 488 at 4°C for 1 h. The cells were then held at 4°C for 45 min (top panel) or transferred to 37°C for 45 min (bottom panel) before being analyzed. Scale bars, 10 µm. All data are expressed as the mean ± SEM of n ≥ 3 independent experiments. *P < 0.05, **P < 0.01, ***P < 0.001, ****P < 0.0001 versus controls, one-way analysis of variance (ANOVA) with Dunnet's multiple comparison test.

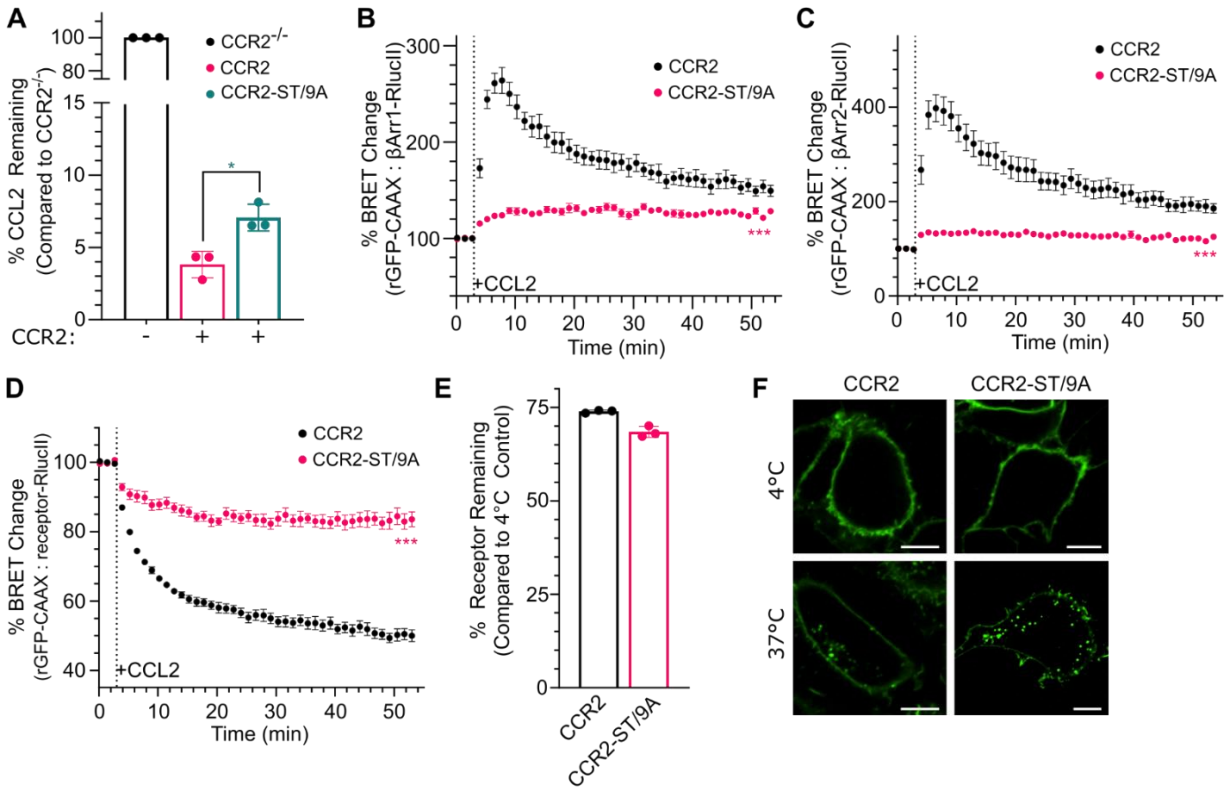

Figure 2.3. CCR2 scavenging of CCL2 occurs independent of receptor phosphorylation. (**A**) HEK293 cells stably expressing CCR2 or CCR2 with nine C-terminal serine/threonine residues mutated to alanine (CCR2-ST/9A), and non-expressing cells were cultured in media containing 5 nM CCL2 for 16 h. Remaining levels of CCL2 were interpolated from CCL2 standards and presented as a percentage of respective non-CCR2 expressing cells. (**B** and **C**) β-arrestin recruitment assessed by ebBRET. Cells expressing CCR2 or CCR2-ST9/A transfected with β-arrestin1- or β-arrestin2-RlucII and rGFP-CAAX were stimulated with 100 nM CCL2 or left untreated. (**D**) CCR2 internalization assessed by BRET. Cells transfected with CCR2-RlucII or CCR2-ST/9A-RlucII and rGFP-CAAX were stimulated with 100 nM CCL2 or left untreated. The BRET ratio changes upon agonist treatment are expressed as a percentage of BRET ratio observed in the untreated controls. (**E**) Constitutive internalization of WT CCR2 and CCR2-ST/9A in HEK293 cells was assessed by pre-label flow cytometry (see Methods). (**F**) Constitutive internalization was visualized by fluorescence confocal microscopy in HEK293 cells expressing SNAP-CCR2 or SNAP-CCR2-ST/9A labeled with cell impermeable SNAP-Surface Alexa Fluor 488 at 4°C for 1 h. Cells were then either held at 4°C for 45 min (top panel) or transferred to 37°C for 45 min (bottom panel) before being analyzed. Scale bars, 10 µm. All data are expressed as the mean ± SEM of $n \geq 3$ independent experiments. *P < 0.05, **P < 0.01, ***P < 0.001, ****P < 0.0001 versus controls, using unpaired t test.

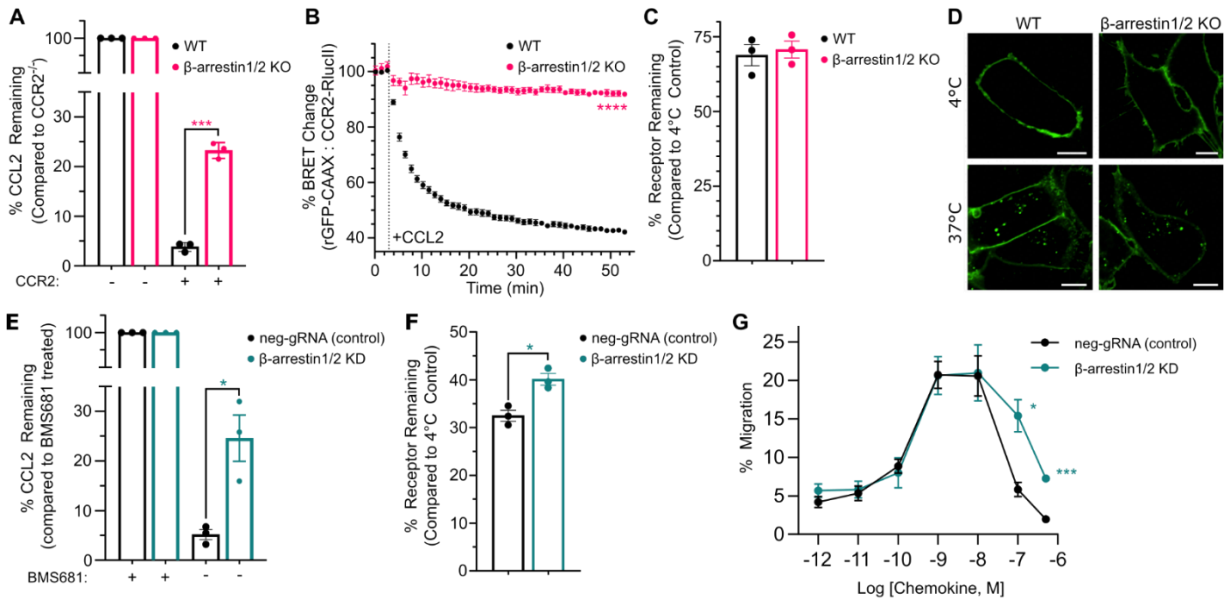

Figure 2.4. β-arrestins are dispensable for constitutive internalization and chemokine scavenging by CCR2. (**A**) WT HEK293 and β-arrestin1/2 KO HEK293 cells stably expressing CCR2 and respective non-expressing cells were cultured in media containing 5 nM CCL2 for 16 h. Remaining levels of CCL2 were interpolated from CCL2 standards and presented as a percentage of respective non-CCR2 expressing cells. (**B**) CCR2 internalization assessed by BRET. Cells transfected with CCR2-RlucII and rGFP-CAAX were stimulated with 100 nM CCL2 or left untreated. The BRET ratio changes upon agonist treatment are expressed as a percentage of BRET ratio observed in the untreated controls. (**C**) Constitutive internalization of WT HEK293 and β-arrestin1/2 KO HEK293 cells stably expressing CCR2 was assessed by pre-label flow cytometry (see Methods). Data are presented as a percentage of surface receptor remaining as compared to non-internalized control. (**D**) Constitutive internalization was visualized by fluorescence confocal microscopy in WT and β-arrestin1/2 KO HEK293 cells expressing SNAP-CCR2 that was labeled with cell impermeable SNAP-Surface Alexa Fluor 488 at 4°C for 1 h. The cells were then held at 4°C for 45 min (top panel) or transferred to 37°C for 45 min (bottom panel) before being analyzed. Scale bars, 10 µm. (**E**) THP-1 cells transduced with non-targeting gRNA (neg-gRNA) and THP-1 β-arrestin1/2 KD cells, treated with vehicle or CCR2 inhibitor BMS681, were cultured in media containing 5 nM CCL2 for 16 h. Remaining levels of CCL2 were interpolated from CCL2 standards and presented as a percentage of non-scavenging control BMS681 treated cells. (**F**) Constitutive internalization of CCR2 in THP-1 neg-gRNA and β-arrestin1/2 KD THP-1 cells was assessed by pre-label flow cytometry (see Methods). Data are presented as a percentage of surface receptor remaining as compared to non-internalized control. (**G**) Transwell migration of THP-1 neg-gRNA and β-arrestin1/2 KD THP-1 cells at various concentrations of chemokine. Data are presented as a percentage of migrated cells as compared to initial number of cells added to each well. All data are expressed as the mean ± SEM of n ≥ 3 independent experiments. *P < 0.05, **P < 0.01, ***P < 0.001, ****P < 0.0001 versus controls, unpaired t test.

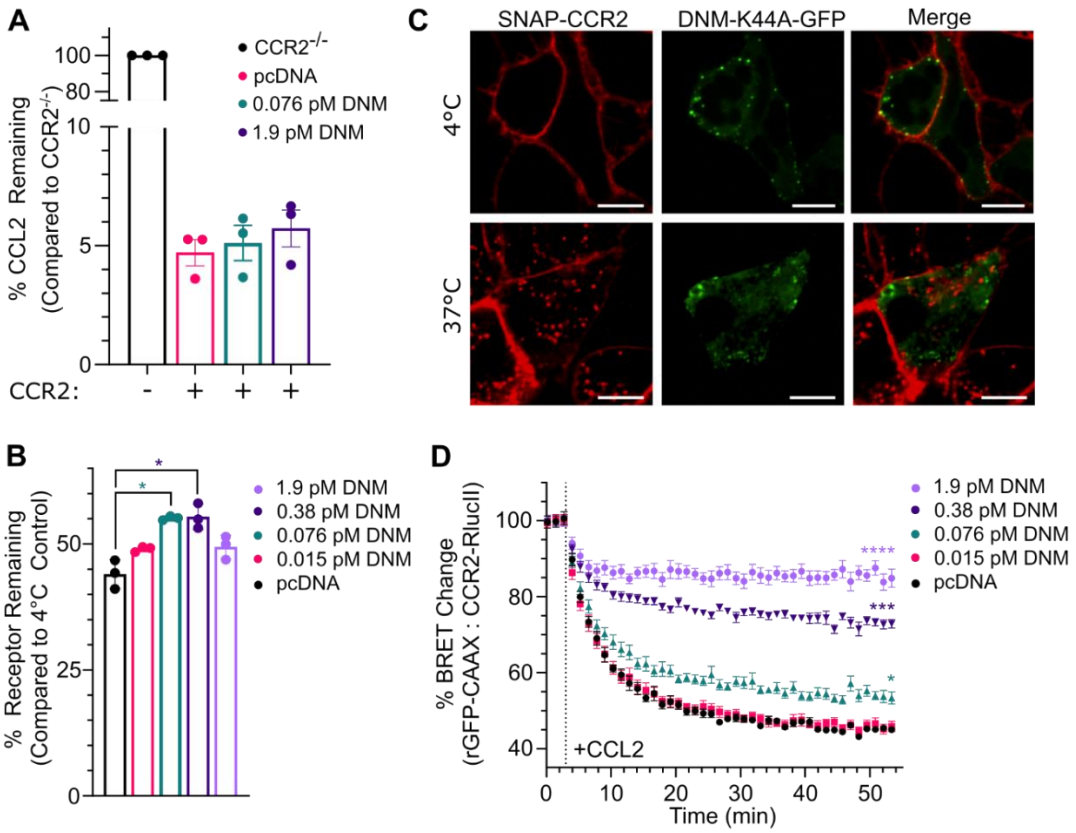

Figure 2.5. Clathrin-mediated endocytosis is not required for CCR2 constitutive internalization or scavenging. (**A**) Non-CCR2 expressing cells and HEK293 cells stably expressing CCR2 were transfected with two different concentrations of a dynamin dominant-negative mutant (DNM2-K44A) or left untransfected. The cells were cultured in media containing 5 nM CCL2 for 16 h. Remaining levels of CCL2 were determined by ELISA and interpolated from CCL2 standards and presented as a percentage of respective non-CCR2 expressing cells. (**B**) Constitutive internalization of CCR2 was assessed by pre-label flow cytometry (see Methods). HEK293 cells expressing CCR2 were transfected with pcDNA or an increasing amount of DNM2-K44A. Data are presented as a percentage of surface receptor remaining as compared to non-internalized control. (**C**) Constitutive internalization in the presence or absence of DNM2-K44A was visualized by fluorescence confocal microscopy in HEK293 expressing SNAP-CCR2 and DNM2-K44A-GFP. SNAP-CCR2 was labeled with cell impermeable SNAP-Surface Alexa Fluor 649 at 4°C for 1 h and then either held at 4°C for 45 min (top panel) or transferred to 37°C for 45 min (bottom panel) before being analyzed. Scale bars, 10 µm. (**D**) CCR2 internalization assessed by BRET. Cells transfected with CCR2-RlucII, rGFP-CAAX, and pcDNA or increasing amounts of DNM2-K44A were incubated in the absence or presence of 100 nM CCL2. The BRET ratio changes on agonist treatment are expressed as a percentage of BRET ratio observed in the untreated controls. All data are expressed as the mean ± SEM of $n \geq 3$ independent experiments. *$P < 0.05$, **$P < 0.01$, ***$P < 0.001$, ****$P < 0.0001$ versus controls, one-way analysis of variance (ANOVA) with Dunnet's multiple comparison test.

Figure 2.6. CCR2 endosomal trafficking, recycling and lack of degradation contribute to scavenging. (**A** to **C**) HEK293 cells were transfected with receptor-RlucII (CCR2, ACKR3 or CXCR4) along with either rGFP-Rab4 (A), rGFP-Rab11 (B) or rGFP-Rab7 (C). Cells were stimulated at 37°C with indicated chemokine or left untreated. Data are presented as a percentage of BRET values compared to untreated controls. (**D** to **F**) HEK293 cells were transfected with rGFP-CAAX along with either CCR2-RlucII (D), ACKR3-RlucII (E) or CXCR4-RlucII (F). Cells were stimulated at 37°C with indicated chemokine and subsequently washed with PBS to remove chemokine or left unwashed. Data are presented as a percentage of BRET values compared to non-chemokine treated controls. (**G**) HEK293 cells stably expressing SNAP-CCR2 were preincubated for 90 min with 10 mg/mL cycloheximide. They were then left untreated or stimulated with 100 nM CCL2 at 37°C for 45 min. Subsequently, cells were washed and remaining SNAP-CCR2 at the surface was blocked at 4°C with SNAP-Surface block for 45 min. Cells were then washed and shifted to 37 °C for 15, 45 or 75 min. Receptors were labeled with SNAP-Surface Alexa Fluor 649 at 4°C following each experimental condition and timepoint. Data are displayed as a percentage of CCR2 detected relative to initial levels of surface CCR2 prior to stimulation (Start). (**H, I**) HEK293 cells expressing FLAG-CCR2 or FLAG-PAR1 were pretreated with 10 μg/mL cycloheximide for 90 min to block de novo protein synthesis, left unstimulated (0 min) or stimulated with 100 nM CCR2 ligand CCL2 or 100 μM PAR1 synthetic ligand TFLLRN for 2 h at 37°C. Equivalent amount of cell lysates were immunoprecipitated with M2 anti-FLAG antibody and immunoblotting detection with anti-FLAG antibody. Cell lysates were analyzed for endogenous α-tubulin as controls (H). Receptor degradation was quantified, and the data (mean ± SEM) shown are expressed as the fraction of receptor remaining compared with untreated control cells as determined from three independent experiments (I). The differences in degradation between stimulated and unstimulated cells were significant for PAR1 but not CCR2. All data are expressed as the mean ± SEM of $n \geq 3$ independent experiments. *$P < 0.05$, **$P < 0.01$, ***$P < 0.001$, ****$P < 0.0001$ versus controls, one-way analysis of variance (ANOVA) with Dunnet's multiple comparison test or unpaired t test.

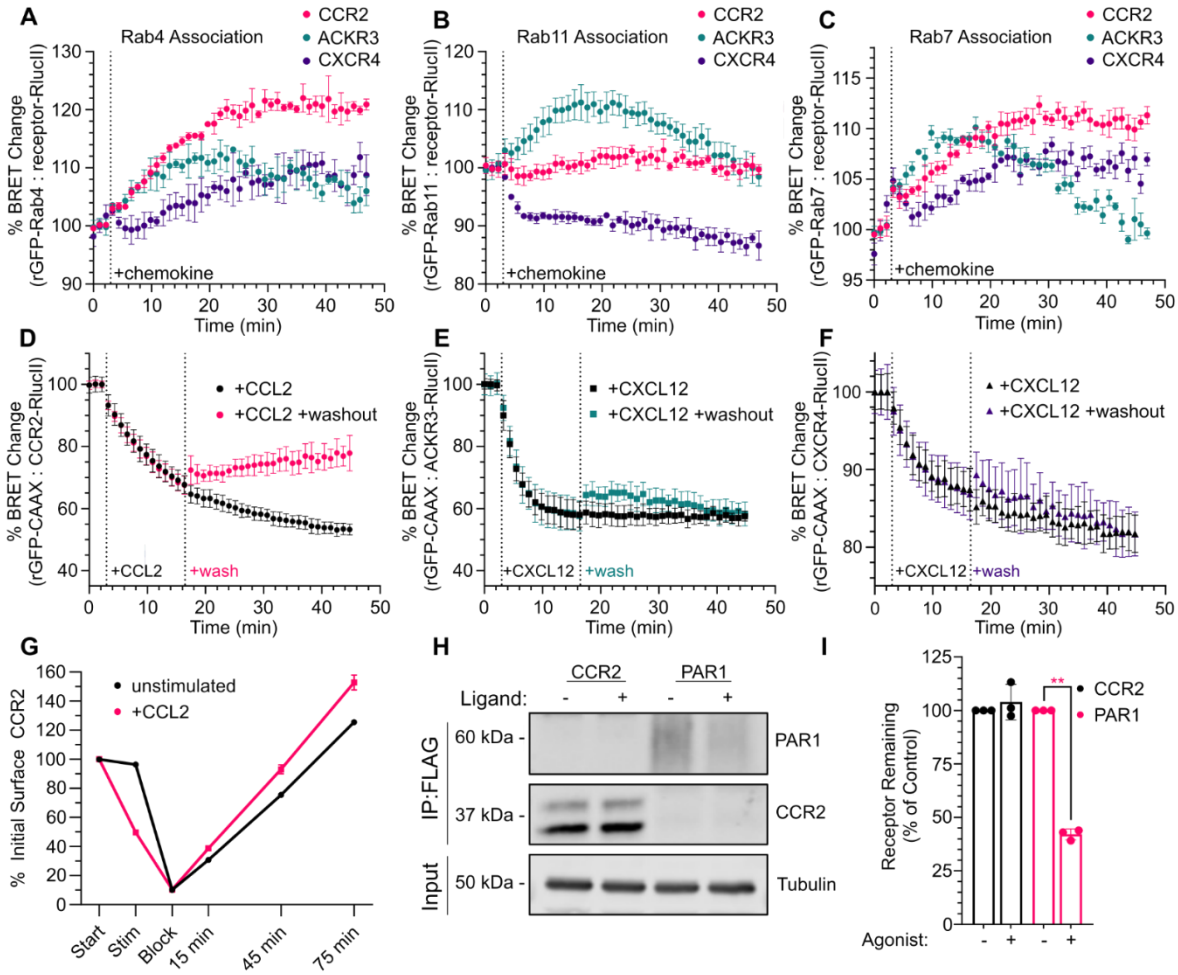
A
Rab4 Association
CCR2
ACKR3
CXCR4
% BRET Change (rGFP-Rab4 : receptor-RlucII)
+chemokine
Time (min)
B
Rab11 Association
% BRET Change (rGFP-Rab11 : receptor-RlucII)
C
Rab7 Association
% BRET Change (rGFP-Rab7 : receptor-RlucII)
D
+CCL2
+CCL2 +washout
% BRET Change (rGFP-CAAX : CCR2-RlucII)
+CCL2
+wash
E
+CXCL12
+CXCL12 +washout
% BRET Change (rGFP-CAAX : ACKR3-RlucII)
+CXCL12
+wash
F
+CXCL12
+CXCL12 +washout
% BRET Change (rGFP-CAAX : CXCR4-RlucII)
+CXCL12
+wash
G
unstimulated
+CCL2
% Initial Surface CCR2
Start
Stim
Block
15 min
45 min
75 min
H
CCR2
PAR1
Ligand:
IP:FLAG
60 kDa -
PAR1
37 kDa -
CCR2
Input
50 kDa -
Tubulin
I
Receptor Remaining (% of Control)
**
CCR2
PAR1
Agonist:

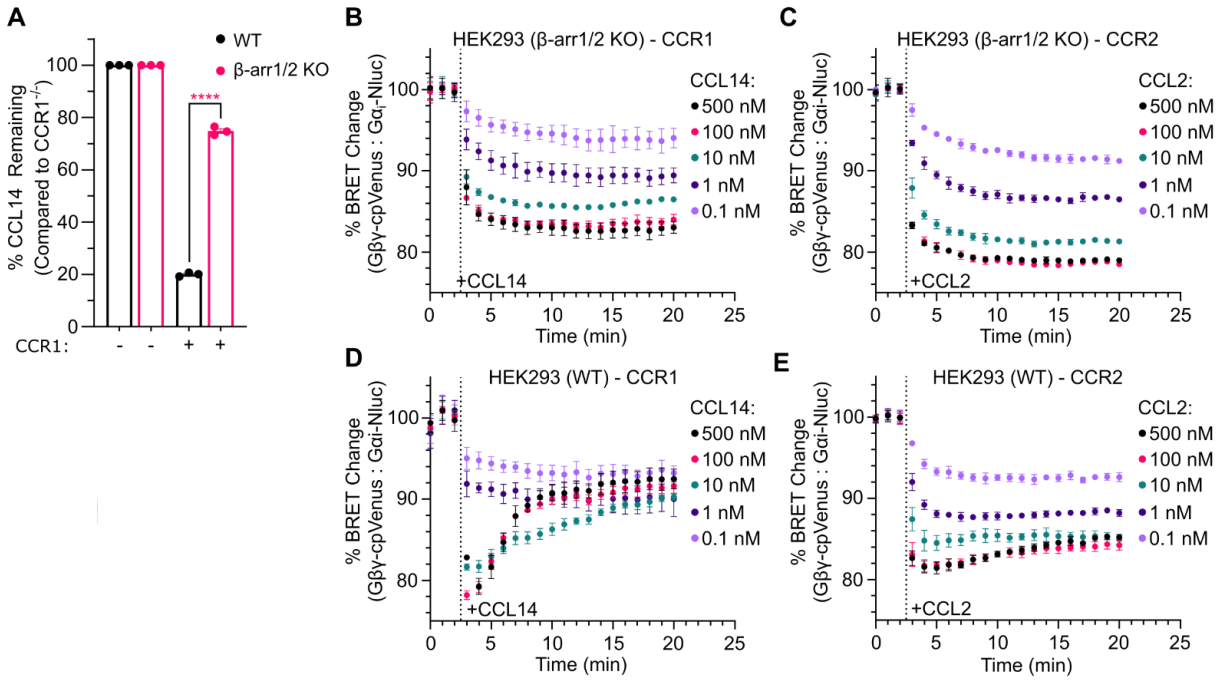

Figure 2.7. CCR1 and CCR2 have distinct mechanisms of chemokine scavenging. (**A**) WT HEK293 and β-arrestin1/2 KO HEK293 cells stably expressing CCR1 and respective non-expressing cells were cultured in media containing 5 nM CCL14 for 16 h. Remaining CCL14 was quantified by ELISA, interpolated from CCL14 standards and presented as a percentage of respective non-CCR1 expressing cells. (**B** to **E**) HEK293 β-arrestin1/2 KO cells (**B** and **C)** or HEK293 WT cells (**D** and **E**) expressing either CCR1 or CCR2 and transfected with an IRES vector coding for Gαi-Nluc and Gβγ-cpVenus were stimulated with 0.1-500 nM CCL14 or CCL2, respectively (indicated by dotted line). The dissociation of the Gβγ- from the Gα-subunit results in a decrease in BRET ratio upon agonist treatment and is expressed as a percentage of the BRET ratio to that observed in the untreated control cells. All data are expressed as the mean ± SEM of n ≥ 3 independent experiments. *P < 0.05, **P < 0.01, ***P < 0.001, ****P < 0.0001 versus controls, one-way analysis of variance (ANOVA) with Dunnet's multiple comparison test or unpaired t test.

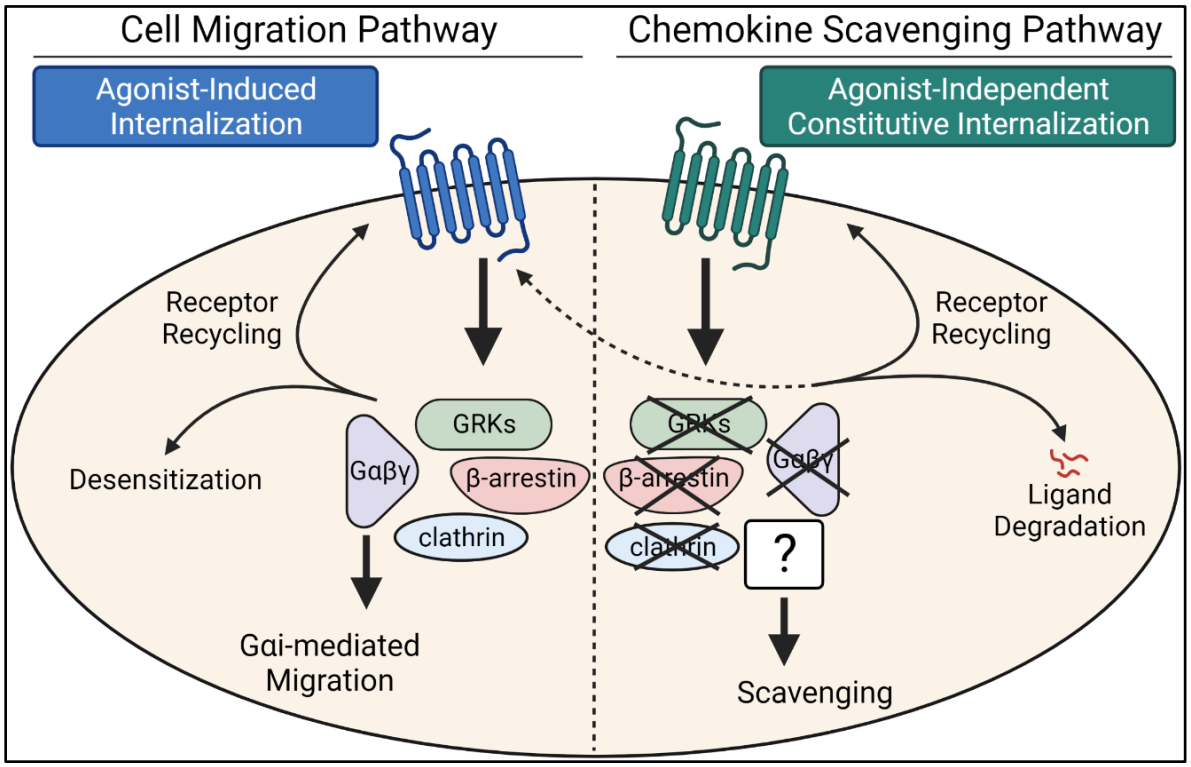

Figure 2.8. CCR2 appears to have two mechanistically distinct functional populations, one that regulates migration (left) and one involved in scavenging (right). The canonical GPCR interactors, including Gαβγ, GRKs, β-arrestins, and clathrin are primarily involved in the CCL2-induced internalization mechanisms and are part of the migratory population. These same interactors are dispensable for the scavenging population of CCR2, which instead can constitutively internalize while passively sequestering extracellular CCL2. The exact mechanisms and regulatory protein interactors involved in the scavenging pathway are yet to be determined. A key aspect of both populations is the ability of CCR2 to recycle to the cell surface to continue to drive G protein-dependent migratory functions as well as continue to scavenge excess chemokine. Additionally, the constitutively internalized receptor may provide non-desensitized receptor (dotted arrow) for the G protein-coupled pathway to allow sustained cell migration.

SUPPLEMENTAL FIGURES

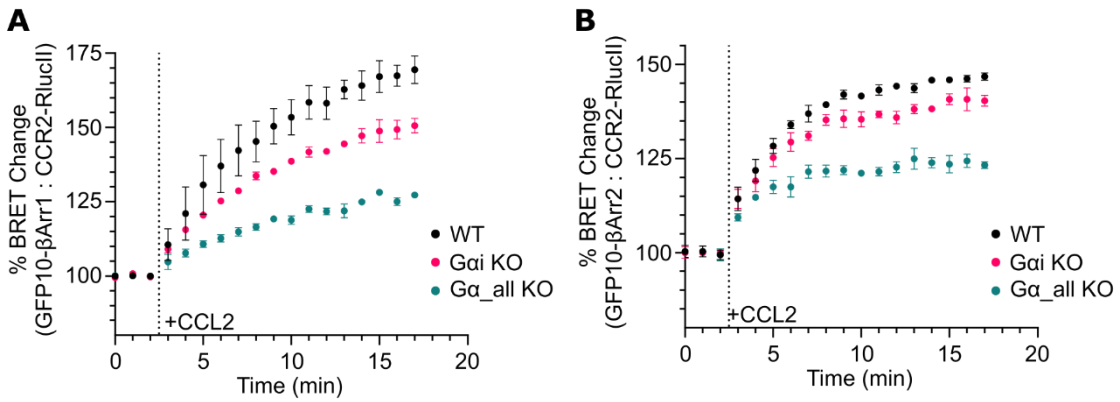

figure 2.S1. Direct recruitment of β-arrestin to CCR2 by BRET. (**A** and **B**) HEK293 cells transfected with CCR2-RlucII and GFP10-β-arrestin1 (A) or GFP10-β-arrestin2 (B) were stimulated with 100 nM CCL2 or left untreated. Data are presented as a percentage of BRET values to untreated controls. All data are expressed as the mean ± SEM of n ≥ 3 independent experiments.

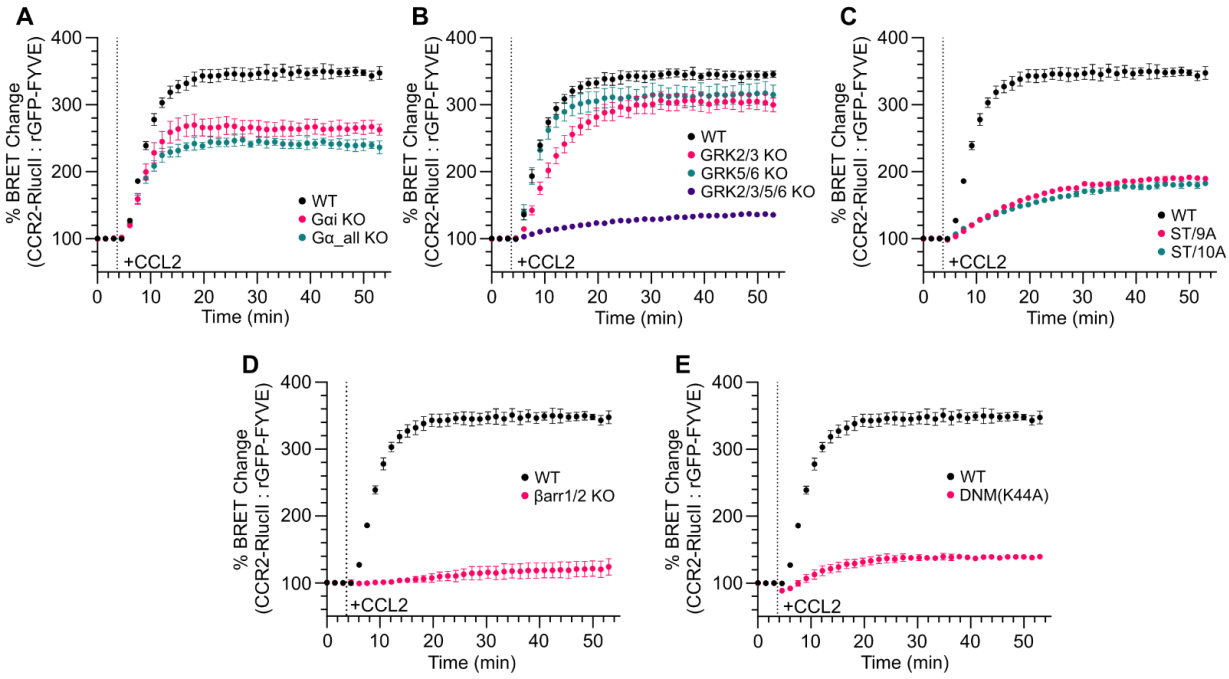

figure 2.S2. CCR2 association with early endosome marker rGFP-FYVE. (**A-B**) HEK293 or indicated KO cells transfected with CCR2-RlucII and rGFP-FYVE were stimulated at 37°C with 100 nM CCL2 or left untreated. (**C**) HEK293 transfected with CCR2-RlucII, CCR2-ST/9A-RlucII, or CCR2-ST/9A-RlucII and rGFP-FYVE were stimulated at 37°C with 100 nM CCL2 or left untreated. (**D**) HEK293 or indicated KO cells transfected with CCR2-RlucII and rGFP-FYVE were stimulated at 37°C with 100 nM CCL2 or left untreated. (**E**) HEK293 cells transfected with CCR2-RlucII and rGFP-FYVE alone or with DNM(K44A) were stimulated at 37°C with 100 nM CCL2 or left untreated. Data are presented as a percentage of BRET values compared to untreated controls. All data are expressed as the mean ± SEM of n ≥ 3 independent experiments.

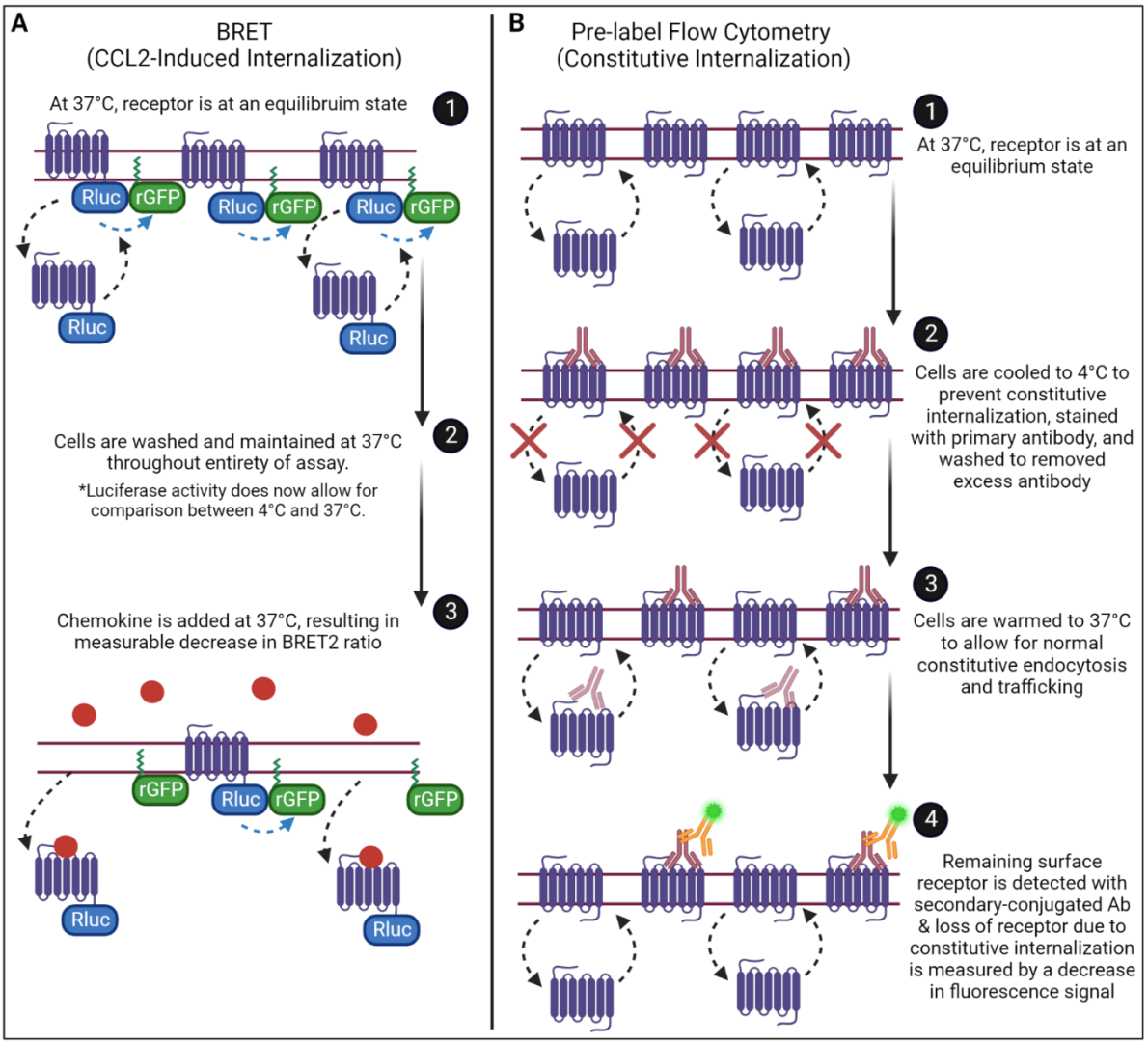

figure 2.S3. Methods for CCL2-induced versus constitutive internalization of CCR2. (**A**) In the BRET-based method of CCL2-induced internalization, cells are maintained at 37°C throughout the experiment, therefore any processes which occur continuously or at an equilibrium state (i.e., constitutive internalization) gives rise to our baseline BRET state. Only after some perturbation, such as addition of CCL2, can we measure a change from the baseline. (**B**) To measure constitutive internalization, a pre-label flow cytometry-based method is used. Cells are chilled to 4°C, preventing internalization, and surface receptor is labeled. Cells are then warmed to 37°C (without ligand), allowing for constitutive internalization and endocytic trafficking of the receptor, resulting in a decrease in labeled receptor at the surface. The amount of original (i.e. pre-labeled) receptor remaining at the surface can then be detected with a fluorescent secondary antibody and loss of receptor due to constitutive internalization quantified by the decrease in fluorescence signal compared to that initial surface receptor at 4°C.

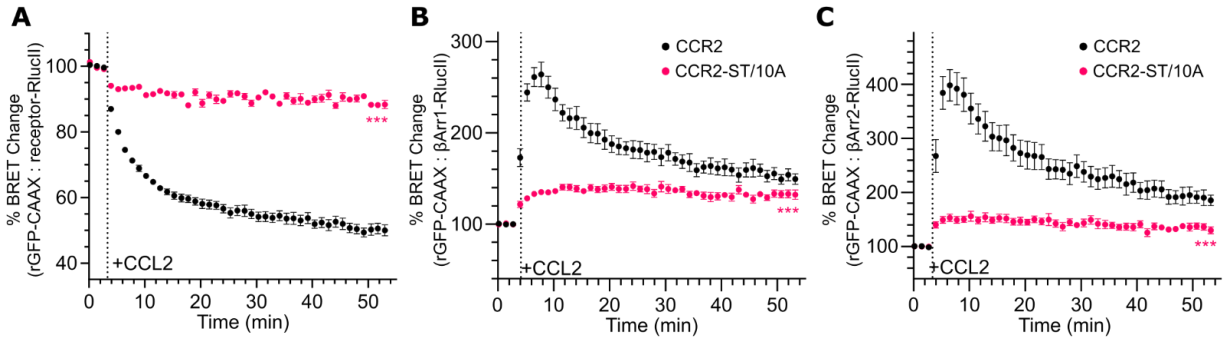

figure 2.S4. CCR2 internalization and β-arrestin recruitment of phosphorylation mutant CCR2-ST/10A. (**A**) CCR2 internalization assessed by BRET. HEK293 cells transfected with rGFP-CAAX and either CCR2-RlucII or CCR2-ST/10A-RlucII were stimulated with 100 nM CCL2 or left untreated. (**B** and **C**) β-arrestin recruitment assessed by ebBRET. Cells expressing CCR2 or CCR2-ST10/A transfected with β-arrestin1- or β-arrestin2-RlucII and rGFP-CAAX were stimulated with 100 nM CCL2 or left untreated. Data are presented as a percentage of BRET values for untreated controls. All data are expressed as the mean ± SEM of $n \geq 3$ independent experiments. *$P < 0.05$ versus controls.

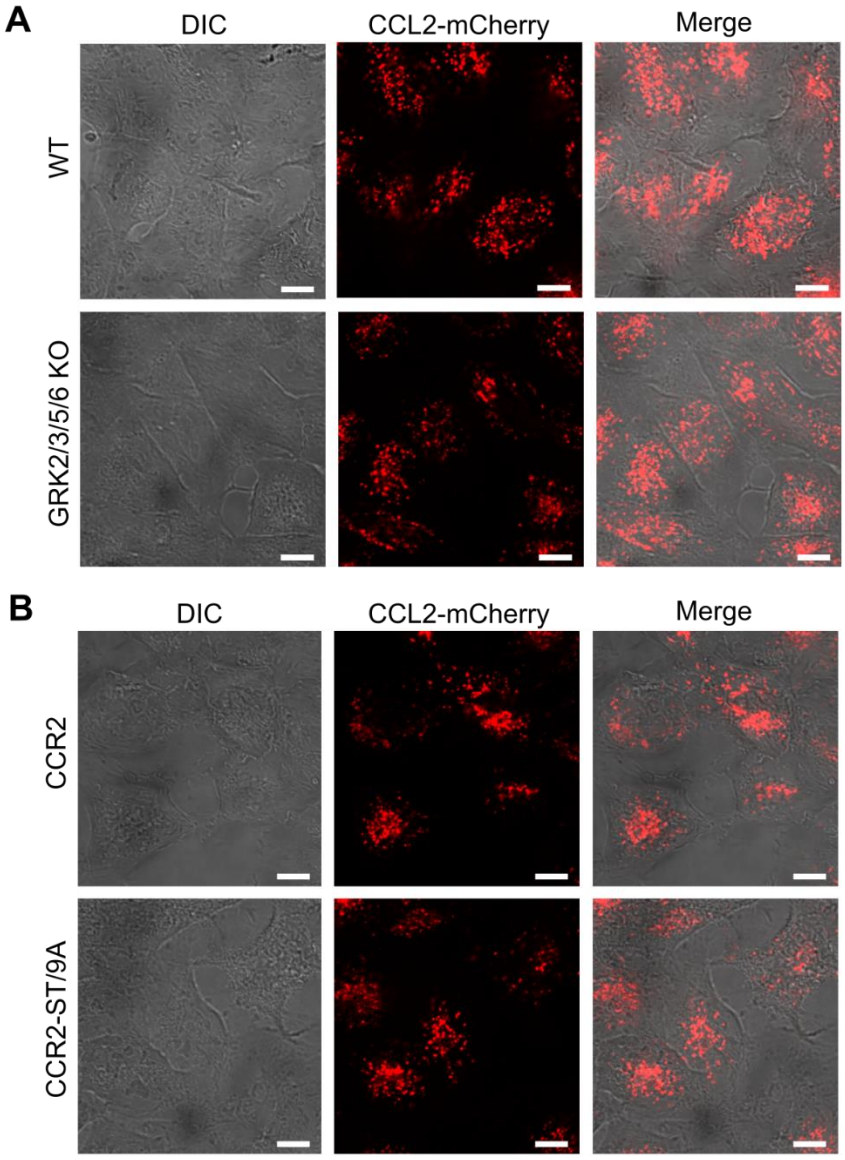

figure 2.S5. CCL2-mCherry is internalized by CCR2 independent of C-terminal phosphorylation. (**A**) WT HEK293A and GRK2/3/5/6 KO HEK293A cells stably expressing CCR2 were cultured in media containing 5 nM CCL2-mCherry. (**B**) HEK293 cells stably expressing WT CCR2 or CCR2-ST/9A were cultured in media containing 5 nM CCL2-mCherry. Live cells were imaged in phenol-red free DMEM media containing 2% FBS on an Eclipse Ti2-E spinning disk field scanning confocal system. Scale bars, 10 μM.

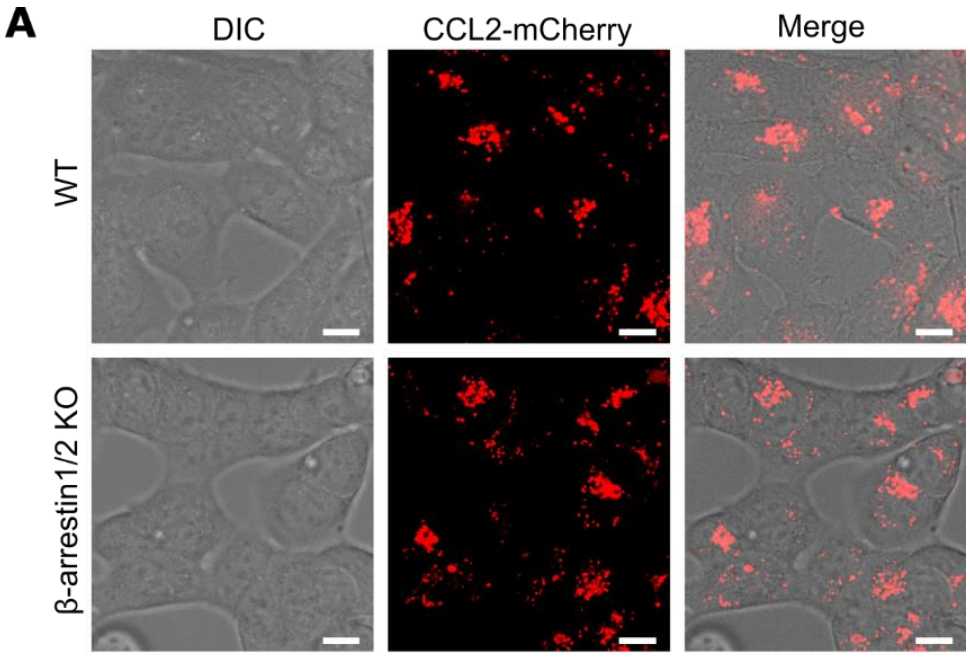

figure 2.S6. CCL2-mCherry is internalized by CCR2 in WT and β-arrestin1/2 KO HEK293 cells. (**A**) WT HEK293 (top) and β-arrestin1/2 KO HEK293 cells (bottom) stably expressing CCR2 were cultured in media containing 5 nM CCL2-mCherry for 16 h. Live cells were imaged in phenol-red free DMEM media containing 2% FBS on an Eclipse Ti2-E spinning disk field scanning confocal system. Scale bars, 10 μM.

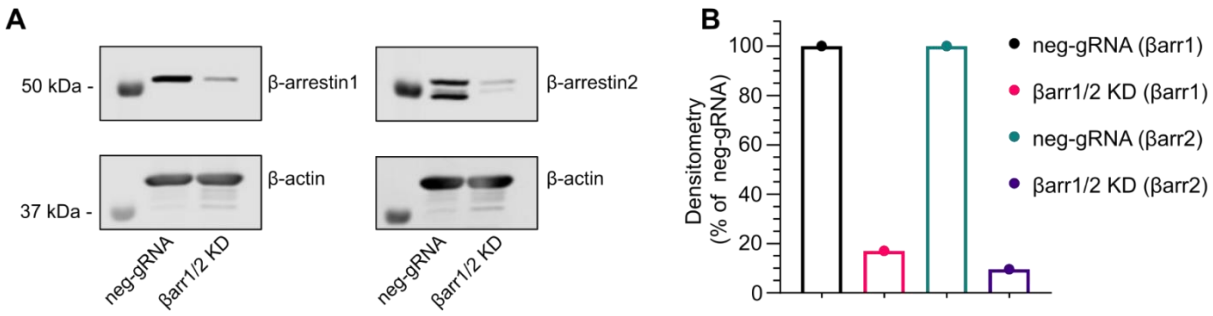

figure 2.S7. CRISPR knockdown of β-arrestin1 and β-arrestin2 in THP-1 cells. (**A**) Western blot probing using anti-β-arrestin1, anti-β-arrestin2, and loading control β-actin of THP-1 non-targeting gRNA lentiCRISPRv2 transduced (neg-gRNA) and THP-1 β-arresitn1/2 KD lentiCRISPRv2 transduced (βarr1/2 KD) cell lines. (**B**) Densitometry of β-arrestin1 and β-arrestin2 knockdown normalized to β-actin loading control and expressed as percent of neg-gRNA control.

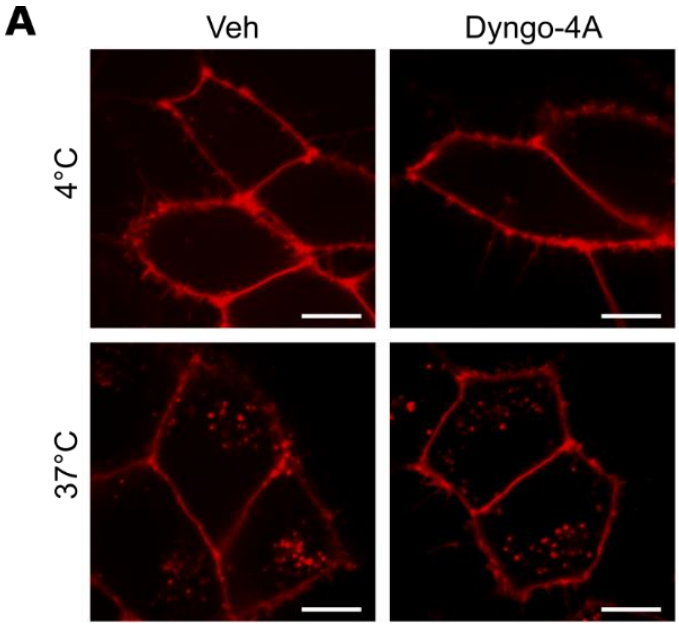

figure 2.S8. Constitutive internalization of CCR2 is unaffected by Dyngo-4a. (**A**) Constitutive internalization was visualized by fluorescence confocal microscopy in HEK293 cells expressing SNAP-CCR2 treated with vehicle or 30 μM Dyngo-4a and labeled with cell impermeable SNAP-Surface Alexa Fluor 648 at 4°C for 1 h and then were either held at 4°C for 45 min (top panel) or transferred to 37°C for 45 min (bottom panel) before being analyzed. Scale bars, 10 μm.

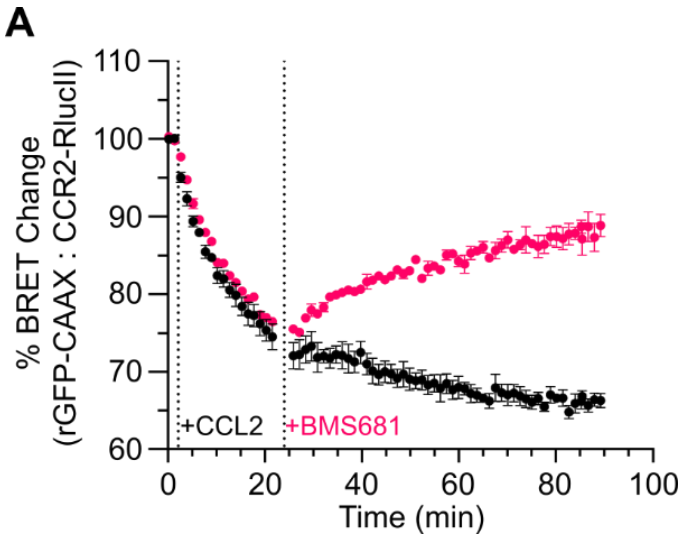

figure 2.S9. CCR2 recycles to the plasma membrane following receptor inhibition with BMS681. (**A**) HEK293 cells were transfected with rGFP-CAAX along with CCR2-RlucII. Cells were stimulated at 37°C with CCL2 (10 nM) and subsequently treated with CCR2 antagonist BMS681 (1 µM) or left untreated. Data are presented as a percentage of BRET values for non-chemokine treated controls. Data is expressed as the mean ± SEM of n ≥ 3 independent experiments.

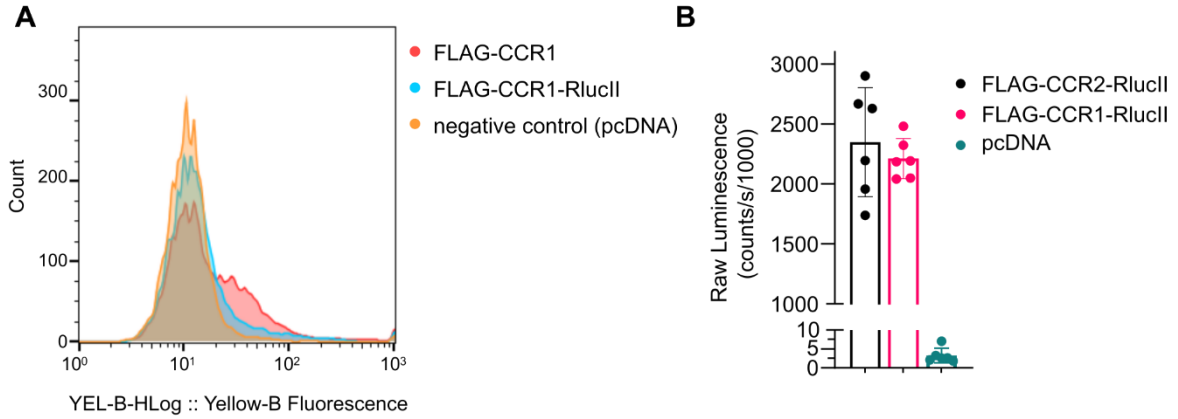

figure 2.S10. RlucII-tagged CCR1 does not express on the cell surface. (**A**) HEK293 cells were transfected with FLAG-CCR1, FLAG-CCR1-RlucII or pcDNA. Twenty-four hours post-transfection, cells were labeled with anti-CCR1 and subsequently stained with secondary PE-conjugated antibody. Surface expression was assessed by flow cytometry. (**B**) HEK293 cells were transfected with FLAG-CCR2-RlucII. FLAG-CCR1-RlucII, or pcDNA. Twenty-four hours post-transfection, RlucII substrate Prolume Purple (2.5 µM) was added to the cells and luminescence was measured using a Spark microplate reader. Data is expressed as the mean ± SEM of n ≥ 3 independent experiments.

Acknowledgements

Chapter 2, in full, is a reprint of the material currently in press at Science Signaling. (T.M. Shroka, I. Kufareva, C.L. Salanga, T.M. Handel (2022)). “The dual function chemokine receptor, CCR2, drives migration and chemokine scavenging by distinct mechanisms.” The dissertation author was the primary researcher and author of this material.

CHAPTER 3

Title: Proximal proteome of C-C chemokine receptor 2 (CCR2) reveals novel endocytic trafficking patterns

INTRODUCTION

The chemokine receptor family, consisting of 22 receptors, makeup the largest family of rhodopsin-like (class A) G protein-coupled receptors (GPCRs) (*1*). These receptors are studied in regard to a variety of different physiological functions but are most notable for their role in development and in the immune response (*2*, *3*). They are also implicated in many disease pathologies, including autoimmune disorders, HIV, cancer, heart disease, and neurological disorders (*4–7*). These receptors have therefore been extensively pursued as therapeutic targets, and although GPCRs have been widely exploited pharmacologically, there are only 3 FDA approved chemokine receptor drugs, none of which are for treatment of any type of immune disorder (*8–12*).

The C-C chemokine receptor type 2 (CCR2) is widely studied in regard to its role in driving the migration of leukocytes to sites of inflammation, as well as its involvement in a wide range of pathophysiologies including rheumatoid arthritis, atherosclerosis, cancer, and neurological disorders (*13–19*). Additionally, within the chemokine receptor family are the atypical chemokine receptors (ACKRs). These four receptors (ACKR1-4) are unique due to the fact that they do not couple to or activate G protein, but rather act as professional chemokine scavengers by which they uptake and remove chemokine from the extracellular environment (*20*). This function has been shown to have a physiologically important role by modulating the amount of available chemokine available to activate other G protein-coupled chemokine receptors and drive certain cellular functions (*21–23*). Intriguingly, CCR2 is able to activate G protein and drive G protein mediated cellular functions such as cell migration, as well as scavenge its chemokine ligands (*24*, *25*). We and others have shown that like ACRKs, this scavenging function of CCR2 is G protein independent. Furthermore, in a

previous study, we revealed that CCR2 is able to scavenge chemokine independent of canonical mediators of GPCR endocytosis, including G protein receptors kinases (GRKs), receptor phosphorylation, β-arrestin, or clathrin (Chapter 2, under-review). Additionally, we determined that CCR2 constitutively internalizes independent of these canonical mediators and it is this constitutive internalization pathway which appears to play a large role in CCR2's scavenging ability. This lead us question what are the mediators of CCR2 trafficking along the canonical β-arrestin/clathrin-mediated endocytosis (CME) and the apparent non-canonical clathrin-independent endocytic (CIE) constitutive pathways.

The existing methods of probing GPCR trafficking are informative, however they often rely on overexpression and modification of the effectors that are being investigated. Additionally, many assays are limited to a single effector or pathway and have poor time resolution. Considering the breadth of pathways and effectors of the endocytic trafficking network, we utilized ascorbate peroxidase APEX2-based proximity labeling proteomics (APEX-MS) to uncover the complex endocytic effectors involved in CCR2 trafficking and function (*26*). This APEX-MS approach has previously been applied successfully to elucidate the spatial and temporal network of other Class A GPCRs, such as angiotensin II type 1 receptor (AT1R) and the mu-opioid receptor (*27, 28*). This method works via the ascorbate peroxidase APEX2, which when exposed to hydrogen peroxide (H_2O_2), rapidly produces short-lived (<1 ms) biotin-phenoxy radicals that covalently tag proximal proteins in a ~20 nm labeling radius (*26*). Following isolation of biotinylated proximal proteins via streptavidin affinity purification, we utilized tandem mass tag (TMT) sample labeling for analysis by quantitative mass spectrometry. This method allows for up to 16 labeled samples to be pooled and analyzed in a single mass spectroscopy experiment, providing relative

quantification of protein abundance while increasing the throughput of the MS data collection (*29*).

We have previously shown that loss of Gα proteins results in drastic decrease in β-arrestin recruitment and a more subtle loss of receptor endocytosis after stimulation with CCL2. Following receptor activation and prior to β-arrestin recruitment, CCR2 is phosphorylated primarily by the G protein receptor kinase (GRK) 2 (*30*, *31*) and is subsequently able to associate with β-arrestins which initiate the endocytic process. Both GRK2 and GRK3 contain a pleckstrin homology (PH) domain which facilitates their recruitment to the plasma membrane (PM) via interaction with Gβγ. The absence of Gα results in the loss of receptor-localized Gβγ and therefore a decrease in GRK2/3 recruitment to the receptor preventing the subsequent interaction with β-arrestin and internalization. Thus, to enrich and probe for pathways or interactions which occur independent of G protein activation and β-arrestin recruitment, we sought to decouple CCR2 from G protein using pharmacological inhibitors, Pertussis toxin (PTx) and the $G\alpha_q$ inhibitor YM-254890. The exotoxin PTx inhibits members of the Gi/o protein family (Gαi, Gαo, and Gαt) by ADP-ribosylation of the C-terminus which prevents the G protein from coupling to the receptor and therefore prevents GDP/GTP exchange of Gα preventing its dissociation from Gβγ (*32*, *33*). Similarly the cyclic depsipeptide YM-254890 inhibits GDP/GTP exchange reaction of $G\alpha_q$ by binding to the hydrophobic cleft thereby stabilizing inactive GDP-bound state, and at higher concentrations has been shown to act as a broad spectrum inhibitor of additional Gα subtypes including $G\alpha_s$, $G\alpha_{11}$, and $G\alpha_{14}$ (*34*, *35*). By preventing the receptor mediated activation of G protein, we therefore prevent the dissociation of Gα from Gβγ and thereby reduce GRK2/3 recruitment and β-arrestin association. With these perturbations in

combination with APEX-MS we aimed to spatially and temporally identify mediators of canonical CME and non-canonical CIE CCR2 trafficking mechanisms.

RESULTS

Production and characterization of CCR2-APEX

From previous receptor-fusion constructs we anticipated that CCR2 would tolerate a large C-terminal tag such as APEX2. Indeed, we observed that the C-terminally tagged receptor (CCR2-APEX) remained functional and had nearly identical internalization properties, chemokine scavenging, β-arrestin recruitment, and G protein activation as untagged CCR2 (**fig. S1**). Next, via lentivirus-based integration, we generated HEK293 CCR2-APEX stable expressing cells. In order to create what we believe to be a more physiologically appropriate level of receptor expression, we FACS sorted for the lowest ~30% of expressors based on surface receptor antibody staining (**fig. S2**). Similarly, we generated and sorted the three APEX spatial reference marker cell lines (Cytoplasmic, EGFP-APEX2; PM, Lyn-EGFP-APEX2; Endosomal, EGFP-FYVE-APEX2) (*28*). Prior to preparation of APEX-MS samples we also confirmed the complete inhibition of G protein with PTx and YM-254890 via Ca+ flux and Gαβγ dissociation (**fig. S3**).

Preparation of the APEX-MS samples were prepared based on methods described by Hung et al. CCR2-APEX expressing cells described above were pretreated with biotin-phenol and vehicle (Normal G) or combination of PTx + YM-254890 (Gα Inhibited). Subsequently, CCR2 was activated with CCL2 at a concentration of 50 nM over a time course of up to 60 minutes (**Fig. 1A**). At selected time points after receptor activation, we

initiated proximal biotin labeling by addition of H_2O_2 for 20 seconds, followed by quenching of the reaction, cell lysis, and capture of biotinylated proteins using streptavidin magnetic beads. Samples were then washed, digested, and labeled using TMT 16-plex. Relative abundance changes of biotinylated proteins after agonist stimulation, was assessed using unbiased quantitative mass spectroscopy.

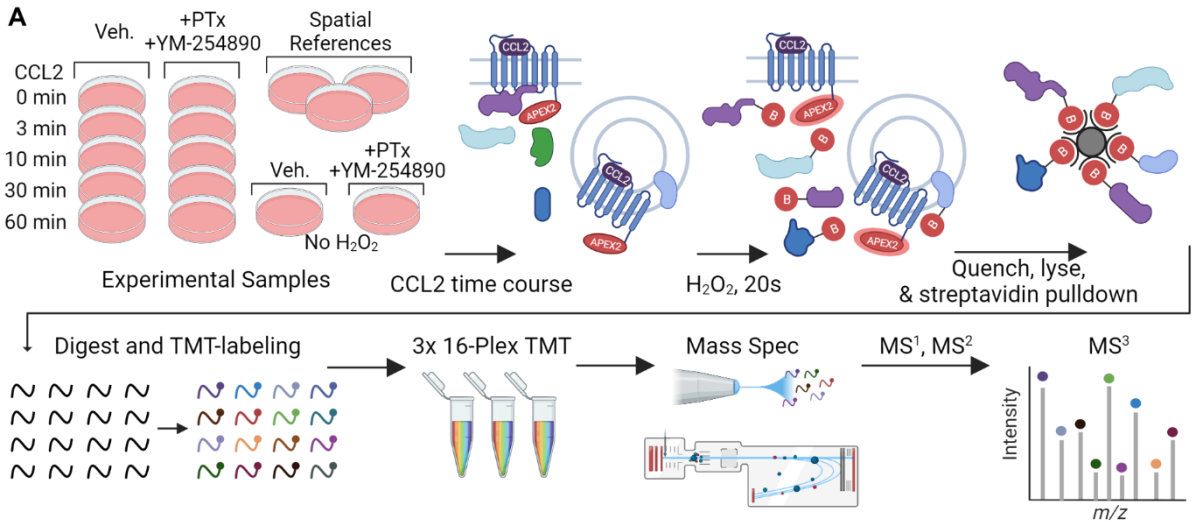

Figure 3.1. CCR2 APEX-MS experimental design. (**A**) HEK293 cells stably expressing CCR2-APEX treated with either vehicle or combination of PTx and YM-254890 are stimulated with CCL2 over a time course of 60 min. Following stimulation period, H_2O_2 is added for 20 seconds, biotinylating proximal proteins (< 20 nm) and immediately quenched. Cells are then lysed, and biotinylated prey proteins are captured by streptavidin pull-down. Following digestion, peptides are TMT-labeled and quantified by mass spectrometric analysis.

Loss of G protein coupling results in subtle differences in CCR2 endocytic trafficking dynamics

We originally sought to decouple CCR2 from canonical endocytic pathways by preventing G protein coupling and therefore perturbing the GRK2/3 recruitment and subsequent interaction with β-arrestin and other typical downstream mediators of internalization (Shroka et al. under-review, (*36*)). Globally, the observed differences in overall biotinylated proximal proteins across the stimulation time course were relatively similar between the two treatment groups. However, the change in proximal proteins is decreased in the 3-minute and 10-minute time points of the G protein inhibitor treated group as compared to the untreated (i.e., Normal G) group, indicated by protein quant fold changes closer to 0 (**Fig. 2 A** and **B)**. This disparity becomes less obvious at the later 30- and 60-min time points. These proteomic differences coincide with our CCR2 BRET-based internalization experimental data, which shows CCR2 internalization is slowed when G protein is inhibited (**Fig. 2C**). Similarly, using proto-oncogene tyrosine-protein kinase Src (SRC) as a marker for the PM (*37*) we observe that the changes in SRC biotinylation quants decreases with a similar trend as our BRET-based internalization data, indicated that CCR2 does appear to leave the PM less efficiently when it is unable to activate G protein (**Fig. 2D**). These results highlight the ability of CCR2 to internalize independent of G protein. This is consistent with previous data (Shroka et al., *25*, *32*) as well as the fact that the ACKRs are able to internalize without coupling to G protein (*39–41*). Along with a lack of incomplete loss of β-arrestin association (**fig. S4 A** and **B**), these results suggest that GRK5/6 mediated receptor phosphorylation may be more involved than previously believed, or that GRK2/3 recruitment to the PM by Gβγ is not as dependent on receptor-mediated Gα activation (*30*,

36, *42*). This also suggest that it may be simply an active confirmation, regardless of G protein coupling, that is able to drive such significant receptor internalization and trafficking along endocytic pathways.

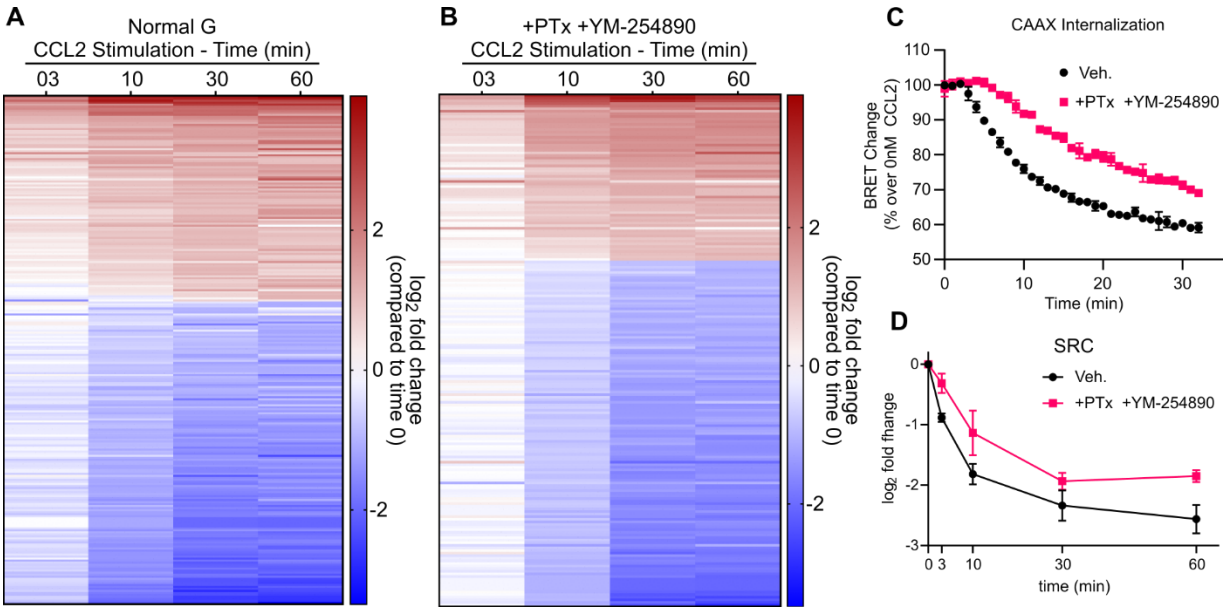

Figure 3.2. Differences in proximal proteins between Normal G and inhibitor treated CCR2-APEX2 samples are most apparent at the 3 and 10 minute time points. (**A** and **B**) Heatmap of untreated (i.e. Normal G) (A**)** and of G protein inhibitor treated (+PTx +YM-254890) (B) showing all proteins with a significant ($p < 0.01$, Log2 fold change > 1 compared to 0 min timepoint) change in biotin labeling following stimulation with CCL2. (**C**) CCR2 internalization assessed by BRET. Cells transfected with CCR2-RlucII and rGFP-CAAX were treated with vehicle or G protein inhibitors PTx and YM-254890 and subsequently stimulated with 100 nM CCL2 or left untreated. The BRET ratio changes upon agonist treatment are expressed as a percentage of the BRET ratio observed in untreated controls. (**D**) Targeted analysis of CCR2-APEX2 internalization using change in SRC biotinylation as a PM localization marker.

Inhibition of $G\alpha_i$ and $G\alpha_q$ has minimal affect on interactors of CCR2 following receptor activation

The proximal protein environment was surprisingly similar between the untreated and G protein inhibited experimental groups. Nevertheless, we sought to identify potential novel interactors which may be involved in G protein dependent and independent pathways. A typical approach in significance determination of individual proteins is to use the statistical analysis method ANOVA to compare conditions and times for a given protein and report on the variance of MS abundance quantities. This does not account for instances where a protein is significantly varied across all conditions but present similar profiles in response to time post ligand addition for both untreated and G protein inhibited conditions. Such cases returned as significantly varied but lacked distinction between conditions. For identifying proteins, a metric that measures differences between these condition-protein time response profiles was developed.

This determination is as follows: First, proteins are analyzed per condition using an adjusted ANOVA through the limma R library (*43*). Subsequently, the protein entries are filtered to include proteins that significantly varied (p-value < 0.05) in at least one of two conditions. Protein data were then reevaluated solely in respect to their time, including both conditions when reprocessing with adjusted ANOVA. Comparisons were made between the maximally significant condition for a protein and its collated significance. If significance is lower when evaluated collectively than individually, this is an indicator of a response that is both significant and varies differently between treatments (**Fig. 3A**).

Due to the high similarity between our treatment groups, many of the most variant proteins appear to not be involved in receptor trafficking and are largely due to the lack of

variance between the 0, 30, and 60 min time points as well as noise within the dataset **(Fig. 3B**). We therefore intend to further assess the difference between the 3-min and 10-min time points due to the observed variance of these samples. We also hope to identify significant and biologically relevant proximal proteins whose biotinylation remains consistent throughout the stimulation time course, which could possibly indicate these proteins are more closely or directly interaction with CCR2 regardless of CCL2 stimulation. Further biological validations of these interactors will need to be pursued; however, this data highlights the power of this computational method which can be implemented to future datasets in order to confidently identify variant proximal interacting proteins. Finally, although difference between the untreated and G protein inhibited groups were not immediately obvious, this study has provided a wealth of information pertaining to the spatial-temporal trafficking of CCR2 following CCL2 stimulation.

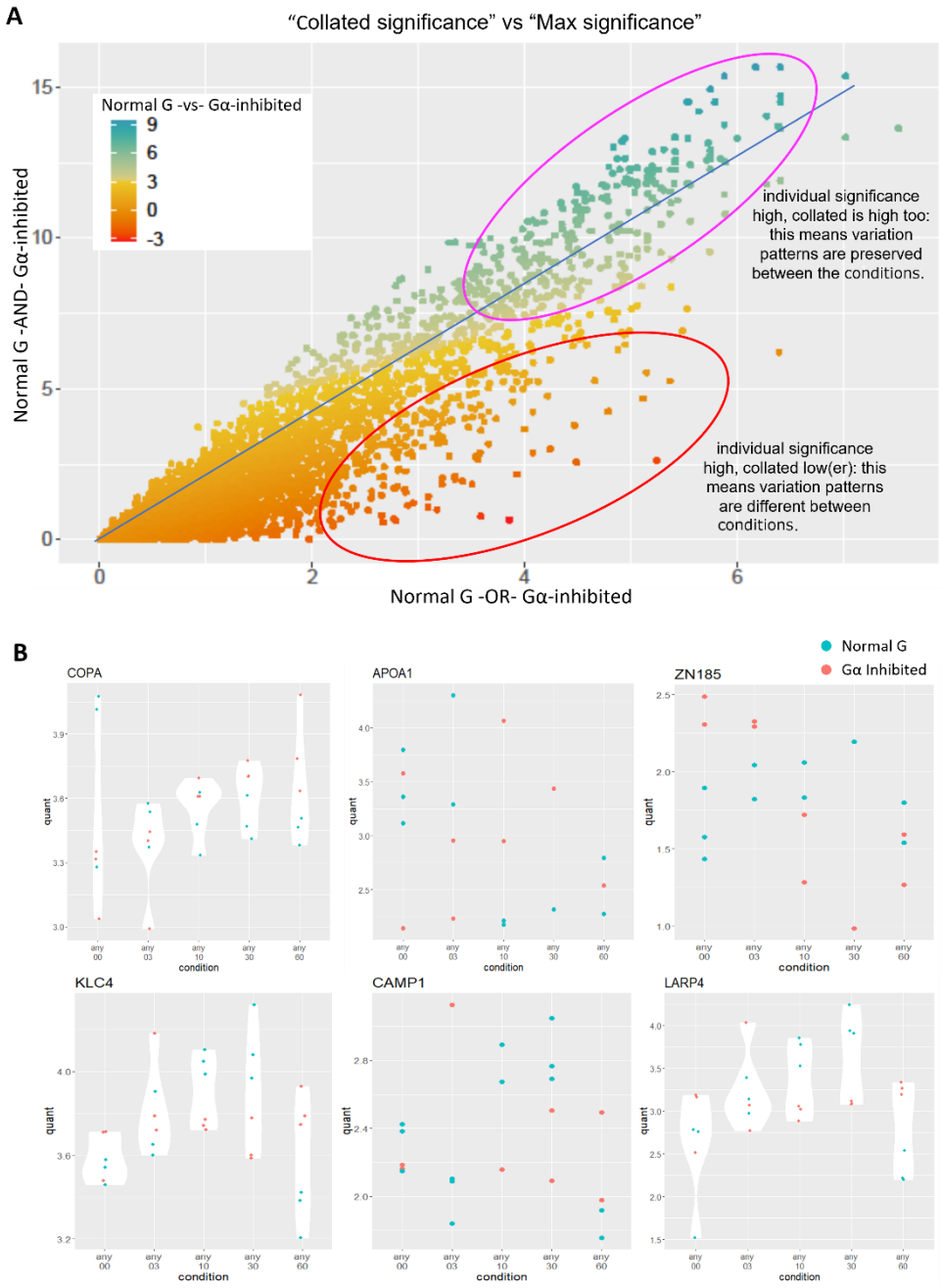

Figure 3.3. Determination of time course differences to identify proteins with high variance between Normal G and Gα inhibited samples. (**A**) Plot of max significance and collated significance between normal and G protein inhibited samples. High "OR" versus "AND" significance of collated data identify proteins with high variance between the two treatment groups. (**B**) Hits of the most variant proteins based on time course differentials.

Proximal proteome time course profiles confirm and expand previous receptor endocytic patterns

The endocytic trafficking of GPCRs involves a strictly regulated network of pathways controlled by an overwhelming wide number of proteins and is critical for the function and fate of internalized receptors. Following ligand-induced activation and endocytosis, the fate of CCR2 is poorly understood. Previous data has shown that following receptor activation, CCR2 is internalized to early endosomes, followed by sorting and fast recycling via the Rab4 mediated endosomal recycling pathway (Shroka et al., in press). Additionally, BRET association data has indicated that CCR2 does not traffic through slow Rab11-mediated trans-golgi network (TGN) but does traffic to Rab7 containing late endosomes (Shroka et al., in press). The fate of CCR2 trafficking through late endosomes is also unclear, with some groups showing CCR2 degradation and lysosome association whereas we have shown essentially no degradation in cultured HEK293 or THP-1 cells (*44*, *45*).

To better interpret the changes in proximal proteins along the CCL2 simulation time course, we performed statistical analysis of peptides with significant MS quant changes over time. Subsequently, for each identified protein within each treatment group, we scored changes in quant changes across the time course. We then explicitly calculated a distance matrix based on p-value of the collated response profiles followed by hierarchical clustering. The hierarchical clusters were then plotted as time course profiles across the CCL2 stimulation timepoints and gene ontology (GO) enrichment analysis was determined for each cluster. Within the time course clustering data, we identified five profiles which

illustrate CCR2's trafficking pattern and location within the endosomal network following ligand stimulation.

Following CCR2 activation, β-arrestin associates with the receptor and acts as a scaffold for internalization machinery including AP2 complex and clathrin, where ultimately the receptor is endocytosed in clathrin coated pits (CPP) (*46*). The time course profile "Cluster 1" (**Fig. 4A**) was identified containing proteins associated with CCP which showed rapid and persistent localization to CCR2-APEX2 (*37*). Within this profile, we observe localization with β-arrestin2 (ARRB2) (**Fig. 4B**), and the proteomic time course profile shows remarkable similarity to the response we observe when measuring β-arrestin2 association to the PM by bioluminescence resonance energy transfer (BRET) following CCR2 activation (**Fig. 4C**). Furthermore, we identify two proteins associated with CCP assembly that coincide with β-arrestin association to CCR2, intersectin 2 (ITSN2) and phosphatidylinositol binding clathrin assembly protein (PICAL) (**Fig. 4 D** and **E**) (*47*, *48*). The identification and MS-based quantification of these known and assumed interactors highlights the advantage of this APEX-MS method as well as the temporal sensitivity.

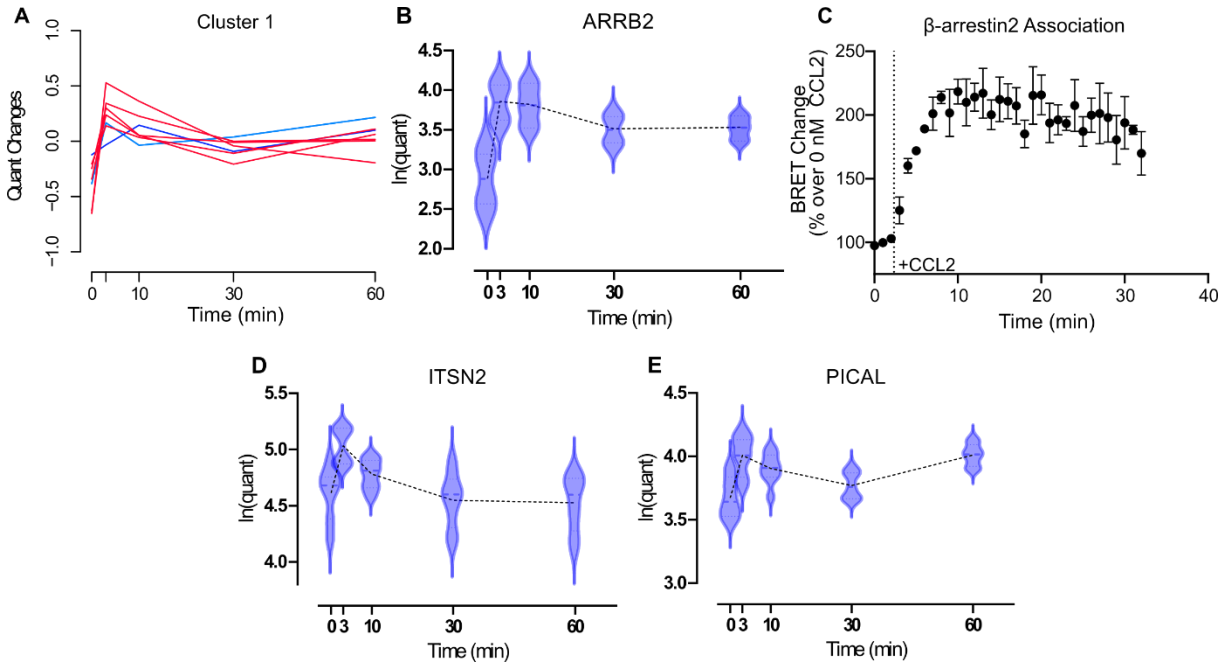

Figure 3.4. Rapid localization with clathrin coated pit assembly machinery and β-arrestin2. (**A**) Hierarchical time course clustering profile "Cluster 1" of proximal proteins with rapid association to CCR2-APEX2. (**B**) β-arrestin recruitment assessed by ebBRET. Cells transfected with β-arrestin2-RlucII and rGFP-CAAX stimulated with 100 nM CCL2 or left untreated. Data presented as a percentage of BRET values for untreated controls. **(C** through **E**) Quant changes of selected proteins belonging to Cluster 1, clathrin coated pit assembly machinery, ITSN2 and PICAL (C and D) and β-arrestin2 (E). Changes in protein quants are plotted as the natural log of quant values of individual peptides identified for each selected protein and averaged across Normal G APEX sample triplicates.

After CCR2 association with β-arrestin and formation of CCPs, the receptor is endocytosed and departs from the PM. Unsurprisingly, we identify a time course profile "Cluster 2" (**Fig. 5A**) containing proteins associated with PM (*37*) which show rapid and persistent decreasing biotinylation, indicative of CCR2-APEX2 internalizing and departing from the PM. Again, with this cluster, the proteomic time course profile shows remarkable similarity to the response we observe when measuring CCR2 dissociation from the PM by bioluminescence resonance energy transfer (BRET) following CCR2 activation (**Fig. 5B**). This similarity is further confirmed by the time course quant changes of known PM markers, proto-oncogene tyrosine-protein kinase Src (SRC), tyrosine-Protein Kinase Lyn (LYN), and Ras-related C3 botulinum toxin substrate 1 (RAC1) (**Fig. 5 C** through **E**).

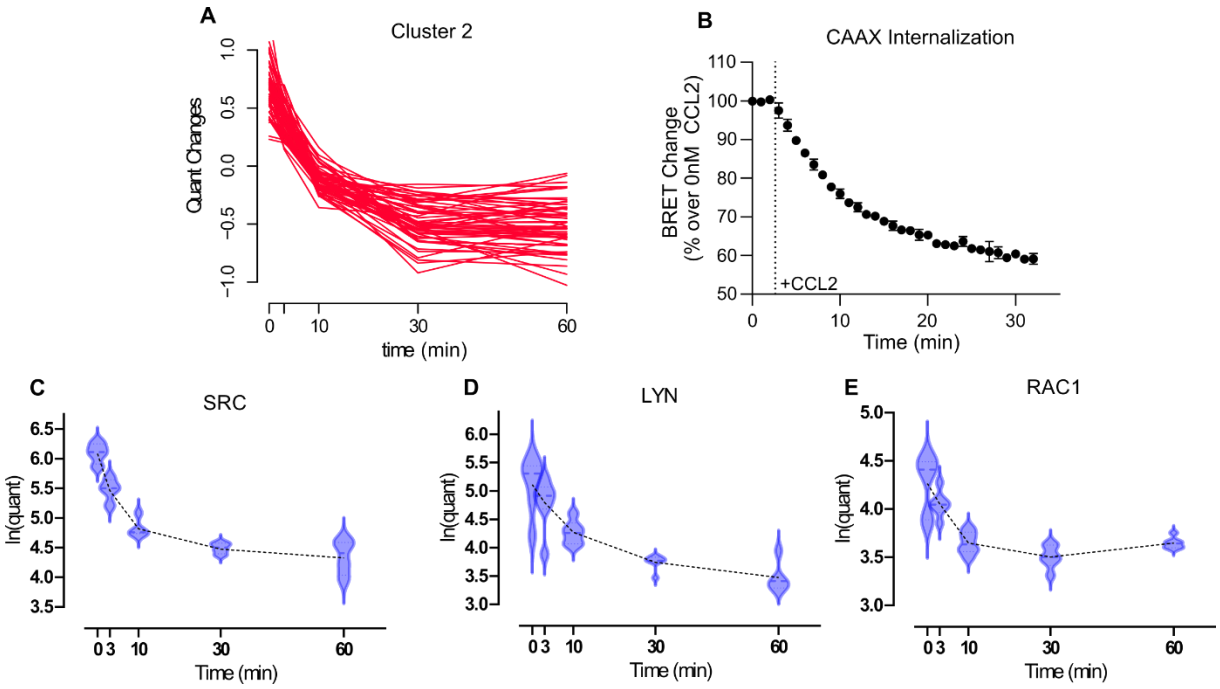

Figure 3.5. Time course profile of receptor departure from the plasma membrane. (**A**) Hierarchical time course clustering profile "Cluster 2" of proximal proteins with rapid dissociation from CCR2-APEX2. (**B**) CCR2 internalization assessed by BRET. Cells transfected with CCR2-RlucII and rGFP-CAAX stimulated with 100 nM CCL2 or left untreated. The BRET ratio changes upon agonist treatment expressed as a percentage of the BRET ratio observed in untreated controls. **(C** through **E**) Quant changes of selected proteins belonging to Cluster 2, markers of cytoplasmic facing side of the plasma membrane, SRC, LYN, and RAC1 (C, D, and E, respectively). Changes in protein quants are plotted as the natural log of quant values of individual peptides identified for each selected protein and averaged across Normal G APEX sample triplicates.

Following receptor internalization along CCP as well as CIE pathways, receptors converge on the early endosome before further endocytic trafficking. Once again, we identify a time course profile "Cluster 3" (**Fig. 6A**) containing proteins associated with early endosomes which show rapid and persistent increase in biotinylation, indicative of CCR2-APEX2 internalizing into early endosomes (*37*). Again, with this cluster, the proteomic time course profile shows remarkable similarity to the response we observe when measuring CCR2 association from the early endosome by BRET following CCR2 activation (**Fig. 6B**). This similarity is further confirmed by the time course quant changes of known early and sorting markers, early endosome antigen 1 (EEA1), small GTPase Rab5C (RAB5C), and sorting nexin 3 (SNX3) (**Fig. 6 C** through **E**) (*49–51*).

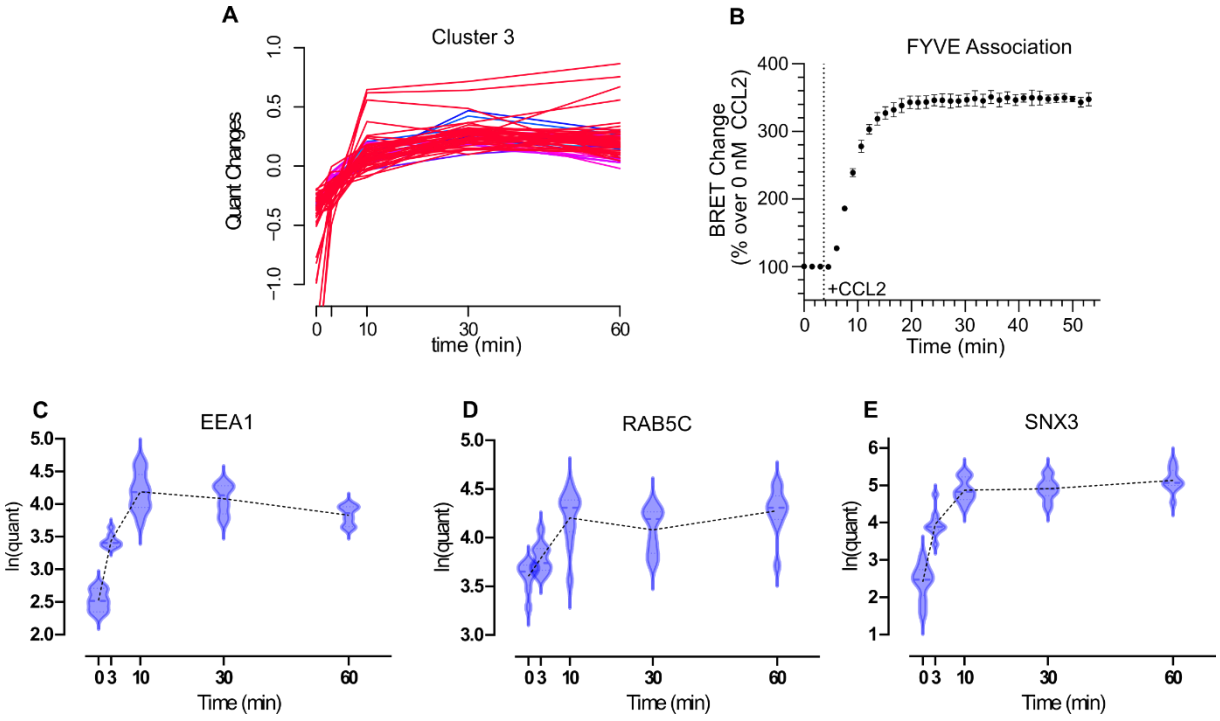

Figure 3.6. Endosomal association time course profile of CCR2-APEX. (**A**) Hierarchical time course clustering profile "Cluster 3" of proteins with rapid and persistent increasing proximity to CCR2-APEX2. (**B**) CCR2 early endosome association assessed by BRET. Cells transfected with CCR2-RlucII and early endosome marker rGFP-FYVE stimulated with 100 nM CCL2 or left untreated. The BRET ratio changes upon agonist treatment expressed as a percentage of the BRET ratio observed in untreated controls. **(C** through **E**) Quant changes of selected proteins belonging to Cluster 3, markers of early endosomal compartment, EEA1, RAB5C, and SNX3 (C, D, and E, respectively). Changes in protein quants plotted as the natural log of quant values of individual peptides identified for each selected protein and averaged across Normal G APEX sample triplicates.

Detailed information regarding the endocytic trafficking of CCR2 is limited and has lacked unbiased and comprehensive evaluation. We have previously investigated CCR2 trafficking into different endosomes using single rGFP-Rab markers, including association into fast recycling (Rab4), trans-golgi endosome (Rab11), and late endosomes (Rab7) (Shroka et al., in press). Additionally, we have investigated whether there is lysosomal degradation of CCR2 and have shown that there is no degradation of CCL2-stimulated receptor detected by western blot analysis in HEK293 or THP-1 cells (Shroka et al., in press). This however is conflicting with previous studies which suggest that CCR2 is partially degraded following endocytosis (*44*, *45*). Once again, our proteomic time course clustering provides rich and confirmatory information regarding the trafficking of CCR2. Time course profile "Cluster 4" (**Fig. 6A**) indicates a slow and gradual localization of CCR2 into late endosomes and lysosomes. This data exemplifies our BRET association data of CCR2 with Rab7A following ligand stimulation (**Fig. 6B**). This same trend of CCR2 association with Rab7A can be observed in our proteomics data by the time course quant changes of the lysosomal Ragulator complex protein Lamtor1 (LTOR1) and small GTPase Ras-related protein Rab7 (RAB7A) late endosome maker (**Fig. 7 C** and **D**). Additionally, although we have previously been unable to observe any degradation of CCR2 following receptor activation, this MS data indicates that CCR2 is potentially being trafficked to lysosomes. We hypothesize that some amount of CCR2, along with CCL2, is trafficked towards degradation pathways however at some point CCR2 is able to escape this pathway, potentially during late endosome-lysosome fusion where CCL2 is degraded but CCR2 is able to 'kiss and run' and recycle along a pathway succeeding the late endosome. This

avoidance of lysosomal degradation is also likely as we observe persistent scavenging even along extended time courses.

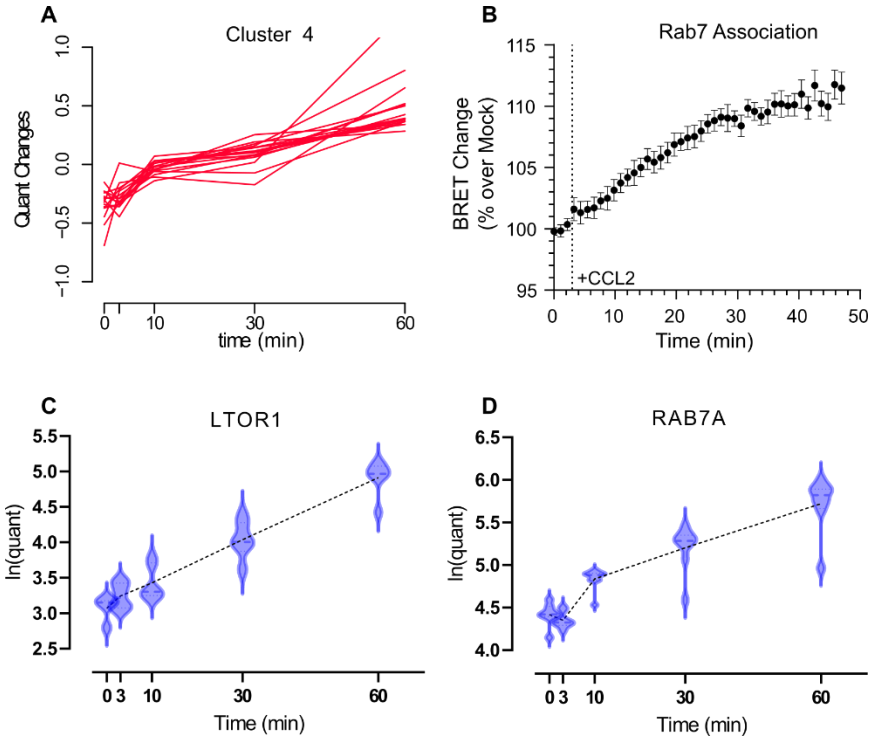

Figure 3.7. Slow and gradual localization of the receptor into late endosomes and lysosomes. (**A**) Hierarchical time course clustering profile "Cluster 4" of proteins with slow and persistent increased localization to CCR2-APEX2. (**B**) CCR2 association with late endosome marker Rab7 assessed by BRET. Cells transfected with CCR2-RlucII and early endosome marker rGFP-Rab7 stimulated with 100 nM CCL2 or left untreated. The BRET ratio changes upon agonist treatment expressed as a percentage of the BRET ratio observed in untreated controls. **(C** and **D**) Quant changes of selected proteins belonging to Cluster 5, markers of late endosomes and lysosomes, LTOR1 and RAB7A (C and D, respectively). Changes in protein quants plotted as the natural log of quant values of individual peptides identified for each selected protein and averaged across Normal G APEX sample triplicates.

Proximal proteome time course profiles identify novel endocytosis patterns

The motivation for these APEX proximity labeling proteomics experiments was to identify novel interactors of CCR2 that potentially influence receptor function, and particularly its scavenging function. As shown in time course Clusters 1-4, our proteomics-based analysis of CCR2 trafficking reliably profiles endocytic trafficking patterns of CCR2 based on changes in the proximal proteome of the receptor following CCL2 stimulation. We therefore sought to identify novel endocytic trafficking patterns of CCR2 which until now, have not been described.

Not surprisingly, we have identified several such proximal proteins in our dataset which have never been associated with CCR2 function, primarily involved in TGN recycling and exocytic pathways (**Fig. 8 & 9**). However, the biological validation and impact of individual proteins remains a labor intensive and difficult task. Furthermore, perturbations of individual interactors may not create a significant response due to compensatory effects of other proteins or pathways. We therefore sought to use our proximal proteome data to identify distinct pathways involved in CCR2 scavenging which could be more robustly disrupted by pharmacological inhibition/activation, mutagenesis, or gene silencing even if the specific perturbed target is not necessarily present within our dataset. This approach allows us to investigate the endocytic pathways and networks involved in CCR2 scavenging on a more global scale as opposed to individual interactors.

Two such pathways that our APEX data revealed to be worth further investigation are the TGN recycling and the exocytic pathway. Time course profile "Cluster 5" (**Fig. 8A**) contains several proteins associated with trans-golgi recycling. We had previous attempted to determine if CCR2 traffics to the TGN using Rab11 as a marker for trans-golgi

endosomes (**Fig. 7B**) and saw no significant association. However, our proteomics time course profile contains several TGN markers, including RAB8A/B, RAB10, and RAB13 (**Fig. 8 C** through **D**) (*52–54*). This data further highlights the limitations of using a single marker for determining receptor endocytic trafficking patterns. Additionally, Rab11 was not detected in our proteomic dataset, further indicating that it may be a poor choice as a TGN marker. This cluster profile highlights a suppression of biotinylated proteins of the TGN endocytic pathway following CCL2 stimulation. Indicating that CCR2 may be basally associated with and trafficking through the TGN and upon stimulation, this pathway of recycling is suppressed in favor of other endocytic networks. It could also be that activation of CCR2 results in a significant release of receptor from the TGN to potentially recover surface expression of receptor. Nevertheless, CCR2's association with the TGN is poorly characterized and may be contributing to its ability to scavenge chemokine. Further biological validation of this pathway will need to be address by using known modulators of TGN trafficking, such as Brefeldin A or nocodazole and their resulting effect on CCR2 function (*55–57*). These inhibitors, which have a much more global effect on the TGN, may provide more direct information as compared to attempting to individually knockout members of the Rab small GTPase family, which could have compensatory affects and lead to unclear conclusions. Indeed, preliminary data (not shown) seems to indicate that Brefeldin A disruption of the golgi-complex prevents CCR2 recycling to the cell surface following constitutive internalization, potentially confirming that under basal conditions CCR2 is internalized and subsequently recycled through the TGN to maintain an equilibrium of surface receptor as well as persistently scavenge chemokine.

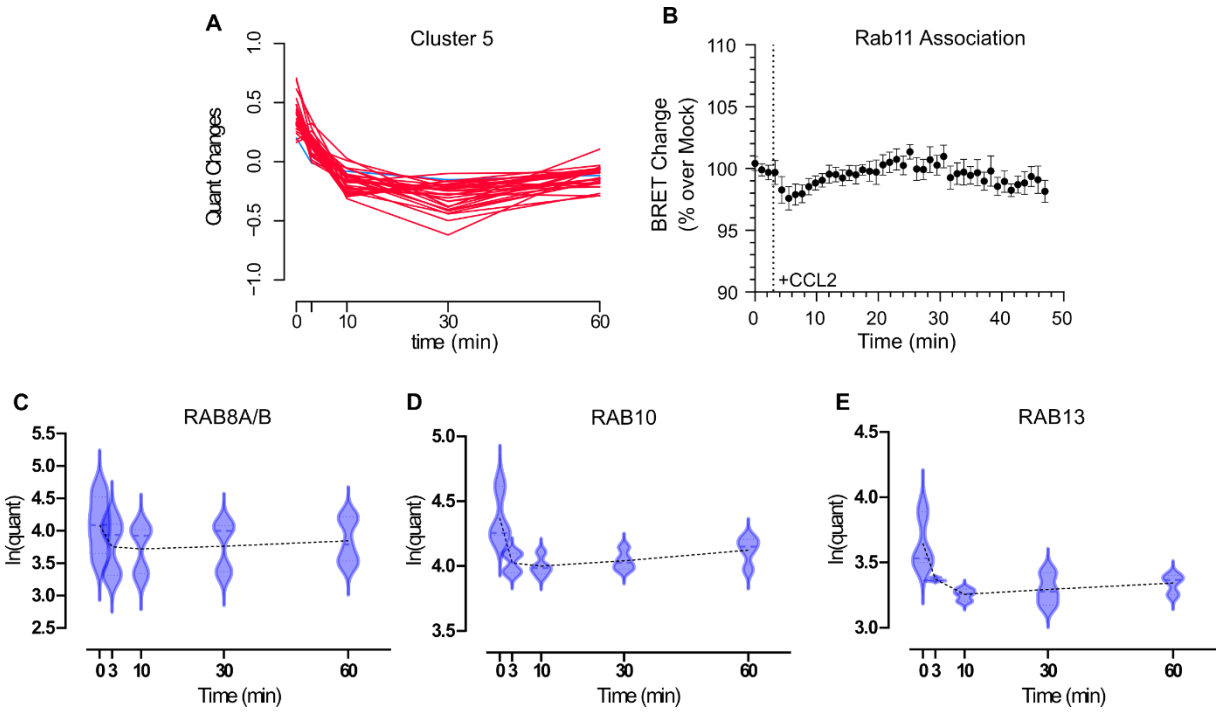

Figure 3.8. Suppression of trans-golgi network interaction following chemokine stimulation. (**A**) Hierarchical time course clustering profile "Cluster 5" of proteins with rapid (10 min) and persistent decrease in proximity to CCR2-APEX2. (**B**) CCR2 association with slow trans-golgi recycling marker Rab11 assessed by BRET. Cells transfected with CCR2-RlucII and early endosome marker rGFP-Rab11 stimulated with 100 nM CCL2 or left untreated. The BRET ratio changes upon agonist treatment expressed as a percentage of the BRET ratio observed in untreated controls. **(C** through **E**) Quant changes of selected proteins belonging to Cluster 4, markers of trans-golgi recycling endosomes, RAB8A/B, RAB10, and RAB13 (C, D, and E, respectively). Changes in protein quants plotted as the natural log of quant values of individual peptides identified for each selected protein and averaged across Normal G APEX sample triplicates.

The second pathway time course profile "Cluster 6" contains several proteins associated with the exocytic pathway and specifically several proteins associated with recycling to the PM (**Fig. 9A**) (*37*) . We had previous shown that CCR2 traffics to fast-recycling endosomes using Rab4 as a marker for recycling endosomes (Shroka et al., in press), but as with Rab11, Rab4 showed poor detection in our MS data. However, our proteomics exocytic time course profile contains several proteins association with exocytic machinery and receptor recycling, Annexin A7 (ANXA7) and Annexin 11 (ANX11) (**Fig. 9 B** and **C**) (*58–60*). This data further highlights the limitations of using single markers for determining mediators of receptor endocytic trafficking.

Involvement of these interactors of the exocytic pathway still needs to be verified with further biological experiments. As with the TGN, the most direct approach could be with the use of global or direct inhibitors of the exocytic pathway or members of the annexin GTPase family. Exocytic blockers such as Bafilomycin A1, botulinum toxin B and tetanus toxin and others have widely been used for the study of synaptic vesicle exocytosis but can be applied to other biological systems as well (*61–63*) and could potentially be a tool for elucidating the exocytic machinery involved in CCR2 trafficking. Additionally, the annexin A7 inhibitor, ABO (6-amino-2,3-dihydro-3-hydroxymethyl-1,4-benzoxazine) which directly binds annexin A7 preventing phosphorylation and thus GTPase activity is another potential target (*64–66*). Moreover, homozygous annexin A7 knockout mice are nonviable and even heterozygous knockouts have severe phenotypes (*67*, *68*), which further rationalizes the use of small molecule inhibitors which may allow for a more tunable inhibitory affect. More targeted perturbations should be explored once broader pathway perturbation is verified to affect receptor function. The identification of proximal proteins of exocytic pathways could

possibly be a result of CCR2's trafficking through the TGN where it is subsequently associated with exocytosis machinery as part of the post-golgi recycling pathway (*69, 70*). Dependent on further validation, this data could indicate a greater involvement of the TGN than previously realized for CCR2 trafficking and scavenging function, and perhaps it is this strong trang-golgi recycling association that allows CCR2 to persistently scavenge chemokine.

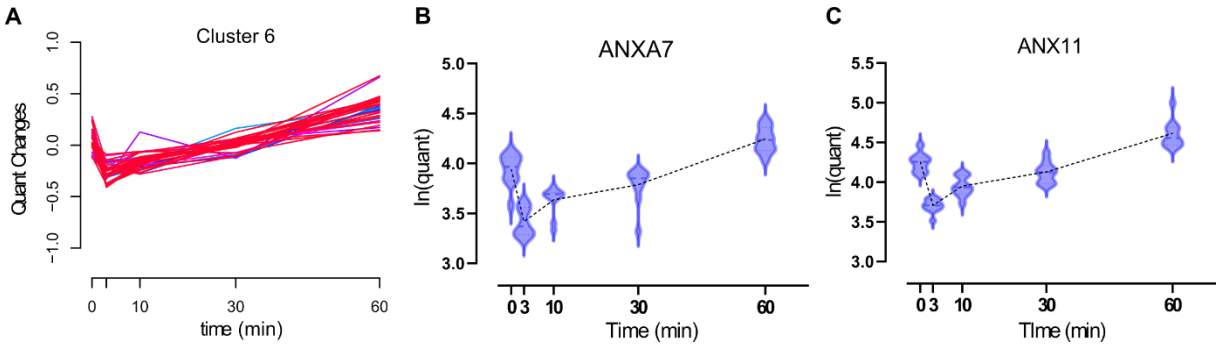

Figure 3.9. Short suppression then increasing association with exocytic machinery following CCL2 stimulation. (**A**) Hierarchical time course clustering profile "Cluster 6" of proteins with rapid (3 min) suppression followed by persistent increase in proximity to CCR2-APEX2. (**B** and **C**) CCR2 association with slow trans-golgi recycling marker Rab11 assessed by BRET. Cells transfected with CCR2-RlucII and early endosome marker rGFP-Rab11 stimulated with 100 nM CCL2 or left untreated. The BRET ratio changes upon agonist treatment expressed as a percentage of the BRET ratio observed in untreated controls.

DISCUSSION

The endocytic trafficking of GPCRs is widely studied and is undoubtedly a critical factor in receptor function, however detailed understanding of the fate of CCR2, and GPCRs in general, following receptor activation is currently incomplete. This is partly due to the primary focus of GPCR biology being activation, G protein signaling, and consequent cellular responses. Although interaction with β-arrestin and receptor internalization is widely studied, more complete information regarding the mechanisms of receptor trafficking further along the endocytic pathways is lacking. Previous studies probing the endocytic trafficking of CCR2, and GPCRs in general, have been sparse and often rely on limited methods, such as co-localization fluorescence microscopy, co-immunoprecipitation (co-IP), and BRET-based association. The application of these methods is limited to a small number of targets or pathways, have constrained time-resolution, and are generally low-throughput. A more completed understanding of CCR2 is required, especially in order to better identify the mechanisms underlying CCR2's often overlooked scavenging function.

With this study, we originally sought to identify novel interactors along G protein-coupled and G protein-independent pathways of CCR2 endocytosis and trafficking which could be influencing CCR2 scavenging. Unfortunately, no obvious proteins have been identified, however the similarity between the two treatment groups reveals several possibilities. Firstly, the observed delay but incomplete loss of CCR2 endocytosis in the presence of G protein inhibitors highlights that GRK2/3 mediated phosphorylation of CCR2 is most efficient when G protein activation is possible due to presence of Gβγ-mediate GRK association but is still able to occur independent of Gα activation, although less efficiently; or it may indicate that GRK5/6 may be more involved in CCR2 phosphorylation and

internalization than previously thought. Secondly, this data indicates that like ACKRs, CCR2 endocytic and scavenging mechanisms do not require G protein-coupling and emphasizes that G protein-dependent pathways play only a small role in CCR2 function. Finally, due to the minimal change observed in CCR2 function and proximal proteome caused by G protein inhibition, we hypothesize that scavenging by CCR2 may be a more significant function than previously realized. Undoubtedly, CCR2 G protein mediated migration of monocytes is a key function of the receptor, however once present at sites of inflammation the migratory function is less vital. Once located in tissue, the scavenging of chemokine becomes the more critical function of CCR2 and is not dependent on G protein-mediated pathways. This CCL2 sequestration by tissue-resident CCR2 expressing cells could also be the primary reason for the observed immunosuppressive effect of CCR2 in certain cancers and further highlights the impact of receptor scavenging and need for further investigation (*71*, *72*).

As shown in this study, the use of time-resolved APEX proximity labeling proteomics in combination with experimental spatial references and gene ontology information can provide a more complete picture of the endocytic trafficking patterns and general interactome of GPCRs. In combination with previous internalization and endocytic trafficking data regarding CCR2 (Shroka et al., in press), our data reveals a possible model for CCR2 trafficking at a constitutive and ligand-induced state (**Fig. 10**). In the absence of ligand, CCR2 is endocytosed along primarily CIE pathways and is trafficked through the TGN and eventually recycled back to the PM. Following CCL2-stimulation, CIE and TGN trafficking is reduced and instead CCR2 is internalized via clathrin-coated pits and associates with Rab4 fast recycling endosomes or to Rab7 containing late endosomes. After

prolonged CCL2 stimulation, CCR2 begins to reassociate with TGN exocytic machinery which we believe is due to TGN trafficking from the late endosome as well as reestablishment of CIE mechanisms as CCR2 begins to return to a more basal like equilibrium state. Further work needs to be done to elucidate more direct or subtle interactors of CCR2 along these pathways which could be playing a functional role, however this dataset provides a means to begin probing CCR2 trafficking in a more informed manner.

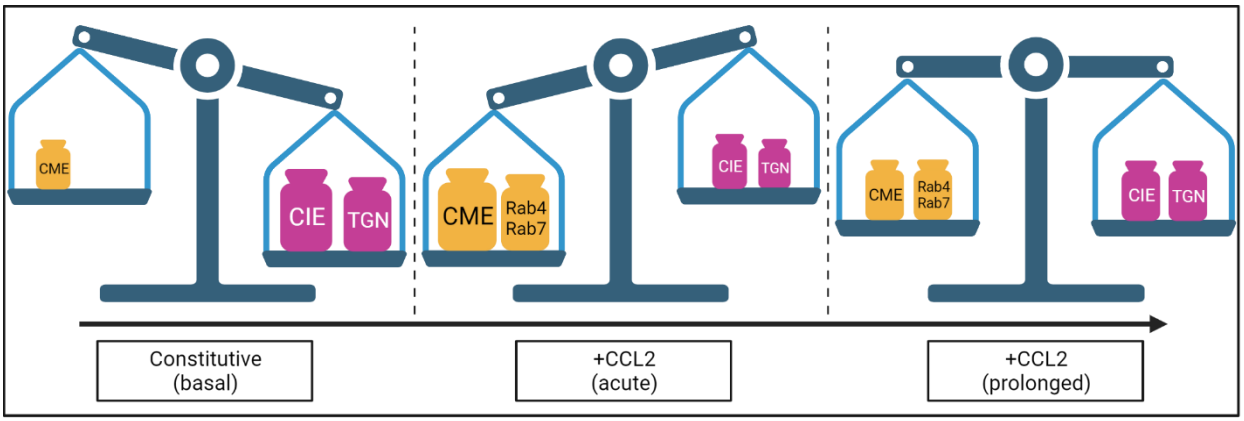

Figure 3.10. Model of CCR2 endocytosis and trafficking pathways across CCL2 stimulation time course. In the absence of CCL2, CCR2 primarily internalizes along CIE pathways and is trafficked through the TGN and recycled back to the cell surface. Following CCL2 stimulation, CCR2 internalization is driven along CME pathways and sorts to Rab4 and Rab7 containing endosomes. After prolonged stimulation with CCL2, CCR2 begins to reassociate with TGN and presumably CIE pathways while CME is reduced as the receptor internalization and endocytic trafficking begins to shift back towards a basal state.

The data provided by these findings can provide a wealth of information in order to better design more focused biological studies potentially targeting previously unexplored pathways or targets. It can also be used to confirm previous results from orthogonal biological methods, which is clearly shown regarding known interactors of CCR2 following receptor activation, including β-arrestin2, AP-2, EEA1, and others which validate previous known interaction and temporal profiles. This method also provides a more granular assessment of receptor interactors. A prime example of the more granular information gained from this study is the identification of proximal receptor interactions within the extensive Rab small GTPase family proteins. This could be a powerful tool for comparing the CCR2 function across different cell types which may have variable expression profiles of key interactors. Ultimately, this APEX-MS study begins to fill gaps in the current understanding of CCR2 endocytic network interactions and the potential implications for CCR2 scavenging, as well as substantiates further functional studies of CCR2, many of which have not been pursued before.

MATERIALS AND METHODS

DNA plasmids and cloning

The pcDNA3.1(+) constructs of β-arrestin1-RlucII, β-arrestin2-RlucII, rGFP-CAAX, rGFP-Rab4 and rGFP-Rab11 (*63*) were kindly gifted by Dr. Michel Bouvier (Université de Montréal, Canada). The rGFP-Rab7 construct was generated by PCR amplification of the Rab7 coding sequence of EGFP-Rab7A, a gift from Qing Zhong (UC Berkeley, CA, USA) (*64*) and in-frame insertion into the XbaI and PmeI sites of rGFP-Rab4 by DNA ligation.

Receptor-RlucII constructs was created by PCR amplification of the coding region of CCR2 and the product was subcloned in-frame at the N-terminus of the RlucII sequence into the pcDNA3.1 RlucII vector. The pcDNA3.1(+) constructs of PM-APEX2, Cyto-APEX2, and Endo-APEX2 were kindly gifted by Dr. Mark Von Zastrow (UC San Francisco, CA, USA) (*28*).

Cell lines

Stable CCR2-APEX2 and all spatial reference APEX2 cell lines were generated in HEK293 cells by lentiviral transduction using pLenti-CMV-Hygro expression vector, a gift from Eric Campeau & Paul Kaufman (University of Massachusetts Medical School, MA, USA) (*65*) and receptor surface expression confirmed by flow cytometry (Guava EasyCyte™ 8HT, Luminex) with an anti-hCCR2-PE (phycoerythrin) antibody (FAB151P, R&D Systems). All APEX2 expressing cell lines were then FAC-sorted for the lower ~30% of expressors with the support of the Flow Cytometry Core at the San Diego Center for AIDS Research. Cell lines were cultured in Dulbecco's modified Eagle's medium (DMEM), supplemented with GlutaMax (Gibco) and 10% fetal bovine serum (FBS) and grown at 37°C with 5% CO_2.

APEX biotinylated protein sample preparation

For CCR2-APEX2 experiment sample preparation the following method was used to perform biotinylation, enrichment and prepare the samples for MS analysis. Cells expressing CCR2-APEX2 were cultured in 15 cm dishes and 16 hrs before sample preparation were treated with PTx (200 ng/mL) or vehicle (PBS). The following day, 1 hr before addition of

chemokine, PTx treated cells were further treated with YM-254890 (100 nM). Cells were then pre-incubated with 500 μM biotin-phenol for 30 min at 37°C. 50 nM CCL2 was added for the noted period of time (0, 3, 10, 30, or 60 min). For the spatial references, cells expressing PM-APEX2, Endo-APEX2, and Cyto-APEX2 were incubated with 500 μM biotin-phenol for 30 min at 37°C, no chemokine was added to these cells. Immediately prior to use, H_2O_2 was diluted to 10 mM final in room-temperature DPBS. APEX labeling was initiated by adding the H_2O_2 DPBS solution at a ratio of 1:10 (i.e. 2.77 mL to 25 mL of media) with the 15 cm dishes containing cells and bioton-phenol culture media (1 mM final H_2O_2) and immediately mixing by gentle shaking. The labeling reaction was allowed to continue for 20 seconds, media was removed, and the cells were washed three times in ice cold quenching buffer (DPBS supplemented with 10 mM sodium ascorbate, 10 mM sodium azide, and 5 mM Trolox). Cells were incubated in quenching buffer for 20 min on ice, quenching buffer was removed, and cells were lysed in RIPA (50 mM Tris, 150 mM NaCl, 1% Triton X-100, 0.5% deoxycholate, 0.1% SDS, pH 7.4) supplemented with 10 mM sodium ascorbate, 10 mM sodium azide, and 5 mM Trolox, protease inhibitors, and 2.5 U/mL benzonase (Roche Complete). Samples were rotated for 1 hr at 4°C, spun down at 15,000 x g for 10 min, the supernatant was collected and frozen at -80°C until streptavidin enrichment.

Streptavidin magnetic beads were washed two times with RIPA buffer (10 bed volumes per wash) and then added to thawed APEX lysates and rotated at 4°C overnight. Using a magnetic stand, streptavidin beads were washed 3 times with 4 M urea, 100 mM NaH_2PO_4 pH 8 followed by four washes of 50 mM HEPES, pH 8.5. Samples were then frozen and saved for peptide digestion and mass spectroscopy analysis.

Quantitative Multiplex Proteomics

Samples were analyzed by quantitative multiplex proteomics at the UCSD Collaborative Center for Multiplexed Proteomics (*66*). Biotinylated proteins bound to magnetic streptavidin beads, were precipitated using a magnetic stand and resuspended in 2mL of 4M Urea in 50mM HEPES. Disulfide bonds were reduced in 5 mM dithiothreitol (DTT) at 47°C for 30 min and free cysteines were alkylated in 15 mM iodoacetamide (IAA) at room temperature in a darkened environment for 20 min. The alkylation reaction was quenched for 15 min at room temperature through the addition of an equivalent volume of DTT as in the reduction reaction. Samples were then precipitated using a magnetic stand and washed with 3mL of 1M Urea in 50mM HEPES. Samples were then resuspended in 2mL of 1M Urea in 50mM HEPES. Proteins bound to streptavidin beads were then digested in solution with 20ug of trypsin (Promega, V5113) at 47°C for 5 hours. Streptavidin beads were precipitated once more using a magnetic stand and the in-solution digest was transferred to a separate Protein LoBind microcentrifuge tube and acidified using trifluoroacetic acid (TFA) to a final concentration of 1%. Samples were desalted using C18 columns (Waters) using manufacturer protocols and dried under vacuum. Samples were subjected to peptide quantification using a Pierce Colorimetric Peptide Quantification Assay kit per the manufacturer's instructions. 50 μg of each sample was separated for further processing.

TMT Labeling

Samples were resuspended in a solution of 30% anhydrous acetonitrile (ACN) with 200 mM HEPES, pH = 8.5. Tandem mass tag (TMTpr0) labels (Thermo Fisher Scientific;

Catalog Number: A44520, Lot Number: XC342532) were suspended in anhydrous ACN to a final concentration of 20 mg/mL, and 7 µL were added to each resuspended sample. Samples were randomized in the TMT 16plex, with the TMT126 channel used as a bridge channel. The labeling reaction was allowed to proceed for 1 h at room temperature, after which excess label was quenched through the addition of 8 µL of 5% hydroxylamine for 15 min. 50 µL of 1% (TFA) was added to each sample, and samples were pooled together into their respective TMT-plex and desalted on C18 columns (Waters) as above. The multiplexed samples were dried under vacuum.

Mass spectrometry-based proteomic analysis

Samples were resuspended in 5% Formic Acid/5% ACN to a final concentration of 1 µg/µL for mass spectrometry analysis. All proteome mass spectrometry data were collected on an Orbitrap Fusion mass spectrometer (Thermo Fisher Scientific) with an in line Easy-nLC. Previously described methods were utilized for data collection.[1]Briefly, samples were loaded on a 30cm glass capillary column packed with 0.5 cm of 5 µm C4 resin followed by 0.5 cm of 3 µm C18 resin, and then 29 cm of 1.8 µm of C18 resin. Following sample loading, peptides were eluted using a gradient of 3% ACN/0.125% FA (A) and 100% ACN/0.125% FA (B) starting at 6% of mixture A and ending in 100% mixture B over a 180 min gradient at a flow rate of 300nL/min, heating the column to 60C.

Data processing and normalization

Raw files were searched using the SEQUEST algorithm in Proteome Discoverer 2.5 against the reference proteome for *Homo sapiens* retrieved July 5th,2022 from UniProt.com.

Data were searched using a precursor mass tolerance of 50 ppm and fragment mass tolerance of 0.6. Static modifications were specified as follows: TMTpro on lysine's and N-termini and carbamidomethylation of cysteines. Dynamic modifications were specified to include oxidation of methionine's. Resulting peptide spectral matches were filtered at a 0.01 FDR by the Percolator module against the decoy database.

Chemokine scavenging ELISA assay

WT non-receptor-expressing or stable receptor-expressing CCR2 or CCR2-APEX2 HEK293 cells were seeded in triplicate in 96-well dishes at 50,000 cells/well and allowed to adhere for ~8 h. Subsequently, media was replaced with DMEM/10% FBS media containing 5 nM CCL2 or CCL14 and incubated for ~16 h. Remaining chemokine levels in the supernatants of cultured cells were measured in triplicate using commercially available CCL2 Invitrogen™ ELISA kits according to manufacturer's instructions (Fisher Scientific, Hampton, NH, USA) and read with a SpectraMax M5 plate reader (Molecular Devices, Sunnyvale, CA, USA). Remaining levels of exogenous chemokine are reported as the percentage of levels in supernatants of the corresponding non-receptor expressing cells.

BRET assays

HEK293 cells were seeded directly into 96-well plates (20,000 cells per well) and transfected the next day using Mirus TransIT-Lt1 transfection reagent at ~70% confluency. Cells were transfected with a BRET donor (1.2 ng of Receptor-RlucII or 0.72 ng of β-arrestin1- or β-arrestin2-RlucII per well) along with 4.8 ng of BRET acceptor per well (for

example, rGFP-CAAX, rGFP-Rab4, rGFP-Rab11 or rGFP-Rab7). All assays were performed ~30 h after transfection, modified from methods as previously described (*63*). Cells were washed once with pre-warmed Tyrode's buffer (140 mM NaCl, 2.7 mM KCl, 1 mM $CaCl_2$, 12 mM $NaHCO_3$, 5.6 mM D-glucose, 0.5 mM $MgCl_2$, 0.37 mM NaH_2PO_4, 25 mM HEPES, pH 7.4), followed by addition of cell-permeable RlucII substrate, Prolume Purple (NanoLight Technologies) at a final concentration of 5 μM, ~3 to 6 min before BRET measurements. Three baseline BRET measurements were performed approximately 1 min apart, followed by the addition of the indicated concentrations of chemokine. Subsequent BRET measurements were taken approximately 1 min apart for 50 min or the indicated times. Values are presented as the percentage of mock treated (no ligand) [$(BRET_{ligand}/BRET_{basal}) \times 100$]. All BRET measurements were read using a Spark microplate reader (Tecan, Männedorf, Switzerland).

Receptor internalization "pre-label" assay

CCR2 receptor surface expression was determined by a pre-label flow cytometry-based internalization assay (*24*, *67*), which measures the number of labeled CCR2 molecules remaining on the cell surface after 45 min of incubation at 37°C. HEK293 cells stably expressing CCR2 or CCR2-APEX2 were labeled with mouse anti-hCCR2 antibody (Clone# 48607, R&D Systems) or its isotype-matched control for 30 min on ice and protected from light. Unbound antibody was washed away with wash buffer (PBS, 0.5% bovine serum albumin (BSA)). Cells were then resuspended in Assay Buffer (DMEM, 0.5% BSA) and either held at 4°C (which prevents receptor trafficking and internalization) or transferred to 37°C with or without 100 nM CCL2 (which allows for normal receptor trafficking) and

incubated for 45 min. After incubation, cells were transferred to wet ice and the remaining surface receptor was labeled with anti-mouse antibody conjugated to PE (Clone# 344701, R&D Systems) for 40 min on ice and protected from light. CCR2 expression was assessed by flow cytometry using a Guava Easycyte™ 8HT flow cytometer (Luminex) and analyzed with FlowJo software (FlowJo, Ashland, OR, USA). The geometric mean fluorescent intensity of analyzed cells was used to quantify surface expression of CCR2 and compared to non-internalized control to determine relative percent of receptor remaining at the surface.

G protein dissociation assay

HEK293 cells expressing CCR2-APEX2 were seeded directly into 96-well plates (15,000 cells/well) and transfected the next day with pIRES Gα-Nluc Gβγ-cpVenus, a kind gift from Dr. Daniel Legler (University of Konstanz, Germany) using Mirus TransIT-Lt1 transfection reagent with cells at ~70% confluency (*68*). Cells were then treated with vehicle or 200 ng/mL PTx for 16 h. After ~30 h post-transfection, cells were washed once with pre-warmed Tyrode's buffer followed by addition of 2.5 µM luciferase substrate coelenterazine-H (Biotium, CA, USA). Three baseline BRET measurements were performed approximately 1 min apart, followed by addition of indicated concentrations of chemokine ligand and subsequent BRET measurements were taken approximately 1 min apart for 25 min or indicated times. All BRET measurements were read using a Spark microplate reader (Tecan, Männedorf, Switzerland).

Gαi activation assay using cAMP sensor using YFP-Epac-RLuc (CAMYEL)

HEK293 cells expressing CCR2 or CCR2-APEX2 were seeded directly into 96-well plates (15,000 cells/well) and transfected the next day with pcDNA3.1 CAMYELv2 and pcDNA3.1 Gαi3 using Mirus TransIT-Lt1 transfection reagent with cells at ~70% confluency (*69*). Cells were then treated with vehicle or 200 ng/mL PTx for 16 h. After ~30 h post-transfection, cells were washed twice with pre-warmed HEPES Buffered Saline Solution (HBSS) with 0.05% BSA, followed by addition of 5 µM luciferase substrate coelenterazine-H (Biotium, CA, USA) ~ 5 min before BRET measurements. Baseline BRET measurements were performed for 3 min, followed by addition of 100 nM CCL2 (final conc.) and another six min of BRET measurements. Forskolin was then added to a final concentration of 10 µM and BRET measurements were taken for 15 minutes. Values are presented as the BRET1 acceptor/donor ratio values [(535 nm)/(460 nm)]. All BRET measurements were read using a VictorX Light luminescence reader (Perkin Elmer, Waltham, MA, USA).

Fura-2 AM Ca^{+} Flux Assay

HEK293 cells expressing CCR2-APEX2 were seeded directly into poly-D-lysine (PDL) coated clear-bottom 96-well black plates (30,000 cells/well) and allowed to adhere for ~8 h. Cells were then treated with vehicle or 200 ng/mL PTx for 16 h. Following PTx treatment, media was removed, cells were washed once with Hank's buffer with HEPES (HHBS), and cells were prepared using Screen Quest™ Fura-2 No Wash Calcium Assay Kit according to manufacturer's instructions (AAT Bioquest, Sunnyvale, CA, USA). For Gq inhibited samples, YM-254890 (50 nM) was added at the same time as the Fura-2 AM assay buffer and incubated at 37°C for 1 h. Baseline fluorescence measurements (excitation/emission)

340nm/520nm and 380nm/520nm were performed, followed by injection of CCL2 ligand and subsequent fluorescent measurements were taken for approximately 2.5 min. Intracellular calcium mobilization was determined by calculating the ratio of 510 nm emission, in response to 340/380 nm excitation and normalized using the baselines reads. All fluorescence measurements were read using a Spark microplate reader (Tecan, Männedorf, Switzerland).

Acknowledgments:

This work was performed with the support of the Flow Cytometry Core at the San Diego Center for AIDS Research (P30 AI036214), the VA San Diego Health Care System, and the San Diego Veterans Medical Research Foundation.

Data Availability: Proteome data was uploaded to massive.ucsd.edu and can be accessed using the following identifiers: (TBD)

REFERENCES

1. F. Bachelerie, A. Ben-Baruch, A. M. Burkhardt, C. Combadiere, J. M. Farber, G. J. Graham, R. Horuk, A. H. Sparre-Ulrich, M. Locati, A. D. Luster, A. Mantovani, K. Matsushima, P. M. Murphy, R. Nibbs, H. Nomiyama, C. A. Power, A. E. I. Proudfoot, M. M. Rosenkilde, A. Rot, S. Sozzani, M. Thelen, O. Yoshie, A. Zlotnik, International Union of Basic and Clinical Pharmacology. [corrected]. LXXXIX. Update on the extended family of chemokine receptors and introducing a new nomenclature for atypical chemokine receptors. *Pharmacol Rev*. **66**, 1–79 (2014).

2. J. W. Griffith, C. L. Sokol, A. D. Luster, Chemokines and Chemokine Receptors: Positioning Cells for Host Defense and Immunity. *Annual Review of Immunology*. **32**, 659–702 (2014).

3. C. E. Hughes, R. J. B. Nibbs, A guide to chemokines and their receptors. *FEBS J*. **285**, 2944–2971 (2018).

4. R. M. Ransohoff, L. Liu, A. E. Cardona, Chemokines and chemokine receptors: multipurpose players in neuroinflammation. *Int Rev Neurobiol*. **82**, 187–204 (2007).

5. Y. Le, Y. Zhou, P. Iribarren, J. Wang, Chemokines and chemokine receptors: their manifold roles in homeostasis and disease. *Cell Mol Immunol*. **1**, 95–104 (2004).

6. J. Wang, H. Knaut, Chemokine signaling in development and disease. *Development*. **141**, 4199–4205 (2014).

7. D. Raman, T. Sobolik-Delmaire, A. Richmond, Chemokines in health and disease. *Exp Cell Res*. **317**, 575–589 (2011).

8. A. E. I. Proudfoot, Chemokine receptors: multifaceted therapeutic targets. *Nat Rev Immunol*. **2**, 106–115 (2002).

9. D. Scholten, M. Canals, D. Maussang, L. Roumen, M. Smit, M. Wijtmans, C. de Graaf, H. Vischer, R. Leurs, Pharmacological modulation of chemokine receptor function. *Br J Pharmacol*. **165**, 1617–1643 (2012).

10. D. J. Scholten, M. Canals, D. Maussang, L. Roumen, M. J. Smit, M. Wijtmans, C. de Graaf, H. F. Vischer, R. Leurs, Pharmacological modulation of chemokine receptor function. *Br J Pharmacol*. **165**, 1617–1643 (2012).

11. Y. L. Kasamon, H. Chen, R. A. de Claro, L. Nie, J. Ye, G. M. Blumenthal, A. T. Farrell, R. Pazdur, FDA Approval Summary: Mogamulizumab-kpkc for Mycosis Fungoides and Sézary Syndrome. *Clin Cancer Res*. **25**, 7275–7280 (2019).

12. M. O'Hayre, C. L. Salanga, T. M. Handel, D. J. Hamel, Emerging Concepts and Approaches for Chemokine-Receptor Drug Discovery. *Expert Opin Drug Discov*. **5**, 1109–1122 (2010).

13. T. O'Connor, L. Borsig, M. Heikenwalder, CCL2-CCR2 Signaling in Disease Pathogenesis. *Endocr Metab Immune Disord Drug Targets*. **15**, 105–118 (2015).

14. S. Singh, D. Anshita, V. Ravichandiran, MCP-1: Function, regulation, and involvement in disease. *Int Immunopharmacol*. **101**, 107598 (2021).

15. B.-Z. Qian, J. Li, H. Zhang, T. Kitamura, J. Zhang, L. R. Campion, E. A. Kaiser, L. A. Snyder, J. W. Pollard, CCL2 recruits inflammatory monocytes to facilitate breast-tumour metastasis. *Nature*. **475**, 222–225 (2011).

16. A. Rogic, I. Pant, L. Grumolato, R. Fernandez-Rodriguez, A. Edwards, S. Das, A. Sun, S. Yao, R. Qiao, S. Jaffer, R. Sachidanandam, G. Akturk, R. Karlic, M. Skobe, S. A. Aaronson, High endogenous CCL2 expression promotes the aggressive phenotype of human inflammatory breast cancer. *Nat Commun*. **12**, 6889 (2021).

17. E. Prat, P. Baron, L. Meda, E. Scarpini, D. Galimberti, G. Ardolino, A. Catania, G. Scarlato, The human astrocytoma cell line U373MG produces monocyte chemotactic protein (MCP)-1 upon stimulation with beta-amyloid protein. *Neurosci Lett*. **283**, 177–180 (2000).

18. R. J. Aiello, B. D. Perry, P.-A. Bourassa, A. Robertson, W. Weng, D. R. Knight, A. H. Smith, K. S. Frederick, A. Kalgutkar, R. P. Gladue, CCR2 receptor blockade alters blood monocyte subpopulations but does not affect atherosclerotic lesions in apoE(-/-) mice. *Atherosclerosis*. **208**, 370–375 (2010).

19. J. Gilbert, J. Lekstrom-Himes, D. Donaldson, Y. Lee, M. Hu, J. Xu, T. Wyant, M. Davidson, MLN1202 Study Group, Effect of CC chemokine receptor 2 CCR2 blockade on serum C-reactive protein in individuals at atherosclerotic risk and with a single nucleotide polymorphism of the monocyte chemoattractant protein-1 promoter region. *Am J Cardiol*. **107**, 906–911 (2011).

20. M. H. Ulvmar, E. Hub, A. Rot, Atypical chemokine receptors. *Exp Cell Res*. **317**, 556–568 (2011).

21. F. Saaber, D. Schütz, E. Miess, P. Abe, S. Desikan, P. Ashok Kumar, S. Balk, K. Huang, J. M. Beaulieu, S. Schulz, R. Stumm, ACKR3 Regulation of Neuronal Migration Requires ACKR3 Phosphorylation, but Not β-Arrestin. *Cell Rep*. **26**, 1473-1488.e9 (2019).

22. P. Abe, W. Mueller, D. Schütz, F. MacKay, M. Thelen, P. Zhang, R. Stumm, CXCR7 prevents excessive CXCL12-mediated downregulation of CXCR4 in migrating cortical interneurons. *Development*. **141**, 1857–1863 (2014).

23. F. Memi, P. Abe, A. Cariboni, F. MacKay, J. G. Parnavelas, R. Stumm, CXC Chemokine Receptor 7 (CXCR7) Affects the Migration of GnRH Neurons by Regulating CXCL12 Availability. *J Neurosci*. **33**, 17527–17537 (2013).

24. B. N. Zhao, J. J. Campbell, C. L. Salanga, L. S. Ertl, Y. Wang, S. Yau, T. Dang, Y. Zeng, J. P. McMahon, A. Krasinski, P. Zhang, I. Kufareva, T. M. Handel, I. F. Charo, R. Singh, T. J. Schall, CCR2-Mediated Uptake of Constitutively Produced CCL2: A Mechanism for Regulating Chemokine Levels in the Blood. *J Immunol*. **203**, 3157–3165 (2019).

25. S. Volpe, E. Cameroni, B. Moepps, S. Thelen, T. Apuzzo, M. Thelen, CCR2 acts as scavenger for CCL2 during monocyte chemotaxis. *PLoS One*. **7**, e37208 (2012).

26. V. Hung, N. D. Udeshi, S. S. Lam, K. H. Loh, K. J. Cox, K. Pedram, S. A. Carr, A. Y. Ting, Spatially resolved proteomic mapping in living cells with the engineered peroxidase APEX2. *Nat Protoc*. **11**, 456–475 (2016).

27. J. Paek, M. Kalocsay, D. P. Staus, L. Wingler, R. Pascolutti, J. A. Paulo, S. P. Gygi, A. C. Kruse, Multidimensional Tracking of GPCR Signaling via Peroxidase-Catalyzed Proximity Labeling. *Cell*. **169**, 338-349.e11 (2017).

28. B. T. Lobingier, R. Hüttenhain, K. Eichel, K. B. Miller, A. Y. Ting, M. von Zastrow, N. J. Krogan, An Approach to Spatiotemporally Resolve Protein Interaction Networks in Living Cells. *Cell*. **169**, 350-360.e12 (2017).

29. A. Thompson, J. Schäfer, K. Kuhn, S. Kienle, J. Schwarz, G. Schmidt, T. Neumann, R. Johnstone, A. K. A. Mohammed, C. Hamon, Tandem mass tags: a novel quantification strategy for comparative analysis of complex protein mixtures by MS/MS. *Anal Chem*. **75**, 1895–1904 (2003).

30. A. M. Aragay, M. Mellado, J. M. Frade, A. M. Martin, M. C. Jimenez-Sainz, C. Martinez-A, F. Mayor, Monocyte chemoattractant protein-1-induced CCR2B receptor desensitization mediated by the G protein-coupled receptor kinase 2. *Proc Natl Acad Sci U S A*. **95**, 2985–2990 (1998).

31. W. Kleibeuker, M. Jurado-Pueyo, C. Murga, N. Eijkelkamp, F. Mayor Jr, C. J. Heijnen, A. Kavelaars, Physiological changes in GRK2 regulate CCL2-induced signaling to ERK1/2 and Akt but not to MEK1/2 and calcium. *Journal of Neurochemistry*. **104**, 979–992 (2008).

32. T. A. Fields, P. J. Casey, Signalling functions and biochemical properties of pertussis toxin-resistant G-proteins. *Biochem J*. **321**, 561–571 (1997).

33. S. Mangmool, H. Kurose, Gi/o Protein-Dependent and -Independent Actions of Pertussis Toxin (PTX). *Toxins (Basel)*. **3**, 884–899 (2011).

34. A. Nishimura, K. Kitano, J. Takasaki, M. Taniguchi, N. Mizuno, K. Tago, T. Hakoshima, H. Itoh, Structural basis for the specific inhibition of heterotrimeric Gq protein by a small molecule. *Proc Natl Acad Sci U S A*. **107**, 13666–13671 (2010).

35. Q. Peng, S. Alqahtani, M. Z. A. Nasrullah, J. Shen, Functional Evidence for Biased Inhibition of G protein Signaling by YM-254890 in Human Coronary Artery Endothelial Cells (2020), p. 2020.08.12.248468, , doi:10.1101/2020.08.12.248468.

36. V. V. Gurevich, E. V. Gurevich, GPCR Signaling Regulation: The Role of GRKs and Arrestins. *Front Pharmacol*. **10**, 125 (2019).

37. M. Ashburner, C. A. Ball, J. A. Blake, D. Botstein, H. Butler, J. M. Cherry, A. P. Davis, K. Dolinski, S. S. Dwight, J. T. Eppig, M. A. Harris, D. P. Hill, L. Issel-Tarver, A. Kasarskis, S. Lewis, J. C. Matese, J. E. Richardson, M. Ringwald, G. M. Rubin, G. Sherlock, Gene Ontology: tool for the unification of biology. *Nat Genet*. **25**, 25–29 (2000).

38. B. N. Zhao, J. J. Campbell, C. L. Salanga, L. S. Ertl, Y. Wang, S. Yau, T. Dang, Y. Zeng, J. P. McMahon, A. Krasinski, P. Zhang, I. Kufareva, T. M. Handel, I. F. Charo, R. Singh, T. J. Schall, CCR2-Mediated Uptake of Constitutively Produced CCL2: A Mechanism for Regulating Chemokine Levels in the Blood. *J Immunol*. **203**, 3157–3165 (2019).

39. M. H. Ulvmar, E. Hub, A. Rot, Atypical chemokine receptors. *Exp Cell Res*. **317**, 556–568 (2011).

40. R. Bonecchi, G. J. Graham, Atypical Chemokine Receptors and Their Roles in the Resolution of the Inflammatory Response. *Front Immunol*. **7**, 224 (2016).

41. L. B. Ford, V. Cerovic, S. W. F. Milling, G. J. Graham, C. A. H. Hansell, R. J. B. Nibbs, Characterization of conventional and atypical receptors for the chemokine CCL2 on mouse leukocytes. *J Immunol*. **193**, 400–411 (2014).

42. Z. Liu, Y. Jiang, Y. Li, J. Wang, L. Fan, M. J. Scott, G. Xiao, S. Li, T. R. Billiar, M. A. Wilson, J. Fan, TLR4 Signaling Augments Monocyte Chemotaxis by Regulating G Protein–Coupled Receptor Kinase 2 Translocation. *J.I.* **191**, 857–864 (2013).

43. limma powers differential expression analyses for RNA-sequencing and microarray studies | Nucleic Acids Research | Oxford Academic, (available at https://academic.oup.com/nar/article/43/7/e47/2414268).

44. N. F. Neel, E. Schutyser, J. Sai, G.-H. Fan, A. Richmond, Chemokine receptor internalization and intracellular trafficking. *Cytokine & Growth Factor Reviews*. **16**, 637–658 (2005).

45. C. Franci, J. Gosling, C. L. Tsou, S. R. Coughlin, I. F. Charo, Phosphorylation by a G protein-coupled kinase inhibits signaling and promotes internalization of the monocyte chemoattractant protein-1 receptor. Critical role of carboxyl-tail serines/threonines in receptor function. *J Immunol*. **157**, 5606–5612 (1996).

46. Clathrin-Dependent Mechanisms of G Protein-coupled Receptor Endocytosis - Wolfe - 2007 - Traffic - Wiley Online Library, (available at https://onlinelibrary.wiley.com/doi/full/10.1111/j.1600-0854.2007.00551.x).

47. C. Pucharcos, X. Estivill, S. de la Luna, Intersectin 2, a new multimodular protein involved in clathrin-mediated endocytosis. *FEBS Lett*. **478**, 43–51 (2000).

48. Q. Xiao, S.-C. Gil, P. Yan, Y. Wang, S. Han, E. Gonzales, R. Perez, J. R. Cirrito, J.-M. Lee, Role of Phosphatidylinositol Clathrin Assembly Lymphoid-Myeloid Leukemia (PICALM) in Intracellular Amyloid Precursor Protein (APP) Processing and Amyloid Plaque Pathogenesis *. *Journal of Biological Chemistry*. **287**, 21279–21289 (2012).

49. J. M. Wilson, M. de Hoop, N. Zorzi, B.-H. Toh, C. G. Dotti, R. G. Parton, EEA1, a Tethering Protein of the Early Sorting Endosome, Shows a Polarized Distribution in Hippocampal Neurons, Epithelial Cells, and Fibroblasts. *Mol Biol Cell*. **11**, 2657–2671 (2000).

50. E. Nielsen, F. Severin, J. M. Backer, A. A. Hyman, M. Zerial, Rab5 regulates motility of early endosomes on microtubules. *Nat Cell Biol*. **1**, 376–382 (1999).

51. P. J. Cullen, H. C. Korswagen, Sorting nexins provide diversity for retromer-dependent trafficking events. *Nat Cell Biol*. **14**, 29–37 (2012).

52. Rab8, a small GTPase involved in vesicular traffic between the TGN and the basolateral plasma membrane. *J Cell Biol*. **123**, 35–45 (1993).

53. H. K. Truchan, L. VieBrock, C. L. Cockburn, N. Ojogun, B. P. Griffin, D. S. Wijesinghe, C. E. Chalfant, J. A. Carlyon, Anaplasma phagocytophilum Rab10-dependent parasitism of the trans-Golgi network is critical for completion of the infection cycle. *Cell Microbiol*. **18**, 260–281 (2016).

54. R. L. Nokes, I. C. Fields, R. N. Collins, H. Fölsch, Rab13 regulates membrane trafficking between TGN and recycling endosomes in polarized epithelial cells. *J Cell Biol*. **182**, 845–853 (2008).

55. S. A. Wood, J. E. Park, W. J. Brown, Brefeldin A causes a microtubule-mediated fusion of the trans-Golgi network and early endosomes. *Cell*. **67**, 591–600 (1991).

56. S.-B. Cheng, E. J. Filardo, Trans-Golgi Network (TGN) as a Regulatory Node for β1-Adrenergic Receptor (β1AR) Down-modulation and Recycling. *J Biol Chem*. **287**, 14178–14191 (2012).

57. W. Yang, B. Storrie, Scattered Golgi Elements during Microtubule Disruption Are Initially Enriched in Trans-Golgi Proteins. *Mol Biol Cell*. **9**, 191–207 (1998).

58. U. Rescher, V. Gerke, Annexins – unique membrane binding proteins with diverse functions. *Journal of Cell Science*. **117**, 2631–2639 (2004).

59. S. L. Sønder, T. L. Boye, R. Tölle, J. Dengjel, K. Maeda, M. Jäättelä, A. C. Simonsen, J. K. Jaiswal, J. Nylandsted, Annexin A7 is required for ESCRT III-mediated plasma membrane repair. *Sci Rep*. **9**, 6726 (2019).

60. H. Shibata, T. Kanadome, H. Sugiura, T. Yokoyama, M. Yamamuro, S. E. Moss, M. Maki, A New Role for Annexin A11 in the Early Secretory Pathway via Stabilizing Sec31A Protein at the Endoplasmic Reticulum Exit Sites (ERES). *J Biol Chem*. **290**, 4981–4993 (2015).

61. A. I. Ivanov, Pharmacological inhibitors of exocytosis and endocytosis: novel bullets for old targets. *Methods Mol Biol*. **1174**, 3–18 (2014).

62. D. H. Woo, Y.-N. Hur, M. W. Jang, C. Justin Lee, M. Park, Inhibitors of synaptic vesicle exocytosis reduce surface expression of postsynaptic glutamate receptors. *Anim Cells Syst (Seoul)*. **24**, 341–348.

63. Y. Feng, S. Yu, T. K. R. Lasell, A. P. Jadhav, E. Macia, P. Chardin, P. Melancon, M. Roth, T. Mitchison, T. Kirchhausen, Exo1: A new chemical inhibitor of the exocytic pathway. *Proceedings of the National Academy of Sciences*. **100**, 6469–6474 (2003).

64. H. Li, S. Huang, S. Wang, J. Zhao, L. Su, B. Zhao, Y. Zhang, S. Zhang, J. Miao, Targeting annexin A7 by a small molecule suppressed the activity of phosphatidylcholine-specific phospholipase C in vascular endothelial cells and inhibited atherosclerosis in apolipoprotein E−/− mice. *Cell Death Dis*. **4**, e806–e806 (2013).

65. W. Lu, X. He, L. Su, B. Zhao, J. Miao, Effects of annexin A7 inhibitor-ABO on the expression and distribution of long noncoding RNA-CERNA1 in vascular endothelial cells apoptosis. *Apoptosis*. **24**, 552–561 (2019).

66. H. Li, N. Liu, S. Wang, L. Wang, J. Zhao, L. Su, Y. Zhang, S. Zhang, Z. Xu, B. Zhao, J. Miao, Identification of a small molecule targeting annexin A7. *Biochimica et Biophysica Acta (BBA) - Molecular Cell Research*. **1833**, 2092–2099 (2013).

67. Loss of Annexin A7 Leads to Alterations in Frequency-Induced Shortening of Isolated Murine Cardiomyocytes | Molecular and Cellular Biology, (available at https://journals.asm.org/doi/10.1128/MCB.21.13.4119-4128.2001).

68. The Anx7(+/-) Knockout Mutation Alters Electrical and Secretory Responses to Ca2+-Mobilizing Agents in Pancreatic β-cells - Abstract - Cellular Physiology and Biochemistry 2012, Vol. 29, No. 5-6 - Karger Publishers, (available at https://www.karger.com/Article/Abstract/186926).

69. J. K. Jaiswal, V. M. Rivera, S. M. Simon, Exocytosis of Post-Golgi Vesicles Is Regulated by Components of the Endocytic Machinery. *Cell*. **137**, 1308–1319 (2009).

70. B. Alberts, A. Johnson, J. Lewis, M. Raff, K. Roberts, P. Walter, Transport from the Trans Golgi Network to the Cell Exterior: Exocytosis. *Molecular Biology of the Cell. 4th edition* (2002) (available at https://www.ncbi.nlm.nih.gov/books/NBK26892/).

71. W. Yao, Q. Ba, X. Li, H. Li, S. Zhang, Y. Yuan, F. Wang, X. Duan, J. Li, W. Zhang, H. Wang, A Natural CCR2 Antagonist Relieves Tumor-associated Macrophage-mediated Immunosuppression to Produce a Therapeutic Effect for Liver Cancer. *EBioMedicine*. **22**, 58–67 (2017).

72. S. Y. Lim, A. E. Yuzhalin, A. N. Gordon-Weeks, R. J. Muschel, Targeting the CCL2-CCR2 signaling axis in cancer metastasis. *Oncotarget*. **7**, 28697–28710 (2016).

73. Y. Namkung, C. Le Gouill, V. Lukashova, H. Kobayashi, M. Hogue, E. Khoury, M. Song, M. Bouvier, S. A. Laporte, Monitoring G protein-coupled receptor and β-arrestin trafficking in live cells using enhanced bystander BRET. *Nat Commun*. **7**, 12178 (2016).

74. Q. Sun, W. Westphal, K. N. Wong, I. Tan, Q. Zhong, Rubicon controls endosome maturation as a Rab7 effector. *Proc Natl Acad Sci U S A*. **107**, 19338–19343 (2010).

75. E. Campeau, V. E. Ruhl, F. Rodier, C. L. Smith, B. L. Rahmberg, J. O. Fuss, J. Campisi, P. Yaswen, P. K. Cooper, P. D. Kaufman, A versatile viral system for expression and depletion of proteins in mammalian cells. *PLoS One*. **4**, e6529 (2009).

76. A. Campeau, R. H. Mills, T. Stevens, L.-A. Rossitto, M. Meehan, P. Dorrestein, R. Daly, T. T. Nguyen, D. J. Gonzalez, D. V. Jeste, V. Hook, Multi-omics of human plasma reveals molecular features of dysregulated inflammation and accelerated aging in schizophrenia. *Mol Psychiatry*. **27**, 1217–1225 (2022).

77. C. T. Gilliland, C. L. Salanga, T. Kawamura, J. Trejo, T. M. Handel, The chemokine receptor CCR1 is constitutively active, which leads to G protein-independent, β-arrestin-mediated internalization. *J Biol Chem*. **288**, 32194–32210 (2013).

78. C. Matti, A. Salnikov, M. Artinger, G. D'Agostino, I. Kindinger, M. Uguccioni, M. Thelen, D. F. Legler, ACKR4 Recruits GRK3 Prior to β-Arrestins but Can Scavenge Chemokines in the Absence of β-Arrestins. *Front Immunol*. **11**, 720 (2020).

79. L. I. Jiang, J. Collins, R. Davis, K.-M. Lin, D. DeCamp, T. Roach, R. Hsueh, R. A. Rebres, E. M. Ross, R. Taussig, I. Fraser, P. C. Sternweis, Use of a cAMP BRET Sensor to Characterize a Novel Regulation of cAMP by the Sphingosine 1-Phosphate/G13 Pathway. *J Biol Chem*. **282**, 10576–10584 (2007).

SUPPLEMENTAL FIGURES

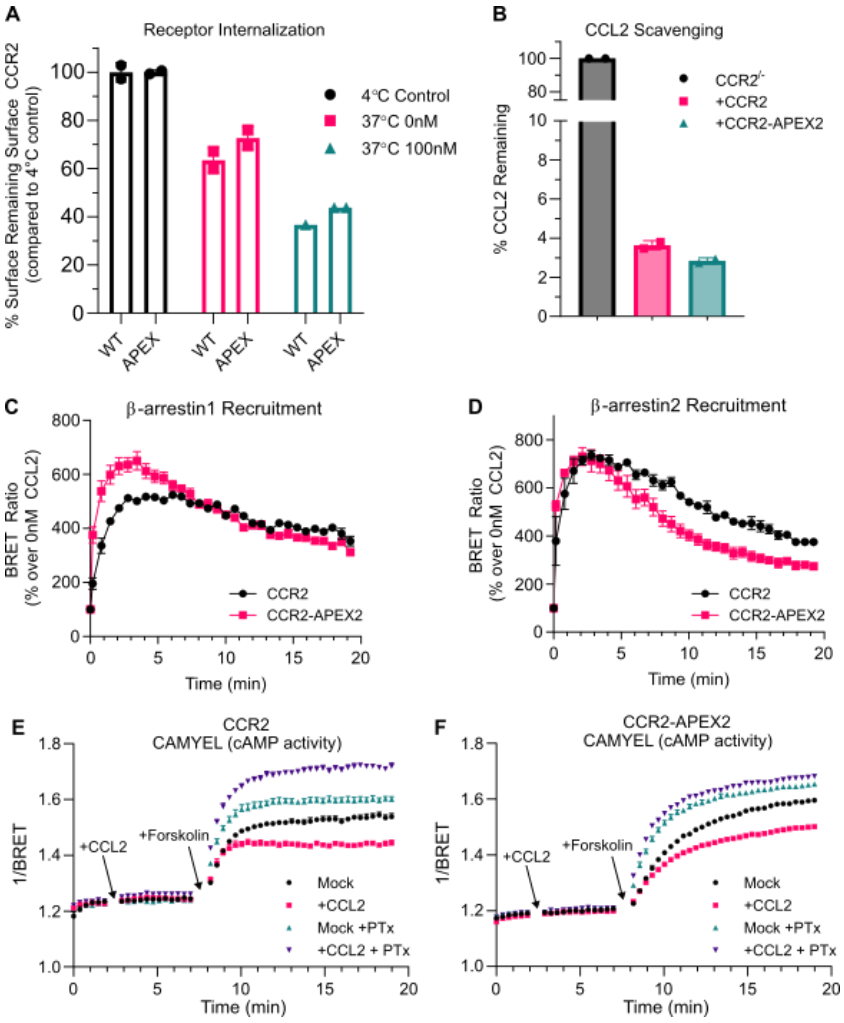

figure 3.S1. Function of CCR2 is unaffected by C-terminal APEX2 tag. (**A**) Constitutive and CCL2-induced internalization of surface labeled CCR2 followed by flow cytometry analysis. Data presented as percentage of surface receptor remaining compared to non-internalized control. Addition of a C-terminal APEX tag does not affect CCR2 internalization. (**B**) HEK293 cells stably expressing WT or APEX-tagged CCR2 and respective non-expressing cells were cultured in media containing 5 nM CCL2. Remaining levels of CCL2 were measured by ELISA, interpolated from CCL2 standards, and presented as a percentage of non-CCR2 expressing cells. (**C** and **D**) β-arrestin recruitment assessed by ebBRET. Cells expressing WT or APEX-tagged CCR2 transfected with β-arrestin1- or β-arrestin2-RlucII and rGFP-CAAX were stimulated with 100 nM CCL2 or left untreated. Data are presented as a percentage of BRET values for untreated controls. C-terminal APEX tag does not hinder β-arrestin recruitment. (**E** and **F**) Activation of Gαi using BRET-based biosensor CAMYEL (cAMP sensor using YFP-Epac-Rluc). C-terminal APEX tag has no affect on CCR2 ability to activate Gαi. Data are presented as 1/BRET.

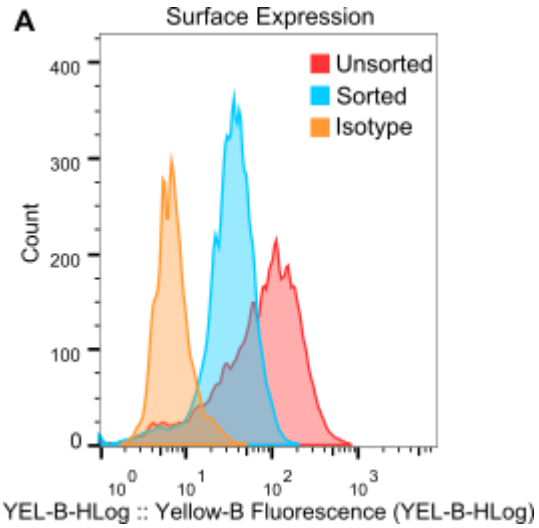

figure 3.S2. Surface expression of CCR2-APEX2 stable HEK293 cells before and after cell sorting. (**A**) Stable CCR2-APEX2 expressing cells were generated in the HEK293 cell line by lentiviral transduction using pLenti-CMV-Hygro expression vector. Surface receptor was labeled with anti-CCR2 PE-conjugated antibody and assessed by flow cytometry. The lower third of expressor were sorted to be used for APEX MS sample preparation.

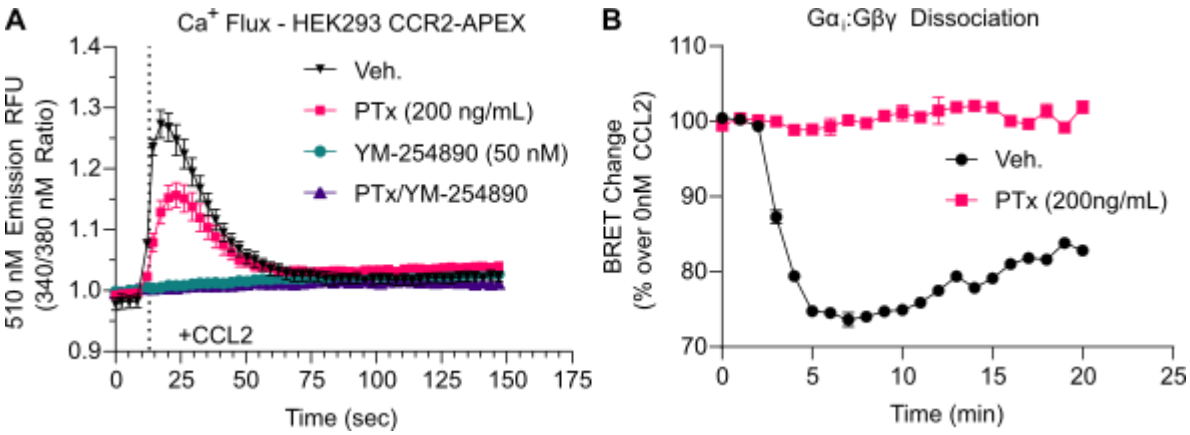

figure 3.S3. G protein inhibitors YM-254890 and PTx are able to completely inhibit G*αq* and G*αi* activation. (**A**) Stable CCR2-APEX2 expressing cells were generated in the HEK293 cell line by lentiviral transduction using pLenti-CMV-Hygro expression vector. Surface receptor was labeled with anti-CCR2 PE-conjugated antibody and assessed by flow cytometry. The lower third of expressor were sorted to be used for APEX MS sample preparation.

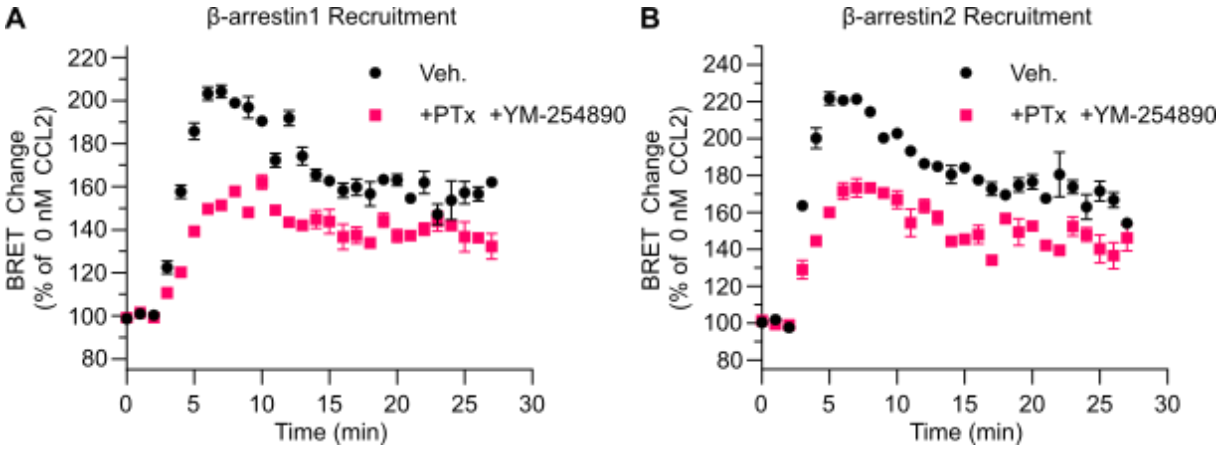

figure 3.S4. Inhibition of Gα results in decreased β-arrestin recruitment following CCR2 activation. (**A**) Stable CCR2-APEX2 expressing cells were generated in the HEK293 cell line by lentiviral transduction using pLenti-CMV-Hygro expression vector. Surface receptor was labeled with anti-CCR2 PE-conjugated antibody and assessed by flow cytometry. The lower third of expressor were sorted to be used for APEX MS sample preparation.

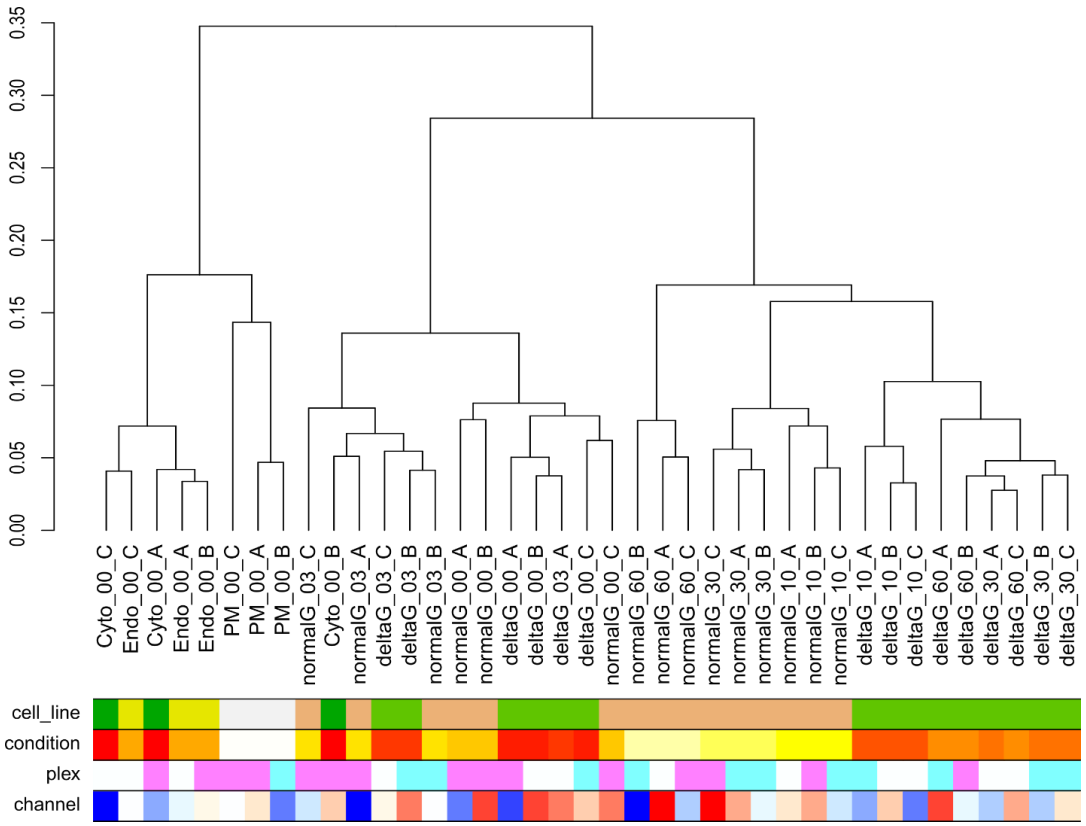

figure 3.S5. Sample correlation-based clustering of CCR2-APEX samples. (**A**) Hierarchical clustering of CCR2-APEX and spatial reference APEX samples following batch effect removal.

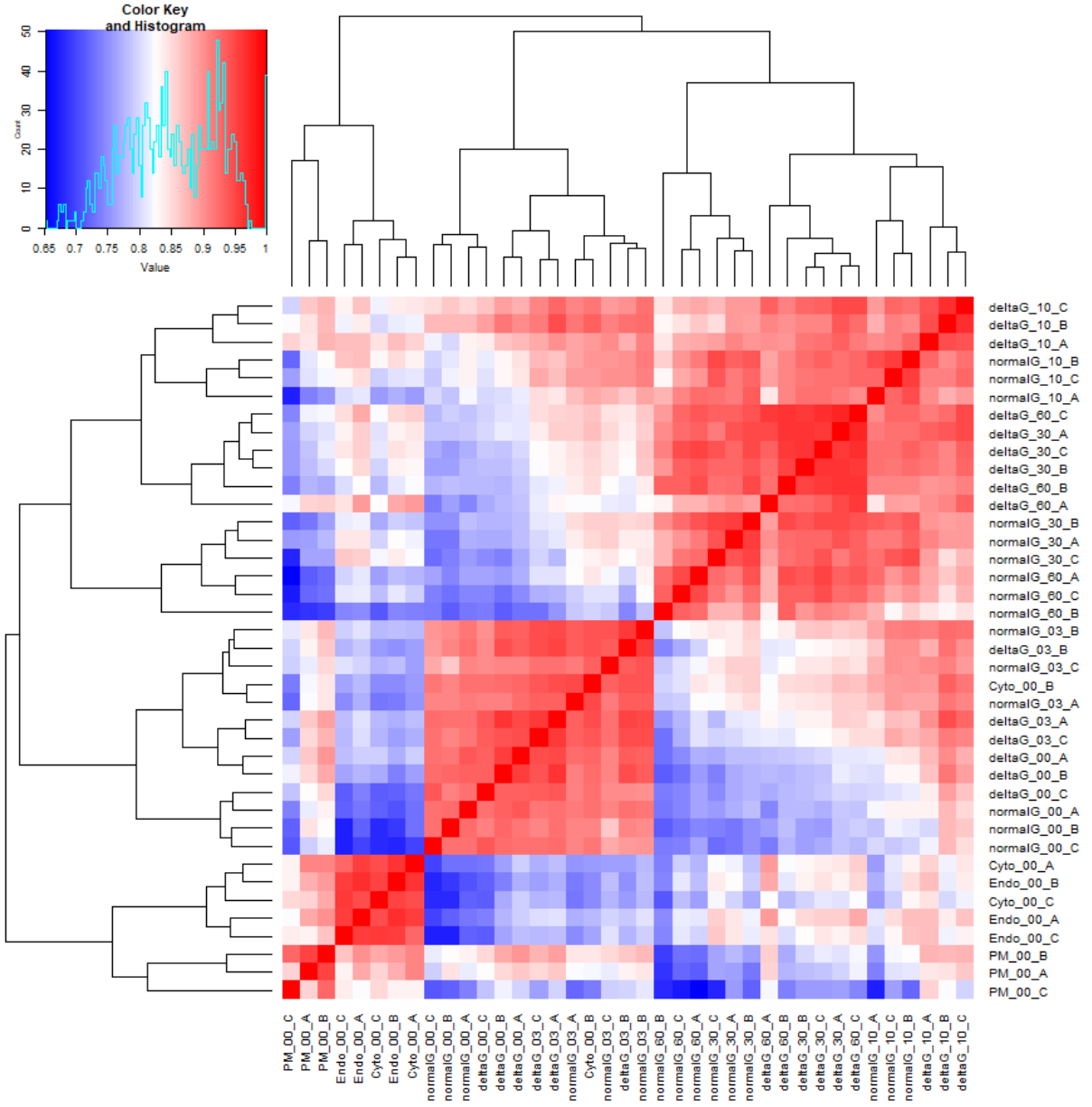

figure 3.S6. CCR2 APEX-MS sample pairwise correlations. (**A**) Heatmap of CCR2-APEX and spatial reference samples pairwise correlations using Pearson correlation coefficient.

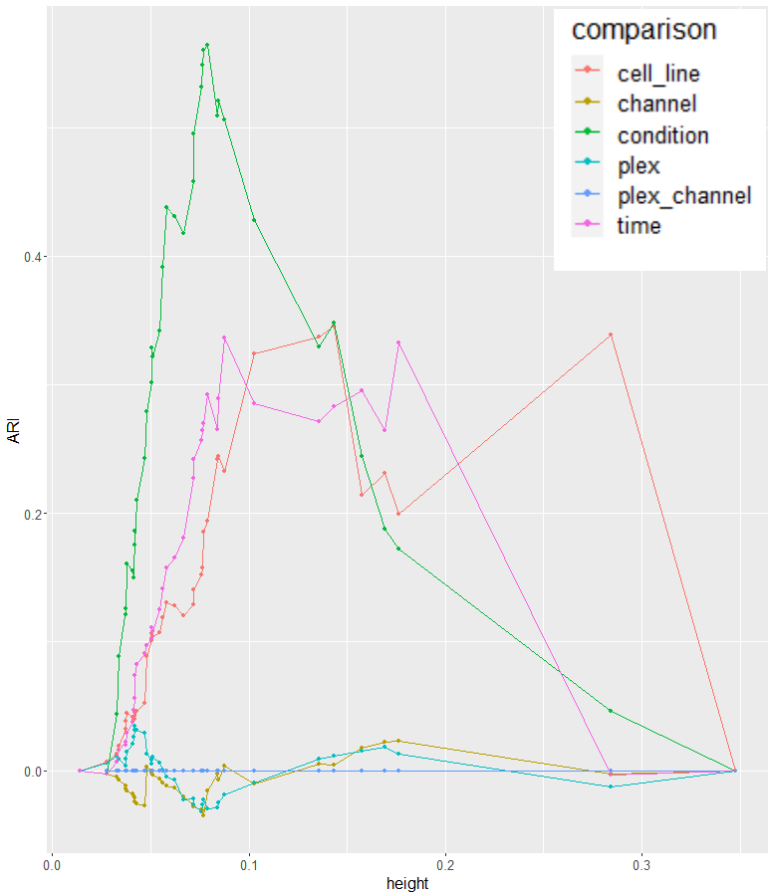

figure 3.S7. Adjusted rand index (ARI) at different dendrogram splits of sample correlation-based clustering. (**A**) Plot indicating ARI value as a measure of consistency within the correlation-based hierarchical clustering, with a higher ARI score indicating more similarity based on a given comparison.

Acknowledgements

Chapter 3 is adapted from a manuscript currently in preparation for submission for publication. (T.M. Shroka, A. Lona, C. Sanchez, C.L. Salanga, I. Kufareva, T.M. Handel (2022)). “Proximal proteome of C-C chemokine receptor 2 (CCR2) reveals novel endocytic trafficking patterns.” The dissertation author was the primary researcher and author of this material.

CHAPTER 4

Conclusions, Discussion and Future Directions

CONCLUSIONS, DISCUSSION AND FUTURE DIRECTIONS

With increasing attention to the effectiveness of immunotherapies for cancer and other inflammatory diseases, chemokine receptors continue to be attractive therapeutic targets within the immune system (*1*). Not surprisingly, many chemokine receptors have already been targeted in clinical trials for a wide variety of pathologies (*2*, *3*); and although these receptors have been widely studied academically and pursued pharmaceutically, there are only three FDA approved therapeutics targeting chemokine receptors, none of which are for treatment of any inflammatory disorder (*4*). CCR2 in particular is currently the target of several ongoing (and recently terminated) clinical trials, for indications such as nonalcoholic steatohepatitis (NASH), nonalcoholic fatty liver disease (NAFLD), type 2 diabetes nephropathy, and pancreatic ductal adenocarcinomas (PDAC) (*5*–*7*). Unfortunately, most drug development efforts targeting CCR2, and chemokines receptors as a whole, fail due to lack of efficacy and inability to reach clinical endpoints. Considering the wealth of information and breadth of academic study encompassing chemokine receptors as well as their therapeutic potential, it is surprising that these receptors have not been better clinically exploited. This raises the question, what information regarding chemokine receptor function is lacking and what information is required to allow for successful pharmacological targeting of these receptors? For example, the ability of G protein-coupled chemokine receptors to be able to scavenge chemokine without becoming desensitized is largely overlooked when considering receptor function. Whereas the biological and phenotypic effects of preventing scavenging of CXCL12 by ACKR3 are exceedingly apparent, stemming from dysregulated function of CXCR4 and the inability of cells to migrate along CXCL12 gradient properly (*8*–*13*); the physiological implications of non-atypical (i.e., G

protein-coupled) chemokine receptors is less apparent. Antagonizing or knocking out chemokine receptors CXCR2, CXCR3, and CCR2 has been shown to result in increased serum levels of their chemokine ligands (*14*, *15*). Furthermore, in CCR2-deficient peripheral blood and resident peritoneal cells, CCR1 showed reduced binding and biologic response to CCL3, suggesting that elevated levels of CCR2 ligands had down-regulated CCR1 (*14*). Studying the implications of loss of scavenging of a G protein-coupled chemokine receptor, such as CCR2, is more difficult compared to the atypical chemokine receptors. This is because when knocking out an atypical receptor, the resulting phenotype is the almost entirely due to the loss of scavenging by that receptor, whereas when knocking out a scavenging receptor with G protein signaling functions, the resulting phenotype is also due to the loss of those G protein-dependent functions, such as the loss of monocyte migration with the loss of CCR2. Therefore, studying the exact role that scavenging by CCR2 plays at a physiological level becomes considerably more difficult. The previous chapters provide a comprehensive analysis of the mechanisms, pathways, and interactors involved in CCR2 scavenging, however several areas require further research to help inform future chemokine receptor research and drug development. The following sections are discrete areas regarding CCR2 and chemokine receptor function that merit further investigation.

β-arrestin/receptor interactions may play a critical role in chemokine receptor function

Arrestins terminate G protein activation by GPCRs following recruitment to the phosphorylated receptor by interacting with and outcompeting G proteins for the same cytoplasmic core location of active GPCRs, as well as by acting as a scaffold for endocytic machinery to take receptor away from the cell surface (*16*). Arrestins are capable of making

extensive electrostatics interactions with the phosphorylated receptor C-terminus as well as interactions with the exposed cytoplasmic face and DRY motif core of the receptor (*17*). Due to its considerable role in receptor function, this interaction between GPCRs and β-arrestin has been the consideration of several structural studies. One such study (*18*), shows clear confirmation of β-arrestins with chimeric β_2V_2R (β_2AR with its C-terminal tail swapped with the tail of vasopressin type 2 receptor (V_2R)), interacting with only the receptor tail and visibly hanging from the receptors, as well as a conformation which β-arrestin is making tight contact with the receptor along the cytoplasmic face of the receptor. The strength of this interaction with β-arrestin may influence both internalization and G protein activation by GPCRs.

As shown in Figure 2.7 (chapter 2, Fig. 7), β-arrestin has drastically different effects on CCR1 and CCR2 functions, both scavenging and G protein activation. Another unusual observation is that CCR1 will not express at the cell surface with even small C-terminal peptide tags. The C-terminal tails of CCR1 and CCR2 are extremely similar in length, Ser/Thr content, and acidic residues content (**Fig. 1A**). Nevertheless, we performed both C-terminal tail truncations as well as CCR1/CCR2 tail swaps to determine if this β-arrestin dependence was due to C-terminal tail differences. We saw no differences in receptor G protein activation with the tail swap mutants in WT (**Fig. 1B**) or β-arrestin1/2 KO cells (**Fig. 1C**), but we did see G protein activation reminiscent of the β-arrestin1/2 KO data (**Fig. 2.7**) in the C-terminal truncation mutants (**Fig. 1D**). This was not entirely surprising, considering we know that the C-terminal Ser/Thr phosphorylation sites are important for β-arrestin recruitment. These results indicate that the C-terminal tail of CCR1 and CCR2 is not the determining factor for how β-arrestin modulates the receptors' functions. We therefore

suspect that following β-arrestin recruitment to the receptor, the interaction between CCR1 and β-arrestin is much stronger potentially due to greater interactions with the receptor core or intracellular face of CCR1, thus preventing CCR1 from further G protein activation. For future experiments, we intend to further investigate not just CCR1 and CCR2, but other chemokine receptor interactions with β-arrestin. One such way we can determine if this interaction varies between receptors is to assess β-arrestin association with endosomal markers by ebBRET. This method tracks β-arrestin trafficking through the endocytic pathways which is driven by its interaction with the receptor. Preliminary data shows drastically varying association of β-arrestin with the early endosome following stimulation of either CCR1, CCR2, or CCR5. We also intend to use fluorescence co-localization microscopy in order to visualize basal levels of association of β-arrestins and receptors, as well as β-arrestins association with endosomal compartments. Furthermore, structure-function approaches can be utilized, including receptor and β-arrestin mutagenesis to determine if specific structural conformations or interactions influence the receptor/arrestin interaction. However, such mutagenesis approaches will need to be carefully considered, as many mutations that would perturb β-arrestin interactions would also impact G protein coupling, which therefore reduces β-arrestin recruitment making certain results more difficult to interpret. Possibly, the most direct approach to determining how these receptors interact with β-arrestin is by cryo-EM structural analysis, similar to Shukla et al. (*18*). Only low resolution negative stain images are needed to visualize these interactions and with our own lab's receptor structure expertise and ongoing collaborations, we are more than capable of investigating these structural interactions.

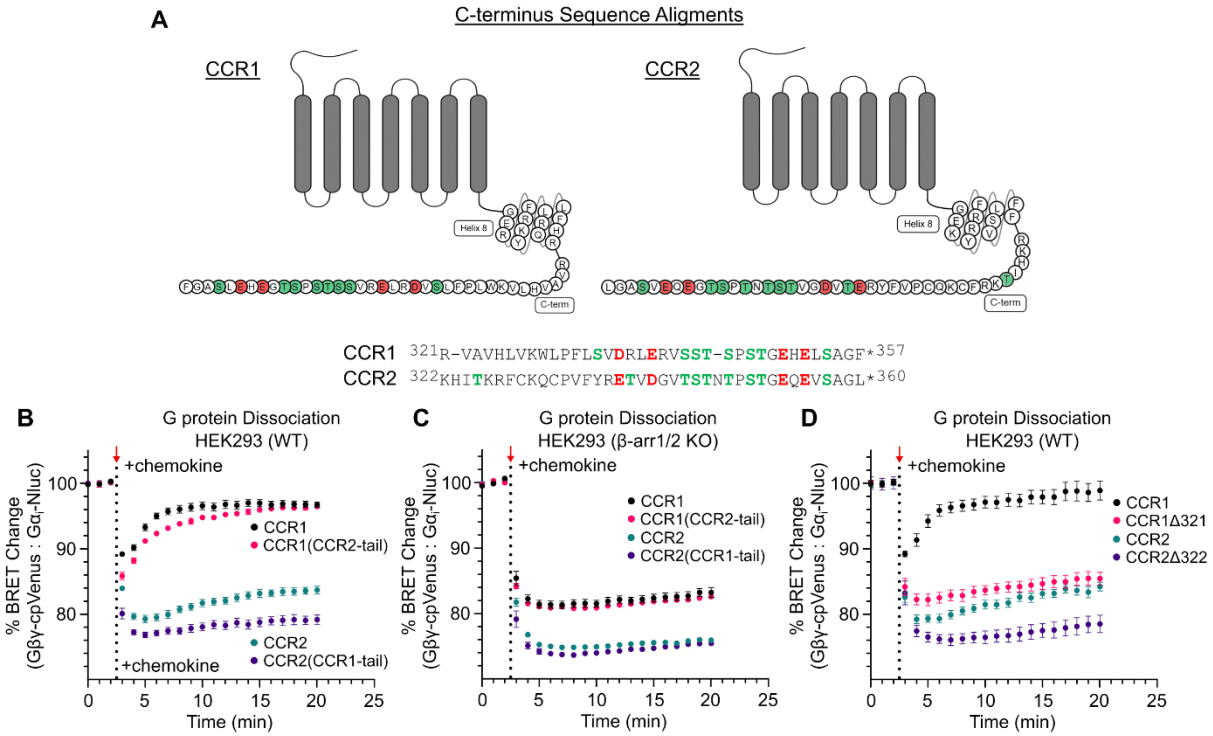

Figure 4.1. C-terminal tail comparisons of CCR1 and CCR2. (**A**) Sequence alignments of CCR1 and CCR2 C-terminal tails. (**B** and **C**) Gαβγ dissociation in HEK293 WT cells (B) or HEK293 β-arrestin1/2 KO cells (C) expressing either CCR1, CCR2, or tail swap mutants and transfected with an IRES vector coding for Gαi-Nluc and Gβγ-cpVenus. Cells were stimulated with 100 nM CCL14 or CCL2 (indicated by dotted line). (**D**) Gαβγ dissociation in HEK293 cells transfected with full length or C-terminal truncated receptors and IRES vector coding for Gαi-Nluc and Gβγ-cpVenus. Cells were stimulated with 100 nM CCL14 or CCL2 (indicated by dotted line).

Ligand selectivity and affinity between chemokines and chemokines receptors and the resultant G protein activation pathways remains unclear

The current knowledge regarding the interoperability of chemokines and chemokine receptors is mostly based off a collection of prior studies over the last several decades and needs to be assessed more thoroughly (*19*). This interoperability could also be a large reason why chemokine receptors have been difficult to target therapeutically. Additionally, the phenomenon of biased signaling continues to be a widely studied field in GPCR biology due to the potential of developing biased agonists for tunable activation of receptor mediated signaling cascades (*20*). We show that CCR2 activates Gαq along with Gαi upon activation by CCL2 (Chapter 3), however Gq mediated cellular responses are widely ignored in studies investigating CCR2 function. Furthermore, chemokine receptors, including CCR2, are able to bind and respond to several different chemokine ligands (Chapter 1, Fig. 1.1), and considering evidence that chemokine receptors can activate multiple downstream pathways (Gαi, Gαq, Gβγ, and β-arrestin) as well as respond to a multitude of natural chemokine ligands, it is possible that certain receptors may possess naturally occurring biased ligands . Since studies regarding chemokines receptors generally focus on their primary ligands, for example our studies focusing on only CCL2, it would be informative to further investigate whether chemokines can act as natural biased ligands preferentially activating separate Gα pathways or β-arrestin. Additionally, the fate of chemokines (i.e., disassociation, endocytic trafficking, and degradation) following receptor binding and whether different chemokines are trafficked differently depending on specific receptor interaction is unknown. Empirical and concise determination of the binding and signaling properties of all the chemokines and chemokine receptors would greatly benefit to the chemokine field. This becomes

challenging due to there being ~50 chemokine ligands and 22 chemokine receptors. Furthermore, accessibility of purified *functional* chemokine is also a major constraint for performing such a study. However, the chemokine receptor family continues to be interesting therapeutics targets although current attempts have had limited efficacy. Greater biological information regarding the properties of individual receptors would help to inform drug design as well as benefit the chemokine receptor field as a whole.

This information would be indispensable when trying to interpret the cellular responses created in an inflammatory environment where there are many different cell types expressing a variety of receptors and in the presence of multiple chemokines.

Clathrin-independent endocytosis mechanism as well as specific endocytic trafficking mediators of CCR2 remain undefined.

Throughout our work, we continue to see that CCR2 constitutively internalizes along CIE pathways and is subsequently able to recycle back to the cell surface. This constitutive internalization and recycling is still poorly understood. Along ligand-induced pathways, which are generally more thoroughly defined, following CCL2 activation CCR2 internalizes to early endosomes, associates with Rab4 endosomes and other retromer-associated markers including SNX3, SNX27, and VP26A (seen in our APEX dataset) and subsequently recycles back to the surface (*21–23*). In the absence of ligand, we observe that CCR2 constitutively internalizes and recycles independent of canonical clathrin-mediated pathways, however the mechanisms underlying this ligand-independent endocytosis and recycling remains unclear. We have begun to hypothesize that CCR2 is internalizing along clathin-independent

pathways of endocytosis, such as macropinocytosis. Considering constitutive macropinocytosis has been shown to occur in several monocytic cells, including CCR2 expressing macrophages (*24*, *25*), we sought to determine whether this was a pathway of CCR2 constitutive endocytosis.

To test whether macropinocytosis is a mechanism for CCR2 scavenging, we treated cells with diacylglycerol (DAG) analog phorbol 12-myristate 13-acetate (PMA), a potent activator of protein kinase C (PKC) (*26*), which activates the macropinocytosis pathway via activation of myristoylated, alanine-rich C kinase substrate (MARCKS) (*27–29*); along which we observe CCR2 to internalize. Along this pathway, we see robust internalization like that of CCL2-induced internalization, however we do not see association with early endosome or Rab4. This is not surprising, as PMA-induced activation of PKC can result in stimulation of macropinocytosis pathways which do not follow typical endocytic trafficking patterns and do not converge on the early endosome (*30*). We do however see rapid recycling of CCR2 to the plasma membrane following the addition of broad PKC inhibitor Go6983, indicating that CCR2 is recycling independent of the Rab4 endocytic pathway. Again, this is not unexpected as Arf6-stimulated macropinosomes are able to rapidly refuse with the membrane to recycle (*31*, *32*). These observations become less exciting when we compare CCR2 to CXCR4, a receptor which is known to be incapable of scavenging and has limited constitutive internalization or recycling. Following PMA treatment, CXCR4 undergoes the same internalization and recycling as CCR2. Additionally, treating CCR2 expressing cells with PMA had no discernable effect on scavenging ability. Although macropinocytosis may be occurring in endogenous CCR2 expressing cells, we have not been able to show a role in chemokine scavenging.

Another clathrin-independent internalization pathway we pursued was caveolin mediated endocytosis. This pathway of CIE is primarily accomplished via caveolin-1, which interacts directly with the PM driving the formation of 50-100 nm omega-shaped membrane invaginations (caveolae) which can interact directly with cytoskeletal components and eventually pinch off from the membrane (*33*). Whether GPCRs localize to or internalize in caveolae is unclear and is likely receptor-specific (*34*). We tested whether CCR2 internalizes via caveolae by generating a caveolin-1 and caveolin-2 dual CRISPR knockout HEK293 cell line. Although the role of caveolin-2 is less understood, we observed that a dual homozygous ($CAV1^{-/-}$ $CAV2^{-/-}$) knockout was not viable and could only achieve heterozygous KO of CAV2 ($CAV1^{-/-}$ $CAV2^{-/+}$), evidence that CAV2 must play some necessary biological role for cell viability. Unfortunately, we observe no effect of loss of caveolins on the ligand-induced or constitutive internalization of CCR2. Further indicating there is some alternative mechanism. There are other such CIE mechanisms we have yet to study, such as fast endophilin-mediated endocytosis (FEME) and clathrin-independent carrier / glycosylphosphatidylinositol-anchored protein enriched early endocytic compartment (CLIC/GEEC) endocytosis (*35*). Further studies directly probing these pathways need to be pursued to better understand CCR2 endocytosis and scavenging.

Endocytosis is not the only aspect of CCR2 scavenging which needs to be further explored. Arguably, the recycling mechanisms of CCR2 along both ligand-induced and constitutive pathways may be the more essential component of CCR2 scavenging. It is known that other GPCRs are able to undergo constitutive internalization along both CME and CIE pathways (*36, 37*). However, the observation that CCR2 can recycle and avoid degradation even in the prolonged presence of extremely high concentrations of ligand

indicate that the endocytic network by which CCR2 traffics is critically important. Probing the endocytic network is incredibly difficult due their being a multitude of pathways and hundreds of proteins involved (*38*). Fortunately, our CCR2 APEX-MS dataset has revealed some promising insights into CCR2 endocytic trafficking patterns. As shown in our APEX data, we see a suppression of TGN association following CCL2-stimulation, potentially indicating that at the basal state, CCR2 is trafficking through the TGN to recycle to the cell surface or that stimulation results in an exit of CCR2 from the TGN potentially to replenish lost surface receptor. Our APEX data also reveals that following CCL2 stimulation, there is a quick decrease then a steady increase in proximity to proteins involved in the exocytic pathway. This also indicates that following activation and endocytosis of the receptor, pathways are activated which result in the replenishment of CCR2 to the cell surface. In order to investigate the role of TGN recycling of CCR2, we have preliminarily tested CCR2 internalization in Brefeldin A treated cells. Brefeldin A is a fungal metabolite that inhibits exchange of ADP ribosylation factor (ARF)-bound GDP for GTP preventing assembly of cytoplasmic coat proteins onto membranes and ultimately resulting in the collapse of the Golgi apparatus (*39*, *40*). In Brefeldin A treated cells, we have observed constitutive and ligand-induced internalization of CCR2, however we appear to inhibit the ability of CCR2 to recover to the surface. Additionally, with prolonged treatment of Brefeldin A, we eventually see a near complete loss of surfacer CCR2, indicating that almost the entirety of the receptor has internalized but has become trapped due to disruption of the TGN. Additional controls and other means of disrupting the TGN will need to be tested to ensure that it is in fact the disruption of the trans-Golgi trafficking that is causing this result and not some other global mechanism. Means by which to perturb the exocytic pathways identified in our APEX

dataset have yet to be explored, however as with the TGN it would be most sensical to broadly inhibit these pathways while testing CCR2 recycling following constitutive and ligand-induced internalization and subsequently apply more direct and target perturbations. Ultimately, non-canonical internalization mechanisms, the TGN recycling pathway, exocytic pathways, as well as other endocytic networks will need to be further probed in order to better elucidate the trafficking and recycling mechanisms of CCR2.

Future experiments and directions

In order to better understand chemokine receptor function and optimistically improve the therapeutic potential of these receptors further studies need to be performed.

As described above, the observed β-arrestin mediated functional differences between CCR1 and CCR2 deserve further investigation. We hypothesize that the strength of interaction between β-arrestin and CCR1 and CCR2 is different, and this may be due to stronger interactions between β-arrestin and the core and intracellular side of CCR1. One way this could be tested is by colocalization immunofluorescence (IF) microscopy. Presumably, if CCR1 and β-arrestin are interacting more strongly than they would show stronger colocalization following endocytosis. Conversely, CCR2 appears to weakly interact with β-arrestin and we would expect less colocalization with CCR2 at the early endosome. Preliminary BRET experiments assessing whether β-arrestin traffics with the receptors to the early endosome have been promising, however the results are difficult to interpret due to the high basal association between CCR1 and β-arrestin. Due to this, colocalization IF in fixed or live cells may be a more informative approach.

The exact endocytic pathways which CCR2 traffics is still unknown. Our BRET-based approaches are limited to individual endosome markers which need to be overexpressed along with a GFP-fusion tag and may not be representative of actual physiological endogenous conditions. Additionally, IF-based approaches are limited to a small subset of markers based on antibody availability or specificity and lacks the throughput and spatial-temporal information that is desired. Our APEX-MS data gives us more informative spatial and temporal data as well as a great coverage of the receptor interactome. However, further biological validation of observations derived from the APEX-MS data need to be performed. Such experiments involve perturbing the pathways identified, such as the TGN and exocytic pathway, and testing these pathways involved in constitutive endocytosis or receptor recycling. Due to there being a vast number of proteins involved in the pathways, many of which may have redundant functionality, preliminarily perturbing these pathways globally as opposed to attempting to identify individual targets may quickly inform us whether they are important for CCR2 function. To do this, pharmacological inhibitors, dominant-negative mutants, and gene-silencing of critical components of the most promising pathway or protein targets could be the most direct means to determine key mediators of CCR2 function and inform more targeted experiments.

Finally, we continue to try and identify novel interactors of CCR2 which are directly involved in and critical for chemokine scavenging. Our CCR2 APEX study was one such attempt to discover novel CCR2 interactors. Another means by which to identify proteins critical for chemokine scavenging by CCR2 is a CRISPR genome-wide or trafficking-wide screen. This could be achieved using either a pooled, or if a trafficking specific library is used, could be done using an arrayed approach. Typically, a CRISPR screen requires a

selection or challenge step, such as in a cancer biology where cells are selected for their ability to resist drug treatment or for increased proliferation. Cells which overcome such challenge are then sequenced for gRNA expression to determine which genes are most significantly associated with cells ability to overcome said challenge. The approach we could take would be to treat CCR2/Cas9 expressing cells with a CRISPR gRNA library followed by addition of fluorescent CCL2. Cells can then be FAC-sorted based on fluorescent intensity of internalized chemokine which should be a semi-quantitative indication of scavenging functionality. Cells with either greater or diminished internalized chemokine can be assessed for gRNA enrichment and potentially inform us which genes are involved in chemokine scavenging.

References

1. V. Mollica Poeta, M. Massara, A. Capucetti, R. Bonecchi, Chemokines and Chemokine Receptors: New Targets for Cancer Immunotherapy. *Front. Immunol.* **10** (2019) (available at https://www.frontiersin.org/articles/10.3389/fimmu.2019.00379).

2. J. E. Pease, R. Horuk, Chemokine receptor antagonists: Part 1. *Expert Opin. Ther. Pat.* **19**, 39–58 (2009).

3. J. E. Pease, R. Horuk, Chemokine receptor antagonists: part 2. *Expert Opin. Ther. Pat.* **19**, 199–221 (2009).

4. Y. L. Kasamon, H. Chen, R. A. de Claro, L. Nie, J. Ye, G. M. Blumenthal, A. T. Farrell, R. Pazdur, FDA Approval Summary: Mogamulizumab-kpkc for Mycosis Fungoides and Sézary Syndrome. *Clin. Cancer Res. Off. J. Am. Assoc. Cancer Res.* **25**, 7275–7280 (2019).

5. T. M. Nywening, A. Wang-Gillam, D. E. Sanford, B. A. Belt, R. Z. Panni, B. M. Cusworth, A. T. Toriola, R. K. Nieman, L. A. Worley, M. Yano, K. J. Fowler, A. C. Lockhart, R. Suresh, B. R. Tan, K.-H. Lim, R. C. Fields, S. M. Strasberg, W. G. Hawkins, D. G. DeNardo, S. P. Goedegebuure, D. C. Linehan, Phase 1b study

targeting tumour associated macrophages with CCR2 inhibition plus FOLFIRINOX in locally advanced and borderline resectable pancreatic cancer. *Lancet Oncol.* **17**, 651–662 (2016).

6. T. M. Nywening, A. Wang-Gillam, D. E. Sanford, B. A. Belt, R. Z. Panni, B. M. Cusworth, A. T. Toriola, R. K. Nieman, L. A. Worley, M. Yano, K. J. Fowler, A. C. Lockhart, R. Suresh, B. R. Tan, K.-H. Lim, R. C. Fields, S. M. Strasberg, W. G. Hawkins, D. G. DeNardo, S. P. Goedegebuure, D. C. Linehan, Targeting tumour-associated macrophages with CCR2 inhibition in combination with FOLFIRINOX in patients with borderline resectable and locally advanced pancreatic cancer: a single-centre, open-label, dose-finding, non-randomised, phase 1b trial. *Lancet Oncol.* **17**, 651–662 (2016).

7. S. L. Friedman, B. A. Neuschwander-Tetri, M. Rinella, A. J. Sanyal, Mechanisms of NAFLD development and therapeutic strategies. *Nat. Med.* **24**, 908–922 (2018).

8. F. Saaber, D. Schütz, E. Miess, P. Abe, S. Desikan, P. Ashok Kumar, S. Balk, K. Huang, J. M. Beaulieu, S. Schulz, R. Stumm, ACKR3 Regulation of Neuronal Migration Requires ACKR3 Phosphorylation, but Not β-Arrestin. *Cell Rep.* **26**, 1473-1488.e9 (2019).

9. C. Tobia, P. Chiodelli, A. Barbieri, S. Buraschi, E. Ferrari, S. Mitola, G. Borsani, J. Guerra, M. Presta, Atypical Chemokine Receptor 3 Generates Guidance Cues for CXCL12-Mediated Endothelial Cell Migration. *Front. Immunol.* **10** (2019) (available at https://www.frontiersin.org/articles/10.3389/fimmu.2019.01092).

10. P. Abe, W. Mueller, D. Schütz, F. MacKay, M. Thelen, P. Zhang, R. Stumm, CXCR7 prevents excessive CXCL12-mediated downregulation of CXCR4 in migrating cortical interneurons. *Dev. Camb. Engl.* **141**, 1857–1863 (2014).

11. E. M. García-Cuesta, C. A. Santiago, J. Vallejo-Díaz, Y. Juarranz, J. M. Rodríguez-Frade, M. Mellado, The Role of the CXCL12/CXCR4/ACKR3 Axis in Autoimmune Diseases. *Front. Endocrinol.* **10** (2019), doi:10.3389/fendo.2019.00585.

12. K. E. Quinn, D. I. Mackie, K. M. Caron, Emerging roles of Atypical Chemokine Receptor 3 (ACKR3) in normal development and physiology. *Cytokine*. **109**, 17–23 (2018).

13. F. Saaber, D. Schütz, E. Miess, P. Abe, S. Desikan, P. Ashok Kumar, S. Balk, K. Huang, J. M. Beaulieu, S. Schulz, R. Stumm, ACKR3 Regulation of Neuronal Migration Requires ACKR3 Phosphorylation, but Not β-Arrestin. *Cell Rep.* **26**, 1473-1488.e9 (2019).

14. A. E. Cardona, M. E. Sasse, L. Liu, S. M. Cardona, M. Mizutani, C. Savarin, T. Hu, R. M. Ransohoff, Scavenging roles of chemokine receptors: chemokine receptor

deficiency is associated with increased levels of ligand in circulation and tissues. *Blood*. **112**, 256–263 (2008).

15. B. N. Zhao, J. J. Campbell, C. L. Salanga, L. S. Ertl, Y. Wang, S. Yau, T. Dang, Y. Zeng, J. P. McMahon, A. Krasinski, P. Zhang, I. Kufareva, T. M. Handel, I. F. Charo, R. Singh, T. J. Schall, CCR2-Mediated Uptake of Constitutively Produced CCL2: A Mechanism for Regulating Chemokine Levels in the Blood. *J. Immunol. Baltim. Md 1950*. **203**, 3157–3165 (2019).

16. X. Tian, D. S. Kang, J. L. Benovic, β-arrestins and G Protein-Coupled Receptor Trafficking. *Handb. Exp. Pharmacol.* **219**, 173–186 (2014).

17. V. V. Gurevich, E. V. Gurevich, The structural basis of arrestin-mediated regulation of G-protein-coupled receptors. *Pharmacol. Ther.* **110**, 465–502 (2006).

18. T. J. Cahill, A. R. B. Thomsen, J. T. Tarrasch, B. Plouffe, A. H. Nguyen, F. Yang, L.-Y. Huang, A. W. Kahsai, D. L. Bassoni, B. J. Gavino, J. E. Lamerdin, S. Triest, A. K. Shukla, B. Berger, J. Little, A. Antar, A. Blanc, C.-X. Qu, X. Chen, K. Kawakami, A. Inoue, J. Aoki, J. Steyaert, J.-P. Sun, M. Bouvier, G. Skiniotis, R. J. Lefkowitz, Distinct conformations of GPCR–β-arrestin complexes mediate desensitization, signaling, and endocytosis. *Proc. Natl. Acad. Sci.* **114**, 2562–2567 (2017).

19. C. E. Hughes, R. J. B. Nibbs, A guide to chemokines and their receptors. *Febs J.* **285**, 2944–2971 (2018).

20. R. T. Strachan, J. Sun, D. H. Rominger, J. D. Violin, S. Ahn, A. Rojas Bie Thomsen, X. Zhu, A. Kleist, T. Costa, R. J. Lefkowitz, Divergent transducer-specific molecular efficacies generate biased agonism at a G protein-coupled receptor (GPCR). *J. Biol. Chem.* **289**, 14211–14224 (2014).

21. P. Temkin, B. Lauffer, S. Jäger, P. Cimermancic, N. J. Krogan, M. von Zastrow, SNX27 mediates retromer tubule entry and endosome-to-plasma membrane trafficking of signalling receptors. *Nat. Cell Biol.* **13**, 715–721 (2011).

22. P. J. Cullen, H. C. Korswagen, Sorting nexins provide diversity for retromer-dependent trafficking events. *Nat. Cell Biol.* **14**, 29–37 (2012).

23. M. N. J. Seaman, The retromer complex – endosomal protein recycling and beyond. *J. Cell Sci.* **125**, 4693–4702 (2012).

24. J. G. Donaldson, Macropinosome formation, maturation and membrane recycling: lessons from clathrin-independent endosomal membrane systems. *Philos. Trans. R. Soc. B Biol. Sci.* **374**, 20180148 (2019).

25. X. P. Lin, J. D. Mintern, P. A. Gleeson, Macropinocytosis in Different Cell Types: Similarities and Differences. *Membranes*. **10**, 177 (2020).

26. K. P. Huang, The mechanism of protein kinase C activation. *Trends Neurosci.* **12**, 425–432 (1989).

27. E. Carballo, D. M. Pitterle, D. J. Stumpo, R. T. Sperling, P. J. Blackshear, Phagocytic and macropinocytic activity in MARCKS-deficient macrophages and fibroblasts. *Am. J. Physiol.-Cell Physiol.* **277**, C163–C173 (1999).

28. R. Ard, J.-C. Maillet, E. Daher, M. Phan, R. Zinoviev, R. J. Parks, S. H. Gee, PKCα-mediated phosphorylation of the diacylglycerol kinase ζ MARCKS domain switches cell migration modes by regulating interactions with Rac1 and RhoA. *J. Biol. Chem.* **296**, 100516 (2021).

29. S. Yoshida, I. Gaeta, R. Pacitto, L. Krienke, O. Alge, B. Gregorka, J. A. Swanson, Differential signaling during macropinocytosis in response to M-CSF and PMA in macrophages. *Front. Physiol.* **6** (2015) (available at https://www.frontiersin.org/articles/10.3389/fphys.2015.00008).

30. J. G. Donaldson, Macropinosome formation, maturation and membrane recycling: lessons from clathrin-independent endosomal membrane systems. *Philos. Trans. R. Soc. B Biol. Sci.* **374**, 20180148 (2019).

31. F. D. Brown, A. L. Rozelle, H. L. Yin, T. Balla, J. G. Donaldson, Phosphatidylinositol 4,5-bisphosphate and Arf6-regulated membrane traffic. *J. Cell Biol.* **154**, 1007–1017 (2001).

32. H. Radhakrishna, R. D. Klausner, J. G. Donaldson, Aluminum fluoride stimulates surface protrusions in cells overexpressing the ARF6 GTPase. *J. Cell Biol.* **134**, 935–947 (1996).

33. A. L. Kiss, E. Botos, Endocytosis via caveolae: alternative pathway with distinct cellular compartments to avoid lysosomal degradation? *J. Cell. Mol. Med.* **13**, 1228–1237 (2009).

34. B. Chini, M. Parenti, G-protein coupled receptors in lipid rafts and caveolae: how, when and why do they go there? *J. Mol. Endocrinol.* **32**, 325–338 (2004).

35. J. J. Rennick, A. P. R. Johnston, R. G. Parton, Key principles and methods for studying the endocytosis of biological and nanoparticle therapeutics. *Nat. Nanotechnol.* **16**, 266–276 (2021).

36. M. Scarselli, J. G. Donaldson, Constitutive Internalization of G Protein-coupled Receptors and G Proteins via Clathrin-independent Endocytosis. *J. Biol. Chem.* **284**, 3577–3585 (2009).

37. J. Hendrik Schmidt, M. Perslev, L. Bukowski, M. Stoklund, F. Herborg, R. Herlo, K. Lindegaard Madsen, Constitutive internalization across therapeutically targeted

GPCRs correlates with constitutive activity. *Basic Clin. Pharmacol. Toxicol.* **126 Suppl 6**, 116–121 (2020).

38. S. R. Elkin, A. M. Lakoduk, S. L. Schmid, Endocytic Pathways and Endosomal Trafficking: A Primer. *Wien. Med. Wochenschr. 1946*. **166**, 196–204 (2016).

39. M. Pavelka, J. Roth, "Brefeldin A-Induced Golgi Apparatus Disassembly" in *Functional Ultrastructure: Atlas of Tissue Biology and Pathology*, M. Pavelka, J. Roth, Eds. (Springer, Vienna, 2010; https://doi.org/10.1007/978-3-211-99390-3_39), pp. 74–75.

40. S. A. Wood, J. E. Park, W. J. Brown, Brefeldin A causes a microtubule-mediated fusion of the trans-Golgi network and early endosomes. *Cell*. **67**, 591–600 (1991).

Acknowledgements

Chapter 4 contains unpublished material. The dissertation author was the primary author of this chapter.

APENDIX

METHODS

Generation of pLenti-CMV stable expressing cell lines

1. Construct design and Gateway Cloning

    1.1. To generate PCR products to be used in the Gateway® BP clonase reaction for insertion into pDONR221 donor vector, attB sites are added to the 5' end of the forward and reverse PCR primers of the desired DNA construct to be expressed. The Kozak sequence and start codon must be included in the PCR product.

        1.1.1. Primers can be designed using OligoPerfect (TermoFisher), SnapGene, or manually following the Gateway manual provided by Thermo Fisher (MAN0000282).

        1.1.2. The DNA construct to be expressed is then PCR amplified and purified by agarose gel electrophoresis. This insures all attB primers are removed which would otherwise inhibit the following BP clonase reaction.

2. BP clonase reaction and creation of pDONR221 entry clone.

    2.1. The propagation of EMPTY pDONR221 DNA needs to be done in ccdB survival competent cells. The empty pDONR221 contains a ccdB toxin expression sequence as part of the cloning selection process which will be replaced following the BP recombination reaction with our desired DNA sequence.

    2.2. Combine 1 µL of 150 ng/µL pDONR222 vector and molar equivalent of attB-PCR product. Add TE buffer (pH 8.0) up to 4 µL. Add 1 µL of BP clonase II enzyme and gently mix.

2.3. Incubate at 25°C for 1 hr.

2.4. Add 1 µL of Proteinase K solution and incubate at 37°C for 10 minute to terminate the reaction.

2.5. Transform 2 µL of the BP reaction into Stbl3 competent cells and plate onto Kanamycin containing plates. NOTE: Some common strains of E. coli (including XL10) are F' and can possibly survive the ccdB negative selection of the empty pDONR221. Use only F- E. coli strains.

3. LR clonase reaction and creation of pLENTI-CMV expression clone.

3.1. After selection and screening of pDONR221 entry clones continue to the LR clonase recombination reaction with pLENTI-CMV destination vector of choice.

3.2. Combine 1 µL of 150 ng/µL pLENTI destination vector and equal molar amount of pDONR221 entry clone. Add TE buffer (pH 8.0) up to 4 µL. Add 1 µL of LR clonase II enzyme and gently mix.

3.3. Incubate at 25°C for 1 hr.

3.4. Add 1 µL of Proteinase K solution and incubate at 37°C for 10 minutes to terminate the reaction.

3.5. Transform 2 µL of the BP reaction into Stbl3 competent and plate onto Carbenicillin containing plates. NOTE: Stbl3 competent cells should be used when cloning lentiviral DNA which contain long terminal repeats (LTRs) in order to prevent unwanted homologous recombination.

3.6. Pick and screen colonies for desired DNA sequence insertion.

4. Alternative one tube BP/LR reaction format

4.1. This can be used to insert the attB-flanked PCR product directly into a destination vector, by combining the BP and LR reactions in a single tube. Saving the need to transform and isolate the pDONR entry clone.

4.1.1. Combine 1 µL of 150 ng/µL pDONR221 vector and equal molar amount of attB-PCR product. Add TE buffer (pH 8.0) up to 6 µL. Add 1.5 µL of BP clonase II enzyme and gently mix.

4.1.2. Incubate at 25°C for 4 hr.

4.1.2.1. Remove 2.5 µL of the BP reaction to be treated with 0.25 µL Proteinase K (37°C for 10 min) and transformed into Stbl3 cells. This is to test efficiency of the BP reaction.

4.1.3. To the remaining 5 µL reaction, add 1 µL of pLENTI-CMV destination vector and 1.5 µL LR clonase II enzyme. Mix gently.

4.1.4. Incubate at 25°C for 2 hr.

4.1.5. Add 1 µL of Proteinase K solution and incubate at 37°C for 10 minutes to terminate the reaction.

4.1.6. Transform Stbl3 competent cells with 2 µL of the reaction and plate onto Carbenicillin containing plates.

4.1.7. Pick and screen colonies for desired DNA sequence insertion.

Chee JY, Chin CF (2015) Gateway Cloning Technology: Advantages and Drawbacks. Clon Transgen 4:138. doi:10.4172/2168-9849.1000138

Hartley JL. Use of the Gateway System for Protein Expression in Multiple Hosts. Curr Protoc Protein Sci. 2003 Feb;Chapter 5:Unit 5.17. PubMed PMID:18429245.

Ptashne, M. (1992). A Genetic Switch: Phage (Lambda) and Higher Organisms (Cambridge, MA: Cell Press).

Generation of lentiCRISPRv2 knockdown cell lines

1. Designing gRNA oligonucleotides

    1.1. Design gRNA oligos using CHOPCHOP v3. For knockout, it is recommended that the gRNA is expected to target all isoforms of the target gene and selected gRNA is downstream of any in-frame ATG sites (designated as green bars in the blue coding region on CHOPCHOP) to avoid expression of truncated proteins.

        1.1.1. Order corresponding forward and reverse oligos, excluding the PAM sequence. Additionally, add a single guanine (G) nucleotide to the 5' end of the forward oligo and a corresponding cytosine (C) to the 3' end of the reverse oligo. The U6 promoter reportedly prefers a G nucleotide to start transcription which can help efficiency of gRNA expression.

        1.1.2. Also add 5' - CACC to the 5' end of the forward Oligo and 5' – AAAC to the 5' end of the reverse oligo. These are the overhanging sequences for insertion into the BsmBI site of the lentiCRISPRv2 construct

            1.1.2.1. Ex. Oligo-F 5' – CACCGNNNNNNNNNNNNNNNNNNN – 3'

                Oligo-R 3' – CNNNNNNNNNNNNNNNNNNNCAAA – 5'

2. Annealing oligos

    2.1. Resuspend oligos to 100 µM in annealing buffer (10 mM Tris pH 8.0, 50 mM NaCl, 1 mM EDTA)

    2.2. Mix equal volumes of the equimolar oligos.

    2.3. Incubate at 95°C for 5 min in heat block water path.

2.4. Turn off the heat block and let cool slowly to room temperature for ~1 hr.

2.5. Store temporally on ice.

3. BsmBI-v2 Golden Gate assembly reaction

3.1. Combine 1 µL of 75 ng/µL lentiCRISPRv2 vector with 2:1 molar ration (insert:vector) of annealed gRNA oligos.

3.2. Bring volume to 8 µL and add 1 µL 10X T4 Ligase Buffer, 0.5 µL BsmBI-v2 enzyme, and 0.5 µL high concentration T4 Ligase (NEB M0202T, 2,000U/µL). NOTE: If using BsmBi-v2 NEBridge® Golden Gate Assembly Kit (NEB #E1602) this already contains HC T4 ligase, simply add 1 µL of reaction mix.

3.3. Run the assembly protocol on a thermocycler, [(42°C, 1 min → 16°C,1 min) x 30 → 42°C, 5 min → 60°C, 5 min].

3.4. Transform 2 µL of the reaction into Stbl3 competent cells and plate onto carbenicillin plates.

3.5. Pick and screen colonies for gRNA insertion.

Improved vectors and genome-wide libraries for CRISPR screening. Sanjana NE, Shalem O, Zhang F. Nat Methods. 2014 Aug;11(8):783-4. doi: 10.1038/nmeth.3047. 10.1038/nmeth.3047 PubMed 25075903

Labun, K., Montague, T. G., Krause, M., Torres Cleuren, Y. N., Tjeldnes, H., & Valen, E. CHOPCHOP v3: expanding the CRISPR web toolbox beyond genome editing. Nucleic Acids Research (2019)

Creating multiple CRISPR gRNA constructs using Multiplex CRISPR/Cas9 Assembly

1. Designing gRNA oligonucleotides

1.1. This system is designed for insertion of up to 7 gRNA into a single Cas9 containing vector.

1.2. Design gRNA oligos using CHOPCHOP v3. For knockout, it is recommended that the gRNA is expected to target all isoforms of the target gene and selected gRNA is downstream of any in-frame ATG sites (designated as green bars in the blue coding region on CHOPCHOP) to avoid expression of truncated proteins.

1.2.1. Order corresponding forward and reverse oligos, excluding the PAM sequence. Additionally, add a single guanine (G) nucleotide to the 5' end of the forward oligo and a corresponding cytosine (C) to the 3' end of the reverse oligo. The U6 promoter reportedly prefers a G nucleotide to start transcription which can help efficiency of gRNA expression.

1.2.2. Also add 5' - CACC to the 5' end of the forward Oligo and 5' – AAAC to the 5' end of the reverse oligo. These are the overhanging sequences for insertion into the Golden Gate Assembly sites of the pX330A-1xN and pX330S-N

1.2.2.1. Ex. Oligo-F 5' – CACCGNNNNNNNNNNNNNNNNNNN – 3'

Oligo-R 3' – CNNNNNNNNNNNNNNNNNNNCAAA – 5'

2. Annealing oligos

2.1. Resuspend oligos to 100 µM in annealing buffer (10 mM Tris pH 8.0, 50 mM NaCl, 1 mM EDTA)

2.2. Mix equal volumes of the equimolar oligos.

2.3. Incubate at 95°C for 5 min in heat block water path.

2.4. Turn off the heat block and let cool slowly to room temperature for ~1 hr.

2.5. Store temporally on ice.

3. BbsI-HF Golden Gate assembly reaction for creation of pX330A-1xN and pX330S-N

    3.1. “N” represents the number of total gRNA for the final product, use whichever vector corresponds to the number of gRNA desired. If using only one gRNA, can be cloned in pX330A-1x2 and subsequently used. Following protocol is if using two gRNA.

        3.1.1. Combine 1 µL of 75 ng/µL pX330A-1x2 and 2:1 (insert:vector) of annealed oligos of first gRNA (about ~0.56 µL of 0.1 µM annealed oligos).

        3.1.2. Combine 1 µL of 75 ng/µL pX330S-2 and 2:1 (insert:vector) of annealed oligos of second gRNA (about ~0.56 µL of 0.1 µM annealed oligos).

        3.1.3. Make master mix by combining (0.5 µL 10X T4 Ligase Buffer, 0.25 µL BbsI-HF, 0.25 µL HC T4 Ligase, and 2.44 µL MilliQ H_2O) per reaction (i.e. X2 if using 2 gRNA inserts).

        3.1.4. Add 3.44 µL of master mix to each vector:insert reaction tube.

        3.1.5. Run the assembly protocol on a thermocycler, [(37°C, 5 min → 16°C,10 min) x 3 → 37°C, 5 min → 80°C, 5 min → 4°C, ∞ min].

        3.1.6. For pX330A-1x2 transform 2 µL of the reaction into XL10 competent cells and plate on Carbenicillin containing plates.

        3.1.7. For pX330S-2 transform 2 µL of the reaction into XL10 competent cells and plate on Spectinomycin containing plates.

        3.1.8. Pick and screen colonies for insertion of gRNA

4. BsaI-HF Golden Gate assembly reaction for recombination of pX330A-1xN and pX330S-N

4.1. Each pX330A-1xN and pX330S-N have BbsI restriction sites and appropriate overhangs for proper insertion depending on the number of insertions. This works due to BbsI recognizing a conserved sequence, but cutting upstream of that recognition site. Therefore the overhangs can be tuned for each insert/vector and allows for the insertion of multiple gRNA and is also the reason for the pX330A-1xN system, which coordinates the proper overhangs for the final recombination.

4.1.1. Combine 1.5 µL of 100 ng/µL pX330A-1x2 and 1.5 µL of 50 ng/µL pX330S-2 for a 2:1 insert:vector ratio). If inserting more than 2 gRNA, add 1.5 µL each of 50 ng/µL pX330S-N.

4.1.2. Make reaction mix by combining 2 µL of 10X T4 Ligase buffer, 1 µL BbsI-HF enzyme, 1 µL HC T4 DNA Ligase, and 13 µL MilliQ H_2O (reduce H_2O by 1.5 µL for each additional pX330S-N clone being used).

4.1.3. Add reaction mix to pX330A/pX330S containing reaction tube.

4.1.4. Run the assembly protocol on a thermocycler, [(37°C, 5 min → 16°C,10 min) x 25 → 37°C, 5 min → 80°C, 5 min → 4°C, ∞ min].

4.1.5. Transform 4 µL of the reaction mix into XL10 competent cells and plate on carbenicillin containing plates. Alternatively, XL1-Blue cells can be used for blue/white colony screening with the addition of X-gal and IPTG to the plates.

4.1.6. Pick and screen colonies for insertion of gRNAs.

Multiplex genome engineering in human cells using all-in-one CRISPR/Cas9 vector system. Sakuma T, Nishikawa A, Kume S, Chayama K, Yamamoto T. Sci Rep. 2014 Jun 23;4:5400. doi: 10.1038/srep05400. PubMed PMID 24954249.

Generation of clonally selected CRISPR knockout cell lines

1. Transfection of cells and generation of conditioned medium

    * This method works best for adherent and easily transfectable cells lines (e.g., HEK293).

    * A Cas9/gRNA containing plasmid should already be generated before the following protocol.

    1.1. Before preparing cells for transfection, save conditioned media form untransfected cultured cells.

        1.1.1. Draw off media from cultured cells and sterile filter through a 0.22 µm filter. Store at 4°C for up to 48 hrs.

    1.2. The day before transfection, seed HEK293 cells to 0.350 $x10^6$ cells/well in a 6-well culture plate. Cells should ideally be ~70% confluent at time of transfection the next day.

    1.3. The next day, following Mirus TransIT-LT1 transfection reagent manufacturer protocol, add 2.5 µg Cas9/gRNA DNA into 250 µL OptiMEM media.

    1.4. Add 7.5 µL TransIT-LT1 reagent and gently vortex for ~3 seconds. And let sit for 20-30 min.

    1.5. Dropwise, add transfection mix to single 6-well containing cells.

    1.6. Culture cells for at 24-48 hours depending on confluency and expression capability of cells.

2. Limiting dilution monoclonal cell isolation

    2.1. Lift cells by trypsinization and break up any clumped cells by pipetting or by passing through a cell strainer.

    2.2. Count cells on ViCell or hemocytometer to determine cell concentration

2.3. Dilute cells to 5 cells/mL in ~10 mL total volume of 1:1 conditioned: fresh media.

2.4. Using a multichannel pipette, transfer 100 µL of 5 cells/mL cell solution to each well of a 96-well plate.

2.5. Leave the cells undisturbed for ~7 days.

2.6. Scan each well of the plate looking for colony grown. Note, single cells tend to prefer the edge of the well and will grow out a colony from there. If multiple colonies are observed in a well this is indicative of multiple single cells being initially seeded and should be discarded/ignored.

2.7. Continue to allow cells to grow and expand into larger culture dish when nearing confluency.

3. Screening monoclonal cell populations for genome editing and knockout.

3.1. Once cells have been efficiently expanded, harvest enough cells for genomic DNA extraction and cell lysis preparation.

3.2. For genome extraction, follow Qiagen genomic DNA extraction kit instructions according to the manufacturer.

3.2.1. Send genomic DNA and appropriate gRNA cut site flanking primers for sanger sequencing. Flanking primers for genomic DNA screening can be found using CHOPCHOPv3 when designing gRNA.

3.2.2. For homozygous genome editing, sequencing chromatograms should be single peaks throughout. Compare sequenced DNA to wildtype. Edited DNA typically has single nucleotide insertions resulting in frame shift and gene silencing.

3.2.3. Whereas for heterozygous genome editing, sequencing chromatograms will have double peaks following gRNA cut site. With one sequencing corresponding to the cut and non-homologous recombination sequence and the other corresponding to the wildtype uncut DNA.

3.2.3.1. NOTE: Double peaks can occur when recombination varies between alleles (e.g. +1 nucleotide and +2 nucleotide on another strand), but this is rare. Analysis of the two separate peak DNA sequences can be analyzed to determine if this is the case.

3.3. For cell lysis, extract cellular protein using RIPA buffer containing protease inhibitors.

3.3.1. Run clonal population lysis and lysate from wildtype cells on appropriate percentage SDS-PAGE gel.

3.3.2. Probe by western blot for protein knockdown comparing to wildtype controls.

3.4. Further expand positively edited clones and freeze down desired populations.

Lentivirus production and transduction

1. Prepare HEK293T cells for lentivirus transfection and virus production.

1.1. The day before transfection seed HEK293T cells in a 6 cm culture dish at 1.4×10^6 cells/well. Cells should be ~70% confluent at time of transfections.

1.2. The day of transfection, combined lentiviral transfer plasmid containing gene of interest, packaging plasmid (pMDLg/pRRE), envelope plasmid (pMD2.G), and

pRSV-Rev plasmid at a ratio of 4:2:1:1. This ratio ensures that majority of viral particles contain transfer plasmid of interest.

1.2.1. Combine DNA in OptiMEM for a DNA concentration of 10 ng/µL. With ~5 µg total DNA for a 6-cm dish transfection.

1.2.2. Add TransIT-LT1 transfection reagent to a ratio of 3:1 (µL reagent:µg DNA). Gently mix by vortexing for ~3 seconds. Let sit for ~20-30 minutes.

1.2.3. Dropwise, add transfection to 6 cm dish containing HEK293T cells.

1.2.4. After ~8 hrs, remove media and replace with fresh media. This step helps remove untransfected DNA.

1.2.5. At 48 hrs post-transfection, draw off media and filter through a 0.45 µm PES filter into a 15 mL conical.

1.2.6. Replace media with minimal amount for additional 24 hrs of growth

1.2.7. The next day (i.e., 72 hrs post-transfection) draw off media and filter through a 0.45 µm PES filter into the same 15 mL conical.

1.2.8. To the viral supe, add 1mg/mL sterile DNAase to a final concentration of 1 µg/mL. Also add 1M $MgCl_2$ to a final concentration of 1 mM. (This is 1 µL of each per 1 mL of viral supe).

1.2.9. Incubate at RT for 30 min followed by 4°C for 2-4 hours.

1.2.10. Store DNA for up to 1 day at 4°C or aliquot into single use amounts and freeze at -80°C. Viral transduction efficiency drops after freeze/thaw and should be stored only temporarily.

2. Transduction by spinfection of adherent or suspension cells.

2.1. Preparation of cells

2.1.1. For adherent cells, seed cells in a 6-well dish the day prior of transduction so they reach a confluence of ~70% the day of infection.

2.1.1.1. The day of transduction, remove media and replace with 1 mL of fresh media just prior to addition of virus.

2.1.2. For suspension cells, the day of transduction, count the cells and bring to a concentration of $2x10^6$ cells/mL and aliquot 1 mL into appropriate number of wells of a 6-well dish.

2.2. Infection with lentivirus

2.2.1. Add 1 mL of virus to each well containing cells, and 1 mL of media to a negative control well containing cells.

2.2.2. Add polybrene to each well for a final concentration of 8 µg/mL. Polybrene stock is typically 10 mg/mL.

2.2.2.1. Polybrene helps facilitate viral particle interaction with the cell and viral uptake. It can however be toxic to some cell types, so should be empirically tested.

2.3. Spinfection

2.3.1. Prewarm a benchtop centrifuge to ~37°C by spinning at max speed for ~15 minutes.

2.3.2. Transfer the transduction plates containing cells and virus to the centrifuge and spin at 800 x g for 90 min.

2.3.3. After the spin, add 0.5 mL of media to help balance the pH of the media.

2.3.4. Leave the cells in virus containing media for ~16-24 hrs.

2.3.4.1. Some cells cannot tolerate being exposed to virus for extended periods. In this case, remove the viral media and replace with fresh following the spinfection step.

3. Expanding and selection of cells

3.1. After the 16-24 hr period, remove the media by aspiration (for adherent cells) or by centrifugation (for suspension cells) and add fresh media to cells.

3.1.1. For suspension cells, spin and replace media then culture in appropriate sized dish.

3.2. The following day (i.e., ~48 hrs post-transduction) passage cells and replace media with antibiotic containing media.

3.2.1. For HEK293: Puromycin 1 – 5 µg/mL, Hygromycin 10 – 50 µg/mL

3.2.2. For THP-1: Puromycin 0.5 – 2 µg/mL

3.2.2.1. Note: For THP-1 cells, "cell death" is usually not observed, however untransduced and negative control cells will stop growing. And positively transduced cells with continue to grow throughout the selection period.

3.3. Continue to passage cells for at least 1 week of selection (longer for suspension or slow growing cells), replacing the antibiotic containing mediate at least once every 3 days. Cells will die more quickly when lifting and passage the cells.

3.4. Once desired period of selection is complete, screen cells for desired stable expression / knockdown / knockout.

A. P. Cribbs, A. Kennedy, B. Gregory, F. M. Brennan, Simplified production and concentration of lentiviral vectors to achieve high transduction in primary human T cells. *BMC Biotechnol*. **13**, 98 (2013).

Bioluminescence resonance energy transfer (BRET) and enhance-bystander BRET

The following protocol is modified from previously reported methods in Namkung et al. 2016.

This protocol can be performed in a 96-well transfection or 6-well transfection format. The 96-well format results in biological replicates as opposed to technical replicates, in addition to the cells being in a more adherent state. Additionally, 96-well transfection can be performed traditionally or via reverse transfection (i.e. addition of transfection DNA at the same time as cell seeding).

1. Preparation and seeding of cells for transfection
    1.1. Seed cells the day before transfection so they reach a confluency of ~70% the day of transfection. For HEK293 seed 0.350 x 10^6 cells/well in a 6-well.
    1.2. If doing 96-well format, seed cells the day before transfection so they reach a confluency of ~70% the day of transfection. For HEK293 seed 0.10 x 10^5 cells/well into a 96-well precoated with poly-D-lysine.
        1.2.1. For poly-D-lysine coating, dilute 1 mg/mL sterile poly-D-lysine stock solution to 50 µg/mL in sterile H_2O and add 70 µL to each, making sure each well is entirely coated (agitate the plate if needed). Incubate at 37°C for 30 min, or RT for at least 1 hr. Aspirate wells and wash once with sterile PBS. Aspirate and let play dry before adding cells.
    1.3. If performing reverse transfection in 96-well plate, seed 0.35 x 10^5 cells/well into poly-D-lysine coated 96-well at time of transfection.
2. Transfection

2.1. DNA amount can be slightly adjusted based on the transfectability and expression capability of the cells being used, but general guidelines are below.

2.2. For 6-well transfection format, DNA ratios are 36 ng receptor-RlucII (a.k.a. Rluc3) DNA and 144 ng rGFP-marker (i.e., CAAX, FYVE, Rab4, Rab11, or Rab7) DNA. For experiments using β-arrestin-RlucII, use a ratio of 21.6 ng β-arresitn-RlucII DNA to 144 ng rGFP-marker DNA.

2.3. For a 96-well format, scale these DNA amounts linearly based on dish surface area, which is 1.2 ng receptor-RlucII DNA (or 0.72 ng β-arrestin-RlucII) and 4.8 ng rGFP-marker DNA.

2.4. Combine appropriate amounts of donor RlucII and acceptor rGFP DNA, along with empirically determined amount of receptor DNA, if needed (e.g., for β-arrestin-RlucII:rGFP-CAAX association), generally between 100 – 500 ng receptor per 6-well, into OptiMEM for a final DNA concentration of 10 ng/µL.

2.5. Add TrandIT-LT1 reagent at a 3:1 ratio (µL reagent : µg DNA). Gentle mix by vortex for ~3 seconds.

2.6. Let sit for ~20-30 minutes.

2.7. Add DNA dropwise to wells.

2.7.1. For reverse transfection, DNA can be added immediately after adding cells to the well.

2.8. Perform assay ~30-48hrs post transfection.

3. Assay protocol

3.1. If using the 6-well format

3.1.1. The day of the assay, remove media and wash cells once with 1 mL PBS. Aspirate PBS and lift cells with 250 µL pre-warmed Accutase for ~7 min. Add 1 mL pre-warmed Tyrode's Buffer (140 mM NaCl, 2.7 mM KCl, 1 mM $CaCl_2$, 12 mM $NaHCO_3$, 5.6 mM D-glucose, 0.5 mM $MgCl_2$, 0.37 mM NaH_2PO_4, 25 mM HEPES and pH 7.4) and lift by pipetting, followed by transfer to a 1.5 mL or 2 mL microcentrifuge tube.

3.1.2. Count cells at a 1:3 dilution (using minimum amount of volume).

3.1.3. Spin cells at 300 x g for 5 min, aspirate supernatant and resuspend to 1.25 x 10^6 cells/mL

3.1.4. Aliquot 80 µL (i.e., 0.1 x 10^6 cells/well) to each well of a white clear bottom (or white bottom) 96-well plate.

3.2. If using the 96-well format

3.2.1. The day of the assay, remove media and wash cells one with 200 µL pre-warmed Tyrode's buffer. Aspirate Tyrode's buffer and add 80 µL pre-warmed Tyrode's buffer to each well.

3.3. Let the cells equilibrate to buffer at 37°C for 1 hr.

3.4. Measure rGFP fluorescence on a microplate reader (400ex /510em).

3.5. If clear, cover the bottom of the plate with white backing stickers.

3.6. Dilute luciferase substrate Prolume Purple to a concentration of 25 µM and add 10 µL to each well (2.77 µM final each well).

3.7. After ~3 min, read the raw luminescence (0.5 integration time) for each well

3.8. Followed by 3 BRET reads 360-440 nm (donor) and 505-575 nm (acceptor) with a 0.2 second integration time.

3.9. Add 10 µL of Tyrode's buffer to mock wells and 10 µL of chemokine containing buffer followed by BRET reads 360-440 nm (donor) and 505-575 nm (acceptor) with a 0.2 second integration time for desired time course.

Y. Namkung, C. Le Gouill, V. Lukashova, H. Kobayashi, M. Hogue, E. Khoury, M. Song, M. Bouvier, S. A. Laporte, Monitoring G protein-coupled receptor and β-arrestin trafficking in live cells using enhanced bystander BRET. *Nat Commun*. **7**, 12178 (2016).

BRET-based receptor recycling assay

This method uses receptor-RlucII and rGFP-CAAX donor:acceptor BRET pairs.

1. Seeding and transfection cells

   1.1. Seed and transfect cells according to the poly-D-lysine coated 96-well Bioluminescence resonance energy transfer (BRET) and enhance-bystander BRET protocol above using receptor-RlucII and rGFP-CAAX BRET pairs.

2. Assay protocol

   2.1. The day of the assay, remove media and wash cells one with 200 µL pre-warmed Tyrode's buffer. Aspirate Tyrode's buffer and add 80 µL pre-warmed Tyrode's buffer to each well.

   2.2. Let the cells equilibrate to buffer at 37°C for 1 hr.

   2.3. Measure rGFP fluorescence on a microplate reader (400ex /510em).

   2.4. If clear, cover the bottom of the plate with white backing stickers.

   2.5. Dilute luciferase substrate Prolume Purple to a concentration of 25 µM and add 10 µL to each well (2.77 µM final each well).

   2.6. After ~3 min, read the raw luminescence (0.5 integration time) for each well

2.7. Followed by 3 BRET reads 360-440 nm (donor) and 505-575 nm (acceptor) with a 0.2 second integration time.

2.8. Add 10 µL of Tyrode's buffer to mock wells and 10 µL of chemokine containing buffer followed by BRET reads 360-440 nm (donor) and 505-575 nm (acceptor) with a 0.2 second integration time for desired time course depending on internalization rate of receptor ~8-15 minutes.

2.9. Wash one group of mock and chemokine treated cells 3x with warm Tyrode's buffer and replace with 100 µL warm Tyrode's buffer.

2.9.1. Similarly, cold 50 mM sodium citrate, pH 4.0 can be used to wash cells. Followed by 2 x washes with pre-warmed Tyrode's buffer and replacement with 100 µL Tyrode's buffer.

2.9.2. Addition of inhibitor (BMS681 for CCR2) can also be used in place of washing. For this method, add 10 µL of vehicle control containing Tyrode's buffer or 10 µL of BMS681 containing Tryode's buffer.

2.10. Continue BRET reads for additional desired time course.

Gαβγ dissociation BRET assay

This protocol is based off previously described method by Matt et al. 2020.

1. Seeding and transfection cells

1.1. Seed cells the day before transfection so they reach a confluency of ~70% the day of transfection. For HEK293 seed 0.350 x 10^6 cells/well in a 6-well.

1.2. If doing 96-well format, seed cells the day before transfection so they reach a confluency of ~70% the day of transfection. For HEK293 seed 0.10 x 10^5 cells/well into a 96-well precoated with poly-D-lysine.

1.2.1. For poly-D-lysine coating, dilute 1 mg/mL sterile poly-D-lysine stock solution to 50 µg/mL in sterile H_2O and add 70 µL to each, making sure each well is entirely coated (agitate the plate if needed). Incubate at 37°C for 30 min, or RT for at least 1 hr. Aspirate wells and wash once with sterile PBS. Aspirate and let play dry before adding cells.

1.3. If performing reverse transfection in 96-well plate, seed 0.35 x 10^5 cells/well into poly-D-lysine coated 96-well at time of transfection.

2. Transfection

2.1. DNA amount can be slightly adjusted based on the transfectability and expression capability of the cells being used, but general guidelines are below.

2.2. For 6-well transfection format, DNA ratios are 250 ng pIRES-Gα-Nluc-Gβγ-cpVenus DNA and 200 ng receptor DNA.

2.3. For a 96-well format, scale these DNA amounts linearly based on dish surface area, which is 6.94 ng pIRES-Gα-Nluc-Gβγ-cpVenus DNA and 5.56 ng receptor DNA.

2.4. Combine appropriate amounts of pIRES-Gα-Nluc-Gβγ-cpVenus and receptor DNA into OptiMEM for a final DNA concentration of 10 ng/µL.

2.5. Add TrandIT-LT1 reagent at a 3:1 ratio (µL reagent : µg DNA). Gentle mix by vortex for ~3 seconds.

2.6. Let sit for ~20-30 minutes.

2.7. Add DNA dropwise to wells.

2.7.1. For reverse transfection, DNA can be added immediately after adding cells to the well.

3. Assay protocol

3.1. If using the 6-well format

3.1.1. The day of the assay, remove media and wash cells once with 1 mL PBS. Aspirate PBS and lift cells with 250 µL pre-warmed Accutase for ~7 min. Add 1 mL pre-warmed Tyrode's Buffer (140 mM NaCl, 2.7 mM KCl, 1 mM $CaCl_2$, 12 mM $NaHCO_3$, 5.6 mM D-glucose, 0.5 mM $MgCl_2$, 0.37 mM NaH_2PO_4, 25 mM HEPES and pH 7.4) and lift by pipetting, followed by transfer to a 1.5 mL or 2 mL microcentrifuge tube.

3.1.2. Count cells at a 1:3 dilution (using minimum amount of volume).

3.1.3. Spin cells at 300 x g for 5 min, aspirate supernatant and resuspend to 1.25 x 10^6 cells/mL

3.1.4. Aliquot 80 µL (i.e., 0.1 x 10^6 cells/well) to each well of a white clear bottom (or white bottom) 96-well plate.

3.2. If using the 96-well format

3.2.1. The day of the assay, remove media and wash cells one with 200 µL pre-warmed Tyrode's buffer. Aspirate Tyrode's buffer and add 80 µL pre-warmed Tyrode's buffer to each well.

3.3. Let the cells equilibrate to buffer at 37°C for 1 hr.

3.4. Measure rGFP fluorescence on a microplate reader (400ex /510em).

3.5. If clear, cover the bottom of the plate with white backing stickers.

3.6. Dilute luciferase substrate coelenterazine H to a concentration of 20 µM and add 10 µL to each well (2.22 µM final each well).

3.7. After ~8-10 min, read the raw luminescence (0.5 integration time) for each well.

3.7.1. Nluc is very bright, make sure BRET values are not over saturated. If so, increase incubation time with coelenterazine H and lower concentration to as low as 0.5 μM.

3.8. Followed by 3 BRET reads 430-485 nm (donor) and 505-590 nm (acceptor) with a 0.1 second integration time.

3.9. Add 10 μL of Tyrode's buffer to mock wells and 10 μL of chemokine containing buffer followed by BRET reads 430-485 nm (donor) and 505-590 nm (acceptor) with a 0.1 second integration time for desired time course.

C. Matti, A. Salnikov, M. Artinger, G. D'Agostino, I. Kindinger, M. Uguccioni, M. Thelen, D. F. Legler, ACKR4 Recruits GRK3 Prior to β-Arrestins but Can Scavenge Chemokines in the Absence of β-Arrestins. Front Immunol. 11, 720 (2020).

Fura-2 Calcium Flux Assay

This assay can be performed in stable, transient, or endogenous expressing cells, as well as adherent or suspense cells. Additionally, this protocol can be performed with or without removing the Fura-2 AM quenching buffer prior to fluorescent reading (usually referred to "wash" vs "no wash" or "1-step" versus "2-step" protocol). Removing the extracellular red quenching buffer (included in the 10X assay buffer), will improve signal intensity, but can result in background due to extracellular Ca^{+} which has bound to any remaining extracellular Fura-2 AM dye.

1. If using adherent cells, cells should be seeded (and transfect, if needed) in 96-well black clear bottom poly-D-lysine coated plates the day before the assay. Cells should be near 100% confluent by the time of the assay.

2. Assay and Fura-2 AM dye buffer preparation

2.1. The day of the assay prepare 1X assay buffer by 1:10 dilution of 10X Pluronic F127 Plus in Hank's Balanced Salt Solution with HEPES buffer (HHBS) [i.e., 100 µL into 900 µL].

2.2. Prepare Fura-2 AM dye-loading solution by adding 20 µL Fura-2 AM to 10 mL of assay buffer (adjust volumes according to volume needed). Solution is stable at RT for up to 2 hrs.

2.3. If cells are known to express high levels of organic anion-transporters, probenecid (1-2 mM) may be added to the dye working solution to prevent expulsion of Fura-2 AM dye.

3. Assay experimental protocol

3.1. For adherent cells

3.1.1. Wash cells 2x with pre-warmed HHBS. After final wash, add 100 µL HHBS to each well

3.1.2. Add 100 µL Fura-2 AM assay buffer dye solution

3.1.3. Incubate at 37°C for 1 hr.

3.2. For suspension cells

3.2.1. The day of the assay, count cells, spin down and resuspend cells to 1 x 10^6 cells/mL in HHBS.

3.2.2. Add 100 µL of cells to each well of a 96-well black clear bottom poly-D-lysine coated plate.

3.2.3. Spin the plate at 130 x g for 5 min and incubate at 37°C for 30 minutes.

3.2.4. Add 100 µL Fura-2 AM assay buffer dye solution

3.2.5. Incubate at 37°C for additional 1 hr.

3.2.5.1. If using the 2-step process, aspirate assay buffer and replace with 200 µL HHBS. This is more difficult with suspension cells, as they will be very loosely adhered to the poly-D-lysine dish.

3.3. After the 1 hr incubation, immediately run the assay plate.

3.3.1. Limit the number of wells per read for shorter time intervals between reads.

3.4. Take 10 baseline reads, measuring Ex/Em 340/520 and 380/520 for each well.

3.5. After 10 baselines reads, using liquid handler, inject 20 µL at 120 µL/s of chemokine in HHBS +1% BSA or HHBS +1% BSA alone.

3.5.1. BSA helps prevent chemokine from sticking to tubes or injector tubing.

3.6. Read plate for remainder of desired time course.

3.7. Calculate the fluorescence intensity ratio (F_{340nm}/F_{380nm}) over the time course. An increase in Ca^{+} flux and binding to Fura-2 AM dye causes a shift in excitation peak from 380 nm to 340 nm.

M. Martínez, N. A. Martínez, W. I. Silva, Measurement of the Intracellular Calcium Concentration with Fura-2 AM Using a Fluorescence Plate Reader. *Bio Protoc*. **7**, e2411 (2017).

G. Grynkiewicz, M. Poenie, R. Y. Tsien, A new generation of Ca2+ indicators with greatly improved fluorescence properties. *J Biol Chem*. **260**, 3440–3450 (1985).

SNAP-tagged receptor labeling and microscopy

For live cell imaging of SNAP-receptor expressing cells, seed and transfect (if necessary) on fibronectin coated plates.

1. Fibronectin coating dishes and preparation of cells

1.1. Dilute fibronectin stock proportional to surface area to be coated. For example, for a 1 cm^2 growth area, make a 10 µg/mL solution for 1 µg/cm^2.

1.2. Add 100 µL/cm^2 of fibronectin solution and incubate at RT for 1 hr.

1.3. Aspirate fibronectin solution and was 1x with PBS.

1.4. Aspirate and allow to dry before adding cells.

1.5. Seed cells at appropriate density so they are ~70% confluent at time of staining.

2. Staining protocol

2.1. For surface staining using SNAP-surface substrates, every step should be performed on ice using cold buffers. Otherwise steps can be performed at 37°C.

2.2. Prepare 4 µM fluorescent SNAP-substrate in complete media (DMEM +10% FBS).

2.3. Add to cells and incubate at 37°C for 30 min (if at 4°C, 45 min).

2.4. Wash the cells three times with complete media.

2.5. Replace buffer with phenol red-free media supplemented with 2% FBS.

2.6. Image the cells using appropriate Ex/Em filter set.

APEX-MS sample preparation

Samples all treatment groups and time points are prepared in batches on separate days, so each replicate is from the same "batch" prepared on the same day. This helps to reduce experimental batch effects within replicates.

Preparation of buffers is critical for experimental success. A stock solution of biotinyl tryramide can be made in DMSO to a concentration of 100 mM and stored at -20°C or 4°C short term.

The quenching buffer should be made fresh and store at 4°C on the day of sample preparation. (Quenching Buffer: DPBS supplemented with 10 mM sodium ascorbate, 5 mM trolox, and 10 mM sodium azide).

1. One or two days before sample preparation, seed cells in 15 cm dishes so they are near 100% confluent at time of biotin labeling protocol.
2. NOTE: Timing of addition of PTx, YM-254890, and biotinyl tyramide vary depending on chemokine stimulation time.
    2.1. PTx should be added to a final concentration of 200 ng/mL 3 hrs before addition of chemokine.
    2.2. YM-254890 Gq inhibitor should be added to 100 nM final concentration (diluted in DPBS) 30 min before addition of chemokine.
    2.3. Pre-incubate cells with 500 µM biotinyl tyramide for 30 minutes total at 37°C. For example, for 60 min CCL2 stimulation add biotinyl tyramide 30 minutes after addition of chemokine. Similarly, for 10 min CCL2 stimulation add biotinyl tyramide 20 minutes before chemokine addition.
3. Stimulate cells with 50 nM CCL2 (final concentration) for appropriate amount of time. For “0 min” timepoint, no CCL2 is added.
4. Immediately prior to use, dilute H2O2 to 100 mM in room temperature DPBS. Add 100 mM of the H_2O_2 DPBS solution to cells to a final concentration of 1 mM H_2O_2 final and immediately rock dish. Allow labeling reaction to continue for 20 seconds.
5. Remove media by pouring off and wash cells 3 times (10 mL/wash) with ice cold quenching buffer.

6. Aspirate final wash and incubate cells on ice with 20 mL ice cold quenching buffer for 20 min.
7. Aspirate quenching buffer and add 6 mL of ice cold quenching RIPA buffer containing protease inhibitor and 2.5U/mL benzonase
8. Briefly agitate plate to dislodge cells, then scrape and transfer to a 15 mL conical centrifuge tube.
9. Rotate at 4°C for 1 hr to complete lysis. Pipette up and down to check on success of lysis.
10. Clarify lysate by centrifugation at 15,000 x g for 15 min at 4°C. Transfer supernatant to a new 15 mL centrifuge tube.
11. Freeze cleared lysates at -80°C until further processing.
12. For streptavidin bead pull-downs, thaw frozen lysates.
13. Wash 500 µL streptavidin magnetic beads per sample with RIPA buffer (10 bed volumes/wash in 15 mL conical centrifuge tubes).
14. Remove supernatant and add beads to the 15 mL conical tube containing lysate.
15. Incubate at 4°C overnight with gentle rotation.
16. Using a magnetic stand, wash beads with three times with 5 mL 4 M urea, 100 mM sodium phosphate pH 8.
17. Using a magnetic stand, wash beads three times with 50 mM HEPES, pH 8.5.
18. Resuspend beads in 1.5 mL 50 mM HEPES, pH 8.5 (deliver buffer). Keep 50 µL of final suspension volume for western sample.
19. Store resuspended beads at -80°C until delivery for mass spectroscopy.

J. Paek, M. Kalocsay, D. P. Staus, L. Wingler, R. Pascolutti, J. A. Paulo, S. P. Gygi, A. C. Kruse, Multidimensional Tracking of GPCR Signaling via Peroxidase-Catalyzed Proximity Labeling. *Cell*. **169**, 338-349.e11 (2017).

V. Hung, N. D. Udeshi, S. S. Lam, K. H. Loh, K. J. Cox, K. Pedram, S. A. Carr, A. Y. Ting, Spatially resolved proteomic mapping in living cells with the engineered peroxidase APEX2. *Nat Protoc*. **11**, 456–475 (2016).